Contents

[43] [44]

Chapter 1

Introduction

In the field of control theory and applications, the H_∞ method is a recently developed method for robust controller design. This method has for the past fifteen years been a popular resarch topic, partly because of the mathematical problems related with the development of the method, but also because of encouraging applications and case studies that have been reported. The fact that many of these applications have been carried out by people from the academic world suggests that such an application requires some insight in the theoretical aspects of the method, including awareness of a number of limitations of the method. The purpose of this thesis is partly to provide yet another case study, thus contributing to the process of making the H_∞ method more accesible for industry, and partly to contribute to the refinement of a method for solving tracking problems.

Central to the H_∞ method is the *standard H_∞ problem*. In this problem, one considers a system of the form

$$\begin{bmatrix} z \\ y \end{bmatrix} = G \begin{bmatrix} w \\ u \end{bmatrix} = \begin{bmatrix} G_{11} & G_{12} \\ G_{21} & G_{22} \end{bmatrix} \begin{bmatrix} w \\ u \end{bmatrix}, \tag{1.1}$$

where z is the to-be-controlled output, y is the measured output, u is the control input and w is the disturbance input. The H_∞ problem is to determine a linear causal control law $u = Ky$ such that, with this control law applied, the closed loop system is stable and there holds

$$\sup_{w \neq 0} \frac{\|z\|_2}{\|w\|_2} < \gamma. \tag{1.2}$$

Here γ is a pre-specified positive constant limiting the effect that the disturbance has on the output. Algorithms based on the solution of the standard H_∞ problem can be used to design a controller that will work well despite the presence of small model uncertainties, and this can be considered as the primary virtue of the H_∞ method.

Tracking problems, where the task is to make the system output follow some tracking trajectory even if the physical plant is not modelled perfectly, can be

solved using the standard H_∞ problem. The property of guaranteed tracking performance in the presence of model uncertainties is denoted *robust performance*. It is common to represent the reference signal by an unknown disturbance signal and then require that the effect this signal has on the tracking error should be bounded. An important distinction is made between one-degree-of-freedom designs where the control law is immediately given by the construction of a feedback law, and two-degrees-of-freedom designs where a feedback law is complemented by a control signal that depends on the reference signal only (feedforward). An example of a popular one-degree-of-freedom design is the mixed sensitivity problem, see Kwakernaak[40]. Examples of two-degrees-of-freedom designs can be found in Limebeer et al.[47] and in Yaesh and Shaked[61]. The three examples mentioned above are all based on a control structure where it is assumed that the signal that one wishes to control is measured directly (where we are here disregarding measurement noise). The range of methods that may be used for a given tracking problem depends on whether this is the case. More problematic than measurement noise is the situation where the signal that is measured depends only indirectly on the signal that one wishes to control. This more general situation where the controlled variable is not assumed to be measured was considered in Shaked and de Souza[57], where formulae for a two-degrees-of-freedom design were given.

For a given industrial control problem it is often important to discuss whether to choose the model as being finite dimensional or infinite dimensional. Relevant questions are whether the parameters of the distributed parameter model can be estimated effectively, and whether the increased complexity of the distributed parameter model results in a significantly improved model. It is also of interest, whether it is possible to take advantage of this extra information in the controller design. In the case study that is treated in this thesis it appears that affirmative answers can be given to at least two of these three questions. The model described in chapter 2 is infinite dimensional as it involves transport of heat and mass along a conveyor. This transport is characterized by a single velocity parameter which is relatively easy to estimate. It is also beyond doubt that the most accurate model that we can formulate for the plant is one that involves a continuous time transport equation, which is thus infinite dimensional. The third issue mentioned above is however more problematic. We base the controller design on a finite dimensional approximation where the quality of this approximation is evaluated by comparing with the tranfer function of the distributed parameter model, and furthermore the transfer function of the distributed parameter model is used directly in a theoretical robust performance test of the controller. An alternative approach would be to choose a finite dimensional discrete time transport model. Unfortunately, the most natural way to do this would involve a rather large sampling time, and it is á priori not obvious, which approach would result in the better controller, but the continuous time formulation has the advantage that we can formulate the model independently of the sampling procedure.

The problem of designing a finite dimensional controller for an infinite dimensional plant has been approached in many different ways in the literature. Most of these approaches fall into two groups: One possibility is to formulate an infinite dimensional control law and then approximate this one directly by an approach which involves the approximation of the solution to Riccati equations in the strong operator norm. Approximation results of this type can be found in Kappel and Salamon[38] and Ito and Morris[35] and specific examples of applications of such an approach can be found in Banks and Burns[4] and in Banks et al.[5]. The second possibility is to immediately approximate the infinite dimensional model by a finite dimensional one and then proceed with techniques developed for finite dimensional systems. The brute force approach is here to use an approximation scheme that is known to converge in an appropriate sense and base the controller design on an approximation of high order, but this approach may be problematic numerically for a number of reasons, specifically problem size. A more satisfactory approach is to design a control law that is robust against a perturbation containing the approximation error, which allows an á priori statement about robust stability, see Glover[26] and Curtain and Glover[15]. An application of this method can be found in Bontsema and Curtain[10], where á priori guaranteed robustness against the approximation error was obtained using an approximation of a moderately high order. This idea is used also in the present thesis. For a more thorough discussion of different approaches the reader is referred to Curtain[14].

When constructing a finite dimensional controller, different types of partial differential equations (PDE) must be treated by different types of approximations. Useful characteristics are here whether or not the solution to the PDE is guaranteed to be smooth and whether or not the model has an eigenfunction decomposition. A characteristic situation appears if the model is a heat equation, in which case the solution has a significant degree of smoothness, see Curtain and Zwart[18] for some examples. A case where eigenfunction decomposition seems to be standard practice is in the modelling and control of a flexible robot arm, see Zakawa et al.[56]. Contrary to these examples, we are in chapter 2 of this thesis dealing with a model where the solution to the PDE is not necessarily smooth. Moreover, an eigenfunction decomposition is not possible. The approximation used in this thesis is chosen according to these observations.

The subject of *Chapter 2* is a case study dealing with the control of a tunnel pasteurizer. The controller design is based on a distributed parameter model, which is approximated by a finite dimensional system. A controller that yields robust tracking performance in the presence of structured perturbations is constructed using a one-degree-of-freedom design based on a sequence of scaled H_∞ standard problems, followed by controller order reduction.

Chapter 3 contains a number of details that were omitted in chapter 2 for the sake of simple exposition. These details include matters as well-posedness and approximations as well as the description of an ad-hoc method which was introduced in order to deal with the high number of structured perturbations of

the system.

Chapter 4 takes as starting point the formulae for a two-degrees-of-freedom H_∞ control law obtained in Shaked and de Souza[57]. The main difference is that in [57] the tracking problem was solved with a finite time horizon and for finite dimensional systems. As a new development we give an infinite time horizon formulation where the signal spaces are based on the class of almost periodic functions. We consider infinite dimensional systems with bounded input and output operators, and give formulae for a so-called loop-shifting procedure, thus extending the formulae to a more general class of systems.

In *chapter 5* the method described in chapter 4 is further developed to meet the presence of structured uncertainties, and formulae for controller order reduction are given.

Chapter 2

Controller Design for a Pasteurization Plant

2.1 Introduction

A tunnel pasteurizer works by slowly moving bottled or canned food products on a conveyor belt through a tunnel, where the products are sprinkled with water from tanks placed above the tunnel. After passing the food products, the water is collected in tanks placed under the conveyor belt, re-heated by heat exchangers if necessary, and then poured into one of the tanks above the tunnel. The tunnel is divided into a number of zones, each of which is furnished with an upper and a lower tank.

We shall in this chapter be concerned with the control of a pasteurization process, and the example to be dealt with is bottled beer. While passing the zones of the tunnel, the beer is first heated above a certain pasteurization threshold temperature, and at the end of the tunnel the beer is cooled down. The objective is to obtain an adequate temperature profile (in time) in each bottle of beer during the pasteurization process. The degree of pasteurization of the beer should naturally be sufficiently high so that it is effective, but on the other hand an excessive degree of pasteurization will deteriorate the taste of the beer. However, it is not immediately a tractable problem to control the history of temperature of each bottle, so instead we content ourselves with controlling the temperature profile of beer along the conveyor belt.

The problem that we shall be concerned with in this chapter is to find a feed-back controller that ensures robust performance in the situation where pasteurization is steadily in progress. The control law is to be based on (filtered) measurements of the temperature of water that is collected after being sprinkled on the bottles in the tunnel. One particular feature of this problem is thus that the variable that we wish to control, namely the temperature profile of beer inside the bottles, is not the same as the measured variable, namely the temperatures

in the tanks beneath the tunnel. The role of actuators is played by a number of heat exchangers.

Tunnel pasteurizers of the type considered in the present work are currently being used in breweries. The control strategy is commonly based on PI controllers. The objective of our work is to suggest an alternative to such decentralized controller designs. As a motivation for this we will demonstrate that, according to our model, the system dynamics of the different zones are highly coupled. As the result of modeling work carried out by several people, e.g. Rudolph and Weiss[54], Heilbuth and Mortensen[32], Jannerup[37], we are able to base the design on a model that has been developed with a controller design in mind. This is important since it is a prerequisite for our approach to the controller design that a reasonably precise, and yet relatively simple, model is available. The model that we use was essentially formulated in Jannerup[37].

We have chosen to base our controller design on modern techniques known as the H_∞ method, see Green and Limebeer[30] and Zhou et al.[63] for background material. Our motivation for this is that uncertainties like small modeling errors and unknown disturbance signals can be taken explicitely into account in the design process. The H_∞ method is basically a worst case design. This is good if the worst case scenario considered in the design is relevant for the physical plant and the objective of the controller, but less appealing if the worst case has only little to do with reality. Therefore, one must make sure to incorporate into the design as much information as possible about the uncertainties. The nature of each uncertainty can be described by the use of frequency weights. Also important is the uncertainty structure that determines, what part of the plant is affected by a given uncertainty. The way we seek to take into account the uncertainty structure is to perform scaling of the input and output variables. Scaling of the inputs and outputs is usually recommended when working with multiple-input multiple-output systems. In H_∞ design with structured uncertainties it is a systematic method to improve the design, and the scaling parameters are determined using an optimization algorithm.

We will consider the control problem from an infinite dimensional systems point of view although the actual controller synthesis algorithm to be used is purely finite dimensional. The basic assumption is thus that the most accurate model that we have is an infinite dimensional one. One of the elements of the H_∞ method is a test for robust performance, which we carry out using the transfer function of the infinite dimensional system.

2.2 The Model

We will in this section give a short description of the model. For a more detailed derivation of the model the interested reader can consult Jannerup[37] and Heilbuth and Mortensen[32].

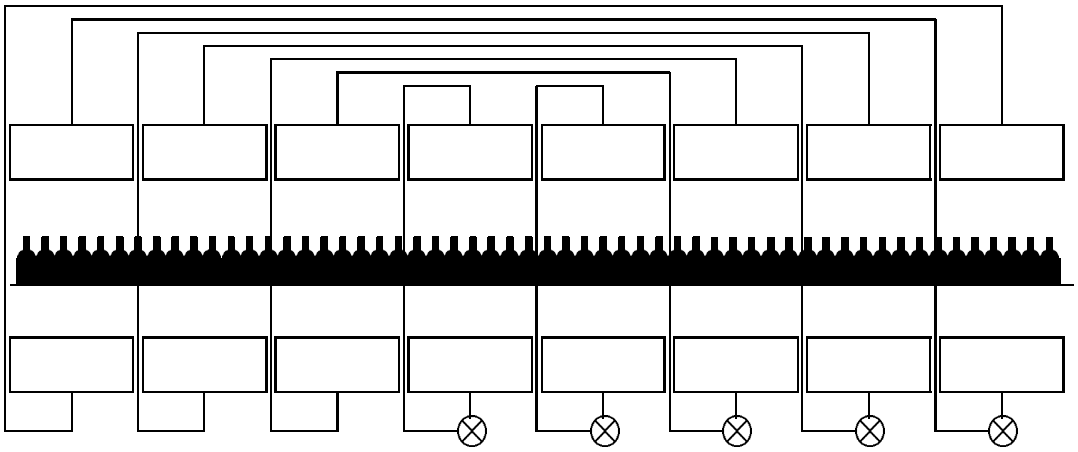

Figure 2.1: A tunnel pasteurizer with upper tanks, lower tanks, heat exchangers (⊗).

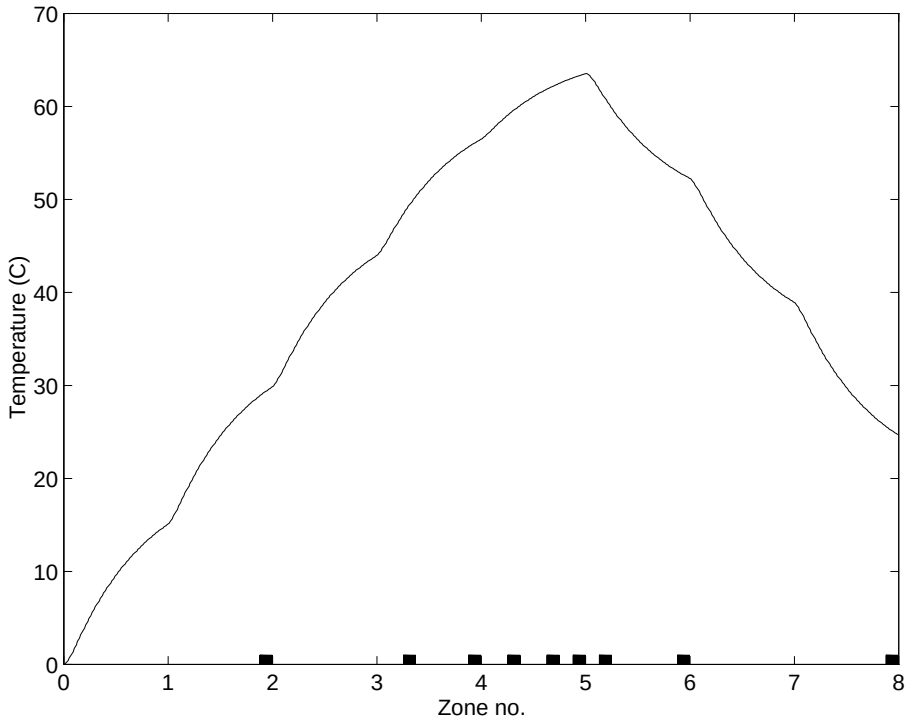

Figure 2.2: Steady state profile of beer along the tunnel. Intervals over which the beer temperature is controlled are marked (■)

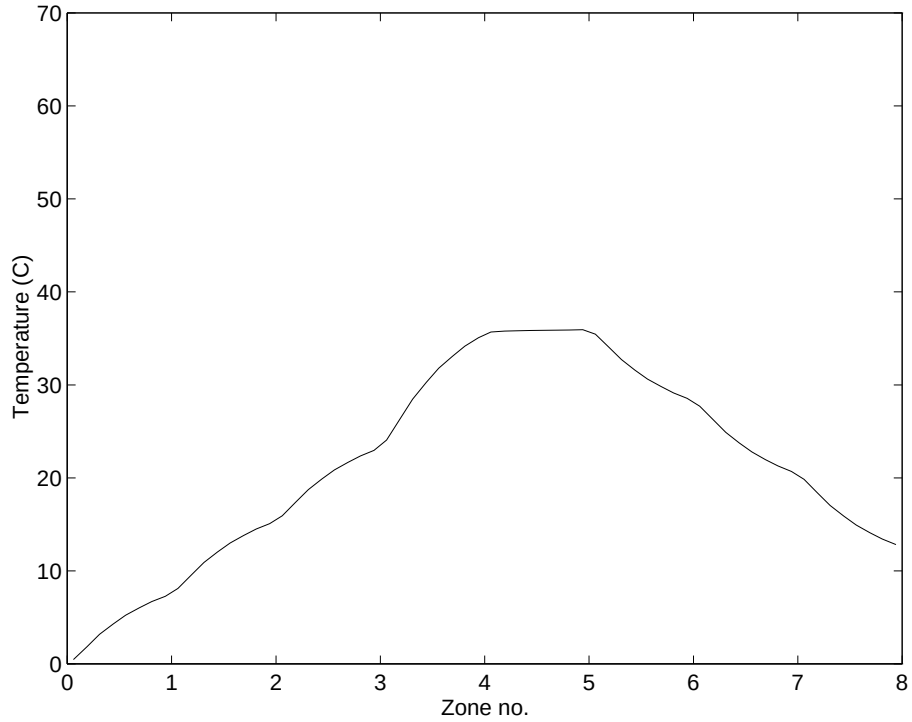

Figure 2.3: Steady state profile of beer along the tunnel when only the 4th heat exchanger is active (open loop control).

In the tunnel a conveyor belt carries each bottle through eight zones. The first three zones are meant for heating the bottles to a temperature that is still below a certain pasteurization threshold. The zones 4-5 are called pasteurization zones. Here heating is continued so that the pasteurization threshold is crossed and the pasteurization takes place mainly in these two zones. The zones 6-8 are cooling zones where the bottles are sprinkled with water of relatively low temperature. The water collected in the tank beneath zone 4 is reheated and then led into the upper tank of zone 4. The same happens in zone 5. The other zones are coupled such that, for example, the water collected beneath zone 3 is led directly to the upper tank of zone 6 as cooling water, while the water from the lower tank of zone 6 is reheated and then led to the tank above zone 3. This structure of water supply is shown in figure 2.1. With this structure, a typical temperature profile of the beer inside the bottles will be as shown in figure 2.2, obtained by simulations of the system, controlled by a feedback controller based on measurements of temperatures in the lower tanks.

The effect that the coupling of zones has on the overall behavior of the plant is demonstrated in figure 2.3, where it is shown that the supply of heat through a single heat exchanger affects the steady state profile throughout the tunnel.

The problem of modeling the entire plant is thus essentially given through the modeling of a single zone. The dynamics related to a typical zone are decomposed into four blocks. These are the inside of the tunnel, the collection of water below

the tunnel with a time delay and the heat exchanger. The collection of water in the upper tank constitutes the final, fourth block. Here a time delay is caused by the transport of water from the heat exchanger to the upper tank. After describing each component for the ith zone, we will conclude with an overview of the whole system.

When considering the ith zone, we denote by a superscript i the variables and parameters specifically related to that zone. Temperatures will, as a rule, be denoted by τ. Time as an independent variable is denoted by t, while T is used when time appears as a model parameter.

2.2.1 The Tunnel of the Pasteurizer.

The effects included in the model of the tunnel are the transport of bottles and the heat transfer between beer, bottles, and the water sprinkled onto the bottles. We assume that the temperatures of glass and beer in the tunnel can each be described by a temperature profile given lengthwise along the conveyor belt. We refer to these temperatures as $\tau_g(t,x)$ and $\tau_b(t,x)$, respectively, where x is the spatial variable along the conveyor belt. It is assumed that the density of bottles on the conveyor belt and the flux of sprinkled water are both constant throughout the tunnel. Also the speed of the belt, v, is assumed constant. The temperature of sprinkled water is assumed to be constant over each zone, but varying in time.

If we could neglect the transport of the conveyor belt, we could model the heat transfer between beer, bottles and sprinkled water as being proportional to the difference in temperature. For example, if we considered one medium with the well defined temperature profile $\tilde{\tau}_1(t,\cdot)$, being in contact with another medium with temperature $\tilde{\tau}_2(t,\cdot)$, then we would take a model of the type

$$\frac{\partial \tilde{\tau}_1}{\partial t}(t,x) = c(\tilde{\tau}_2(t,x) - \tilde{\tau}_1(t,x)).$$

Now, taking into account the water of temperature τ_5^i being sprinkled onto the bottles, and the transport of the conveyor belt, energy flow considerations, etc., (see Jannerup[37]) lead to the transport equation

$$\frac{\partial \tau_g}{\partial t} = -v\frac{\partial \tau_g}{\partial x} - (c_1+c_2)\tau_g + c_2\tau_b + c_1\tau_5^i \tag{2.1}$$

$$\frac{\partial \tau_b}{\partial t} = -v\frac{\partial \tau_b}{\partial t} + c_3\tau_g - c_3\tau_b \qquad , \ t \in [0,\infty), \ x \in (x_{i-1}, x_i) \tag{2.2}$$

where (x_{i-1}, x_i) is the interval of the ith zone. The constants c_1, c_2, c_3 depend on many different factors, for example the material (glass, water, beer), the flux of sprinkled water, and the speed of the conveyor belt.

For the first zone we impose zero boundary condition at the left side. This is based on the essential assumption that the temperature at the entrance of

the tunnel is known and constant, so that the zero boundary condition can be obtained by a standard substitution. For the zones 2-8 we simply impose that the temperature at the left end of the ith zone is equal to the temperature at the right end of the $(i-1)$st zone.

Since we are interested in measuring and controlling temperatures, the main concern is whether the energy flow inside the tunnel is modelled correcly. Therefore, the modeling errors that we consider will be the error in energy flow from the tanks above the tunnel to, firstly, the beer in the bottles, and, secondly, to the tanks placed beneath the tunnel.

2.2.2 The Lower Tanks

While passing the tunnel, the sprinkled water exchanges heat with the bottles. Afterwards it is collected in tanks under the conveyor belt. Denoting the temperature in the ith lower tank by τ_2^i, the temperature in the ith upper tank by τ_5^i, and the temperature profile of glass along the belt by $\tau_g(\cdot)$, the dynamics of this tank is described by the model

$$\frac{d\tau_2^i}{dt}(t) = -a_3^i\tau_2^i(t) + a_3^i\left(a_4^i(x_i - x_{i-1})\tau_5^i(t - T_E^i) + a_5^i\int_{x_{i-1}}^{x_i}\tau_g(t - T_E^i, x)dx\right), \tag{2.3}$$

where a_3^i, a_4^i and a_5^i are constants. The delay T_E^i models the time that it takes for the water to fall from the bottles into the lower tanks. We are assuming that there is no loss of energy to the surroundings, so from energy flow considerations we have the relation

$$(a_4^i + a_5^i)(x_i - x_{i-1}) = 1. \tag{2.4}$$

2.2.3 The Heat Exchangers

On the physical plant, the control signal is the electric current in a valve on the heat exchanger. Here we are assuming that there is a static relation between this current and the power being released inside the heat exchanger. In our design we can therefore simplify matters. We thus consider the power u^i that is released inside the heat exchanger as the control signal.

Let η denote the steam temperature in the heat exchangers, and let τ_4^i denote the temperature of the water immediately after passing the ith heat exchanger, and let τ_2^j be the temperature of the water entering the ith heat exchanger, i.e. the temperature of the jth lower tank. As already indicated in the notation above we let the jth lower tank be connected to the ith heat exchanger. From Jannerup[37] we then have the following dynamic relation

$$\frac{\beta}{\eta - \tau_2^j}\frac{d(\tau_4^i - \tau_2^j)}{dt} = -(\tau_4^i - \tau_2^j) + ku^i \tag{2.5}$$

where β and k are positive real numbers. This nonlinear model is based on empirical observations and is obtained by parameter fitting of a first order model, with a constant stationary gain k, and with a time constant of the form

$$\frac{\beta}{\eta - \tau_2^j}. \tag{2.6}$$

For the controller synthesis we need a linear, nominal model. We therefore assume that the value of τ_2^j that appears in the denominator of (2.6) has the constant nominal value $\hat{\tau}_2^j$. Furthermore, we eliminate the variable τ_4^i by the substitution

$$\tau_3^i = \tau_4^i - \tau_2^j \tag{2.7}$$

and arrive at the linear differential equation

$$\frac{d\tau_3^i}{dt} = -a_1^i \tau_3^i + b^i u^i, \tag{2.8}$$

where a_1^i and b^i are positive constants. Notice that we have here considered one of those zones that are actually equipped with a heat exchanger, i.e. $i \in \{1, ..., 5\}$. In the other cases, equation (2.7) would still be relevant but with $\tau_3^i = 0$.

We consider the linearization to be the main source of modeling error for the heat exchanger. In view of this we must make sure that the controller works well even if the temperature in the jth lower tank deviates from the nominal value $\hat{\tau}_2^j$.

2.2.4 The Pipes and the Upper Tanks

After passing the heat exchangers the water is led through pipes which gives rise to a time delay, and into the upper tanks which is modelled by a first order system. These two effects are here modelled in one single equation describing how the temperature τ_5^i of water in the upper tank is affected by the temperature rise τ_3^i in the heat exchanger and the temperature τ_2^j in the lower tank.

$$\frac{d\tau_5^i}{dt}(t) = -a_2^i \tau_5^i(t) + a_2^i(\tau_3^i(t - T_D^i) + \tau_2^j(t - T_D^i)). \tag{2.9}$$

T_D^i is the delay of the ith pipe. The parameter a_2 is a constant specific to the ith upper tank, that depends on the constant flux of water through the pipe.

Examples of modeling errors are unprecise knowledge of the delay, and that energy loss to the surroundings is neglected.

2.2.5 Overview of the Model

We will now describe the overall model considering all of the zones and every component at the same time. In order to do this we need a slightly more compact

notation. Define the diagonal matrices $a_1 = \mathrm{diag}\{a_1^1, ..., a_1^5\}$, $a_2 = \mathrm{diag}\{a_2^1, ..., a_2^8\}$, etc., and $b = \mathrm{diag}\{b^1, ..., b^5\}$. To handle the permutation that is introduced by the coupling of the 8th, 7th and 6th lower tanks to the 1st, 2nd and 3rd heat exchangers, respectively, we introduce the permutation matrix a_6. Also, to handle the situation that there are only 5 heat exchangers we introduce a_7, defined as follows,

$$a_6 = \begin{bmatrix} & & & & & 0 & 0 & 1 \\ & & & & & 0 & 1 & 0 \\ & & & & & 1 & 0 & 0 \\ & & & 1 & 0 & & & \\ & & & 0 & 1 & & & \\ 0 & 0 & 1 & & & & & \\ 0 & 1 & 0 & & & & & \\ 1 & 0 & 0 & & & & & \end{bmatrix}, \quad a_7 = \begin{bmatrix} 1 & & & & & \\ & 1 & & & & \\ & & 1 & & & \\ & & & 1 & & \\ & & & & 1 & \\ 0 & 0 & 0 & 0 & 0 & \\ 0 & 0 & 0 & 0 & 0 & \\ 0 & 0 & 0 & 0 & 0 & \end{bmatrix}. \tag{2.10}$$

We also introduce the functions χ^i, defined by

$$\chi^i(x) = \begin{cases} 1 & \text{for } x \in (x_{i-1}, x_i) \\ 0 & \text{elsewhere} \end{cases}, \quad i \in \{1..8\}, \tag{2.11}$$

and the variables

$$\tau_1(t,x) = \begin{bmatrix} \tau_g(t,x) \\ \tau_b(t,x) \end{bmatrix}, \tag{2.12}$$

$\tau_2 = [\tau_2^1, ..., \tau_2^8]'$, etc. The equations of the overall linearized model now read

$$\frac{\partial \tau_1}{\partial t}(t,x) = -v\frac{\partial \tau_1}{\partial x}(t,x) + \begin{bmatrix} -c_1 - c_2 & c_2 \\ c_3 & -c_3 \end{bmatrix} \tau_1(t,x) + c_1 \sum_{i=1}^{8} \begin{bmatrix} \chi^i(x) \\ 0 \end{bmatrix} \tau_5^i(t), \quad x \in (x_0, x_8) \tag{2.13}$$

$$\tau_1(t, x_0) = 0 \tag{2.14}$$

$$\frac{d\tau_2^i}{dt}(t) = -a_3^i \tau_2^i + a_3^i a_4^i (x_i - x_{i-1}) \tau_5^i(t - T_E^i) + a_3^i a_5^i \int_{x_{i-1}}^{x_i} \begin{bmatrix} 1 & 0 \end{bmatrix} \tau_1(t - T_E^i, x) dx, \qquad i = 1..8 \tag{2.15}$$

$$\frac{d\tau_3}{dt} = -a_1 \tau_3 + bu \tag{2.16}$$

$$\frac{d\tau_5}{dt}(t) = -a_2 \tau_5(t) + a_2(a_7 \tau_3(t - T_D) + a_6 \tau_2(t - T_D)), \tag{2.17}$$

where, with an abuse of notation, $\tau_3(t - T_D)$ means $\tau_3^i(t - T_D^i)$ for every i.

2.3 System Formulation and Model Reduction

In order to use the H_∞ method, we must write the model as a linear system of the form

$$\begin{aligned} \frac{d\psi}{dt} &= A\psi + B_1 w + B_2 u && (2.18)\\ z &= C_1\psi + D_{11} w + D_{12} u && (2.19)\\ y &= C_2\psi + D_{21} w + D_{22} u. && (2.20) \end{aligned}$$

Here, $\psi(t)$ is the state, $u(t)$ is the control input, $w(t)$ is an unknown disturbance input, $z(t)$ is the to-be-controlled output, and $y(t)$ is the measured output. The meaning of u and y is evident, while the meaning of w and z is problem dependent. We let one component of w represent (indirectly) the reference signal in a tracking problem, and the tracking error is represented by a number of components of z. The remaining components of w and z are introduced to account for the modeling errors. All signals are vector valued, in finite or infinite dimensional spaces. A, B_1, etc., will be matrices, or, in the latter case, linear operators. The linear model made up by the equations (2.13)-(2.17) can be written in this formulation, and the system will be infinite dimensional. We will use this system to test whether a controller candidate satisfies our specifications for performance and robustness.

For the actual synthesis we need a finite dimensional system. This system is obtained by approximation of the infinite dimensional system. The aim of this approximation is not to approximate the operators, A, B_1, etc., but rather to approximate the system as an input-to-output map. Having obtained an appropriate finite dimensional system, a number of modern algorithms are available for the controller synthesis. The algorithms that we have chosen have one feature in common, namely that each step in the synthesis is reformulated as the problem of making the H_∞ norm of a particular system small. In line with this, the H_∞ norm also plays a role in the model reduction.

Let us now turn to the actual system formulation. Each of the equations (2.13)-(2.17) gives rise to a subsystem. The overall system of the form (2.18)-(2.20) is to be formed as an interconnection of these subsystems, which, as part of the design process, is enhanced with frequency weight systems. In the remainder of this section we will focus mainly on the subsystem representing the dynamics of the tunnel.

The model of the dynamics inside the tunnel, given by the transport equation (2.13), can be rewritten as a system where the system operator is

$$A_1 = \begin{bmatrix} -v\frac{\partial}{\partial x} - c_1 - c_2 & c_2 \\ c_3 & -v\frac{\partial}{\partial x} - c_3 \end{bmatrix}, \qquad (2.21)$$

defined on its domain

$$D(A_1) = \{\phi \in (L^2(x_0, x_m))^2 \text{ such that } \frac{\partial \phi}{\partial x} \in (L^2(x_0, x_m))^2,$$

ϕ is absolutely continuous , and $\phi(x_0) = 0\}$.

This operator has the following properties (see chapter 3). A_1 generates a strongly continuous semigroup, and thereby satisfies a fundamental well posedness assumption of our approach. Furthermore, this semigroup is exponentially stable and the spectrum of A_1 is empty. The latter information is useful in the sense that it warns us against searching for an eigenfunction decomposition of the system.

The inputs of the tunnel is the vector of temperatures, τ_5, of water in the upper tanks. The outputs of the tunnel fall in two groups. Firstly, we take for each zone the average temperature of water falling into the lower tanks. This temperature is given by

$$a_4^i(x_i - x_{i-1})\tau_5^i + a_5^i \int_{x_{i-1}}^{x_i} \left[\begin{array}{cc} 1 & 0 \end{array}\right] \tau_1(x)dx, \quad i = 1 \ldots 8, \tag{2.22}$$

cf. equation (2.15). Secondly, we take a number of average values of the beer temperature profile. We have chosen nine intervals, distributed as shown in figure 2.2. Writing the jth of these intervals as $[\hat{x}_j, \hat{x}_j + \xi_j]$, the corresponding component $\hat{z}^j$ of the to-be-controlled output can be written

$$\hat{z}^j = \frac{1}{\xi} \int_{\hat{x}_j}^{\hat{x}_j + \xi_j} \left[\begin{array}{cc} 0 & 1 \end{array}\right] \tau_1(x)dx, \quad j = 1 \ldots 9. \tag{2.23}$$

The transfer functions related to the tunnel can be calculated explicitely, see chapter 2. Let us first consider the transfer matrix $\Theta(s)$ from the temperatures $\tau_5(s)$ in the upper tanks to the average temperatures of water falling into the lower tanks. Introduce the notation

$$\begin{aligned} c_4 &= \sqrt{(c_1 + c_2 + c_3)^2 - 4c_1c_3} && (2.24)\\ \zeta^s(x) &= e^{-(c_1+c_2+c_3-c_4+2s)x/2v} && (2.25)\\ \eta^s(x) &= e^{-(c_1+c_2+c_3+c_4+2s)x/2v}. && (2.26) \end{aligned}$$

We consider two special cases: The case where the lower tank is placed after the upper tank, and the case where the upper and lower tanks in question belong to the same zone. The third possibility, where the lower tank is placed before the upper tank is trivial, and the corresponding entry is zero. For $i < j$:

$$\begin{aligned} \Theta_{ji}(s) &= \frac{2a_5^j v c_1(-c_1 - c_2 + c_3 + c_4)}{(c_1 + c_2 + c_3 - c_4 + 2s)^2 c_4} && (2.27)\\ &\quad \cdot (\zeta^s(x_{j-1} - x_i) + \zeta^s(x_j - x_{i-1}) - \zeta^s(x_{j-1} - x_{i-1}) - \zeta^s(x_j - x_i))\\ &\quad + \frac{2a_5^j v c_1(c_1 + c_2 - c_3 + c_4)}{(c_1 + c_2 + c_3 + c_4 + 2s)^2 c_4}\\ &\quad \cdot (\eta^s(x_{j-1} - x_i) + \eta^s(x_j - x_{i-1}) - \eta^s(x_{j-1} - x_{i-1}) - \eta^s(x_j - x_i)). \end{aligned}$$

For $i = j$:

$$\begin{aligned}\Theta_{ii}(s) &= a_5^i \frac{c_1(-c_1-c_2+c_3+c_4)}{(c_1+c_2+c_3-c_4+2s)c_4}\left(x_i - x_{i-1} - \frac{2v(1-\zeta^s(x_i-x_{i-1}))}{c_1+c_2+c_3-c_4+2s}\right)\\ &+ a_5^i \frac{c_1(c_1+c_2-c_3+c_4)}{(c_1+c_2+c_3+c_4+2s)c_4}\left(x_i - x_{i-1} - \frac{2v(1-\eta^s(x_i-x_{i-1}))}{c_1+c_2+c_3+c_4+2s}\right)\\ &+ a_4^i(x_i - x_{i-1}). \end{aligned} \tag{2.28}$$

Next we consider the transfer matrix $\Pi(s)$ from the temperatures in the upper tanks to the chosen averages of the beer temperature profile. For simplicity, these averages are taken over intervals that are contained entirely in one of the zones. We consider again two special cases: first the case where the interval $[x_{i-1}, x_i[$ of the ith upper tank does not intersect with the interval $[\hat{x}_j, \hat{x}_j + \xi_j[$ of the jth component of the controlled variable.

$$\begin{aligned}\Pi_{ji}(s) &= \frac{4c_3c_1v}{c_4(c_1+c_2+c_3-c_4+2s)^2}\\ &\cdot(\zeta^s(\hat{x}_j - x_i) + \zeta^s(\hat{x}_j + \xi_j - x_{i-1}) - \zeta^s(\hat{x}_j - x_{i-1}) - \zeta^s(\hat{x}_j + \xi_j - x_i))\\ &- \frac{4c_3c_1v}{c_4(c_1+c_2+c_3+c_4+2s)^2}\\ &\cdot(\eta^s(\hat{x}_j - x_i) + \eta^s(\hat{x}_j + \xi_j - x_{i-1}) - \eta^s(\hat{x}_j - x_{i-1}) - \eta^s(\hat{x}_j + \xi_j - x_i)). \end{aligned} \tag{2.29}$$

In the second case where $[\hat{x}_j, \hat{x}_j + \xi_j[\subset [x_{i-1}, x_i[$, we find

$$\begin{aligned}\Pi_{ji}(s) &= \frac{2c_3c_1}{c_4(c_1+c_2+c_3-c_4+2s)}\\ &\cdot\left(\xi_j - \frac{2v(\zeta^s(\hat{x}_j - x_{i-1}) - \zeta^s(\hat{x}_j + \xi_j - x_{i-1}))}{c_1+c_2+c_3-c_4+2s}\right)\\ &- \frac{2c_3c_1}{c_4(c_1+c_2+c_3+c_4+2s)}\\ &\cdot\left(\xi_j - \frac{2v(\eta^s(\hat{x}_j - x_{i-1}) - \eta^s(\hat{x}_j + \xi_j - x_{i-1}))}{c_1+c_2+c_3+c_4+2s}\right). \end{aligned} \tag{2.30}$$

Notice that, while $\Theta(s)$ is lower triangular, $\Pi(s)$ is lower block triangular in such a way that when the interval $[\hat{x}_j, \hat{x}_j + \xi_j[$ is placed before the interval of the zone $[x_{i-1}, x_i[$ then the corresponding entry in $\Pi(s)$ is zero. Notice also that, the singularities at $s = -c_1 - c_2 - c_3 \pm c_4$ are not poles, and that Θ and Π can be extended to be analytic on $\mathbb{C}$ by taking the limit in these points.

We will now turn to the reduction of the tunnel dynamics to a finite dimensional system. The transfer matrices $\Theta(s)$ and $\Pi(s)$ are approximated by stable real-rational transfer matrices $\Theta^N(s)$ and $\Pi^N(s)$, such that the maximum approximation error across frequencies

$$\left\| \begin{bmatrix} \Theta(s) \\ \Pi(s) \end{bmatrix} - \begin{bmatrix} \Theta^N(s) \\ \Pi^N(s) \end{bmatrix} \right\|_\infty \tag{2.31}$$

is small. Furthermore, the error must be particularly small at low frequencies, since this frequency area is critical for good tracking performance.

The construction of Θ^N and Π^N is carried out in two steps. In the first step we construct a preliminary, finite dimensional system. Each interval $[x_{i-1}, x_i]$ is divided into a number subintervals of equal length, h, and over each subinterval the temperature profile $\tau_1(t,\cdot)$ is approximated by its average value. Consider now the nth subinterval, $[(n-1)h, nh]$, and assume that this interval is contained in $[x_{i-1}, x_i]$ where, for simplicity, we let $x_0 = 0$. We introduce the notation

$$\Sigma = \begin{bmatrix} -c_1 - c_2 & c_2 \\ c_3 & -c_3 \end{bmatrix} \tag{2.32}$$

$$M = e^{\frac{h}{v}\Sigma} + \frac{v}{h}\Sigma^{-1}\left(I - e^{\frac{h}{v}\Sigma}\right) \tag{2.33}$$

$$\hat{\tau}_{1,n}(s) = \frac{1}{h}\int_{(n-1)h}^{nh} \hat{\tau}_1(s,x)dx. \tag{2.34}$$

After taking the Laplace transform and integrating, the transport equation (2.13) leads to

$$\hat{\tau}_{1,n}(s) = (sI - \Sigma)^{-1}\left(-\frac{v}{h}\hat{\tau}_1(s,nh) + \frac{v}{h}\hat{\tau}_1(s,(n-1)h) + \begin{bmatrix} c_1 \\ 0 \end{bmatrix}\hat{\tau}_5^i(s)\right). \tag{2.35}$$

We use the approximation

$$\hat{\tau}_1(s,nh) \approx \hat{\tau}_{1,n}(s) + M\left(\hat{\tau}_1(s,(n-1)h) + \Sigma^{-1}\begin{bmatrix} c_1 \\ 0 \end{bmatrix}\hat{\tau}_5^i(s)\right). \tag{2.36}$$

For the dynamics of the average value $\hat{\tau}_{1,n}(s)$, when this average is taken over an interval contained in the ith zone, we thus obtain in the frequency domain

$$\left(sI - \Sigma + \frac{v}{h}I\right)\hat{\tau}_{1,n}(s) \approx \frac{v}{h}(I-M)\hat{\tau}_1(s,(n-1)h) + (I - \frac{v}{h}M\Sigma^{-1})\begin{bmatrix} c_1 \\ 0 \end{bmatrix}\hat{\tau}_5^i(s). \tag{2.37}$$

The approximating, finite dimensional system can now be constructed by subsequently applying the approximation (2.36). This approximation can be regarded as a modification of the well-known average approximation, which would be obtained by putting $M = 0$ in (2.36). The reason for using (2.36) rather than the usual average approximation is that the resulting rational transfer matrix fits the transfer matrix $[\Theta(s)' \;\; \Pi(s)']'$ exactly in steady state ($s = 0$). With a discretization grid of 8 subdivisions per zone, we found that the approximation in H_∞ norm was satisfactory. This was evaluated by performing a μ-test on the linear, infinite dimensional plant with the controller applied, see section 2.4.5.

In the second step the finite dimensional system is further reduced using optimal Hankel norm approximation, see appendix A.2 for definition, and see Glover[25] or Green and Limebeer[30] for background material. The idea with

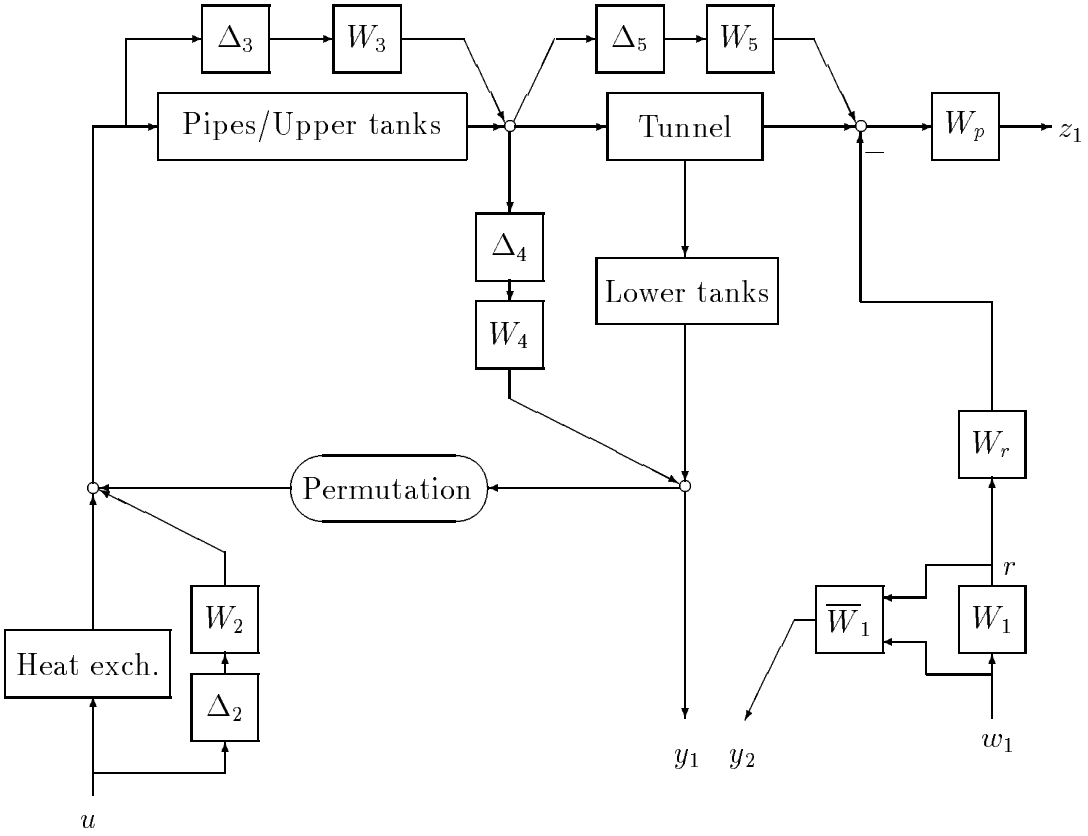

Figure 2.4: Structure of robust performance problem. With nominal subsystems, perturbations, weighting systems, reference signal r and tracking error z_1.

this step is to obtain a system of lower order but with roughly the same behaviour when considered as an input-output map. Hankel norm approximation is considered as one of the most efficient methods for model reduction of finite dimensional linear systems.

The remaining subsystems given by the equations (2.15), (2.16), (2.17), are more straightforward to handle. The delays in (2.15) and (2.17) are replaced by the first order Padé approximation

$$e^{-sT} \approx \frac{2 - sT}{2 + sT} \tag{2.38}$$

in order to obtain good approximation for low frequencies.

2.4 Controller Synthesis

The control problem to be solved is a tracking problem. We want the beer temperature profile along the belt to follow a pre-specified profile, with a temperature tolerance of 1 °C, even though we do not have a perfect model of the plant. The $\mathcal{H}_\infty$ method is appropriate for such a controller design because here the tracking problem and the robustness requirement can be formulated in the standard framework. In the design process one must specify how large uncertainties one will allow while demanding that the system still shows satisfactory performance. The synthesis algorithm will then give one of two answers: It will either result in a controller that is prepared for the worst possible uncertainty of the specified size and structure, or, as the second possibility, the algorithm will produce the warning that the resulting controller is not guaranteed to meet the given requirements.

In figure 2.4 it is shown how we describe the physical plant as a nominal system subject to model uncertainties, represented by perturbations $\{\Delta_i\}$ and frequency weights $\{W_i\}$. The signals flowing from one subsystem to the other are each a vector of temperatures, except for the control input u, which is the power released in the heat exchangers. The disturbance signal w_1 determines the tracking trajectory in such a way that the trajectory to be tracked is given by $W_r r$.

The controller synthesis may be split into four parts:

1. Specify the uncertainty structure.
2. Specify magnitude and spectral content of modeling errors.
3. Specify required performance.
4. Find the best possible H_∞ controller for the enhanced system resulting from items 1-3.

Once the uncertainty structure is chosen, we use this structure throughout the design. Items 2 and 3 may result in conflicting desing objectives, as there is a trade-off between allowing large modeling errors and requiring high performance. If the H_∞ controller of item 4 is not satisfactory, we must adjust the choices made in items 2 and 3.

2.4.1 The Uncertainty Structure

The first decision to be made in an H_∞ design is to specify the uncertainty structure. We have chosen to use a relatively high number of uncertainty components, as shown in figure 2.4. The perturbation Δ_2 has five components, while Δ_3, Δ_4, Δ_5 have each eight components, which makes 29 independent perturbations.

The high number of perturbations turned out to be critical for the synthesis algorithms. In order to justify our choice of uncertainty structure we list the following key observations.

1. The measured output y and the temperature profile that is supposed to follow a given trajectory do not coincide. In a steady state situation there is however some correlation between the two signals, and the major source for this correlation is that they both depend fairly directly on the temperatures τ_5 in the upper tanks. This information is incorporated into the design by placing the uncertainties $W_4\Delta_4$ and $W_5\Delta_5$ as shown in figure 2.4.

2. The plant has an internal feedback since the water is led from the lower tanks and back into the upper tanks. This feedback has an enormous influence on the behaviour of the plant. The effect of model uncertainties is also influenced by this feedback, and it is desirable to specify the uncertainties in such a way that the frequency weights can be chosen without taking the influence from the feedback into account. The feedback induced by the cross coupling of zones causes the plant to have a significant integrating effect, and therefore the influence of this will be largest for low frequencies.

The clearest interpretation of the control problem as a worst case design is obtained when all of the uncertainties are model uncertainties rather than exogeneous disturbance signals. Partly for this reason, two natural uncertainties are omitted. Firstly, measurement noise is not included explicitely in our uncertainty formulation. However, we have made sure that the frequency weight W_4 does allow high frequency disturbance to affect the measured output y. This does not give an entirely satisfactory representation of measurement noise, so we therefore rely on the inherent conservatism in the H_∞ design to obtain robustness towards measurement noise. Another uncertainty not considered explicitely is that the temperature of entering bottles may vary in time. However, temperature differences will be largely reduced while the bottles are passing the first three zones. We have therefore chosen, not to complicate the design further by modeling this variation in temperature of entering bottles as an exogeneous disturbance signal but, instead, to assume that a reasonably large tracking bandwith will enable the controller to handle this uncertainty satisfactory.

2.4.2 Uncertainty Frequency Weights in the Synthesis

Each of the uncertainties in figure 2.4 has the form $W_i\Delta_i$, where Δ_i is a diagonal matrix of perturbation systems. The assumptions made on the perturbations are that each perturbation Δ_i is linear, stable and normalized so that the inequality

$$\|\Delta_i z\|_2 \leq \|z\|_2 \tag{2.39}$$

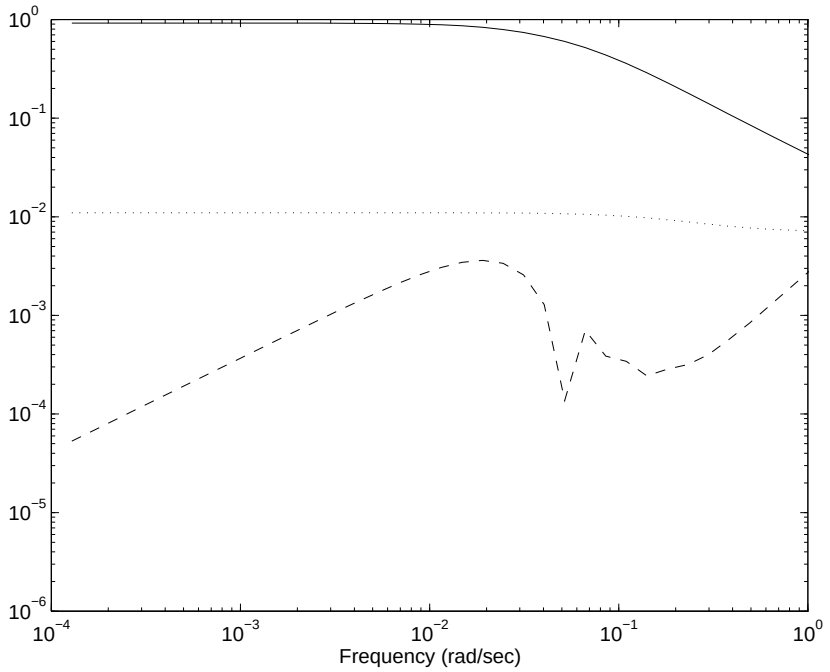

Figure 2.5: Transfer functions related to the ith upper tank and the ith lower tank: $(-)$ magnitude of $(s + a_3^i)^{-1} a_3^i e^{-sT_E^i} \Theta_{ii}(s)$, $(\cdot\cdot)$ frequency weight used in synthesis, $(- \; -)$ approximation error.

holds for every L^2 signal z of appropriate dimensions. Given that Δ_i is normalized, the frequency weight W_i must be chosen to shape the spectral content of the modeling errors such that $W_i \Delta_i$ gives an adequate representation of the set of uncertainties that the controller should be able to handle.

Concerning the frequency weights $W_2, \ldots, W_5$ we make the following general considerations. At low frequencies, the model is assumed to give a relatively good description of the plant, and therefore the frequency weights should have here a small magnitude. At high frequencies the model is poor, and most part of the signals can be considered as being due to unmodelled dynamics or noise. However, the modeling of heat transfer leads to a system where the dynamics are well damped, and this is true also for the unmodelled dynamics. From a modeling point of view it is therefore reasonable to let most of the weighting systems have low magnitude also at high frequencies. This means that most of the weighting systems naturally have their largest magnitude in between, in a middle frequency range.

It turned out that our procedure for taking the structure of the perturbations into account, see section 2.4.4, showed very little flexibility across frequencies. This ment that in the case of W_4 we ended up using roughly the same magnitude over the whole frequency range, see figures 2.5 and 2.6.

The perturbations Δ_4 and Δ_5 each have 8 independent components, one for

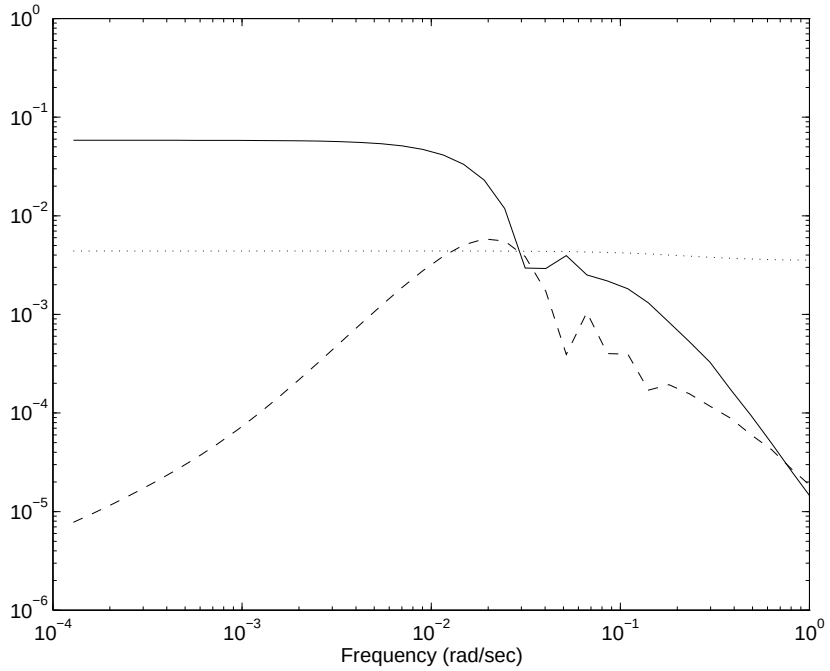

Figure 2.6: Transfer functions related to the $(i-1)$st upper tank and the ith lower tank: $(-)$ magnitude of $(s+a_3^i)^{-1}a_3^i e^{-sT_E^i}\Theta_{i,i-1}(s)$, $(\cdot\cdot)$ frequency weight used in synthesis, $(--)$ approximation error

each zone. The weighting matrix $W_4(s)$ is lower triangular and $W_5(s)$ is lower block triangular, conforming to the structure of the transfer matrices $\Theta(s)$ and $\Pi(s)$ respectively. In this way we let 16 independent perturbations account for all uncertainty related to the tunnel. In particular, we assume a certain correlation between uncertainties that are related to the same upper tank while affecting different components of the tracking error z_1.

The uncertainties $W_4\Delta_4$ and $W_5\Delta_5$ are very different in the way they affect the system. $W_5\Delta_5$ affects the tracking error, which implies a direct constraint on the obtainable performance. On the other hand, $W_5\Delta_5$ does not affect the dynamics of the nominal system and controller. $W_4\Delta_4$ is not related directly to performance, but the fact that it makes part of the internal loop of the plant poses another severe problem for the controller synthesis algorithm. With respect to the attainable γ-value of the full order H_∞ controller there was a trade-off between the magnitudes of W_4 and W_5. When it came to the reduced order controller, it was interesting to notice that this trade-off was changed significantly. With the reduced order controller it was much harder to deal with a large contribution from $W_4\Delta_4$. As a consequence, it was necessary to take controller order reduction into account when adjusting the frequency weights, thus complicating the iterative design procedure.

As shown in figure 2.5 and figure 2.6, we have chosen the frequency weight

W_4 such that the uncertainty $W_4\Delta_4$ almost contains the approximation error that arises when approximating the transport equation and the delay that models the time that it takes for the water to fall into the lower tanks. Ideally, the uncertainty $W_4\Delta_4$ should cover the whole approximation error. This idea was used in Bontsema and Curtain[10] in the control of flexible structures. However, in the present problem we consider the problem of robustness against approximation errors to be less critical than when controlling flexible structures, and we therefore take the point of view that almost covering the approximation error is sufficient. That this is indeed a sensible compromise is evaluated in the robust performance test in section 2.4.5. Based on the same attitude, the uncertainty $W_3\Delta_3$ did also not completely cover the approximation error.

The weight W_5 was chosen such that $W_5\Delta_5$ did clearly not include the approximation error. See section 3.2 for further remarks about the role of $W_5\Delta_5$. The weight W_2 was given a very small magnitude at low frequencies, where the assumption is that the steady state gain of the heat exchangers is well known (and well defined). A large magnitude was specified for higher frequencies in order to account for the error commited when linearizing the model of the heat exchangers. See appendix A.6 for the precise details of the frequency weights.

As a simple way of describing the allowed inaccuracy of the model we perturbed some of the parameters and compared the bode plot of the variation of the transfer functions. In figure 2.8 and figure 2.9 is shown the modeling error that would follow from uncertainty in certain parameters, compared to a frequency weight that is of larger magnitude than the one used in the synthesis. It is clear from those figures that the magnitude of perturbations considered in the synthesis accounts for only small variations in the plant parameters. However, due to the inherent conservatism in the design, it is á priori likely that the controller can handle larger variations in parameters. Another point worth bearing in mind is that part of the modeling error is due to unmodelled dynamics. For example, the density of bottles on the conveyor belt can vary in time, and this is not described by simply varying some of the parameters of the transfer functions.

2.4.3 Performance Specification

The desired temperature profile of the beer along the tunnel is represented by $W_r r$. We have chosen 9 intervals over each of which we wish to control the average temperature of beer. Therefore, W_r is a matrix of dimension 9×1. The desired performance level is specified through the static weight matrix W_p. When choosing W_p it is necessary to bear in mind that, the tracking error $z_1(t)$ is measured in the Euclidian norm and the desired H_∞ controller is one that makes the maximum amplification from any L^2 signal w_1 to the tracking error z_1 less than 1.

The reason for letting the tracking trajectory depend on an unknown disturbance the way we do is to make the problem fit into the $\mathcal{H}_\infty$ standard problem.

This procedure is widely used, and is suggested for example in Francis[22]. We are, however, using a different formulation of the tracking problem. This way of implementing the tracking trajectory enables us to focus on robust tracking in steady state, and on the frequency bandwidth of the tracking ability of the system. Once the controller is designed, the idea is to let y_2 be constant and equal to 1 under normal operation.

The weight $\overline{W_1}$ is static. The idea is that the reference signal $r = W_1 w_1$ should be known on-line by the controller, and it would therefore seem appropriate to simply let r be a component of the measured output y. Instead we put $y_2 = \overline{W_1}[r\ w_1]' = (1-\epsilon)r + \epsilon w_1$, where the regularization parameter $\epsilon > 0$ is introduced for technical reasons. This is necessary in order not to violate assumption $A2$ of the ARE solution of the H_∞ problem, see appendix A.1. It turned out that this regularization was even more critical when doing controller order reduction, which step was ruined when choosing ϵ smaller than approximately 0.05.

As cut-off frequency for the reference signal we chose $3 \cdot 10^{-4}$ rad/sec. Notice that we are demanding the whole vector of beer temperatures to follow a trajectory of this bandwidth. For this to be possible, the bandwidth of the controller must be much larger than $3 \cdot 10^{-4}$, which means that the cut-off frequency of the reference signal gives no precise á priori information on how fast the controller reacts, for example on step changes of the reference signal.

2.4.4 The H_∞ Synthesis Algorithm

We will in this section briefly describe the algorithm used for finding an H_∞ controller. The system shown in figure 2.4 can be written on the form (2.18)-(2.20). The perturbations $\Delta_2, ..., \Delta_5$ are removed, and each independent perturbation is replaced by a component of the disturbance input w and the to-be-controlled output z, as indicated in figure 2.7 We then define $w = [w_1', w_2', w_3', w_4', w_5']'$ and $z = [z_1', z_2', z_3', z_4', z_5']'$. With 29 independent perturbations and 9 components in the tracking error, we introduce the diagonal scaling matrices

$$\Lambda = \begin{bmatrix} \lambda_1 & & 0 \\ & \ddots & \\ 0 & & \lambda_{29} \end{bmatrix}, \quad D_l = \begin{bmatrix} I_9 & 0 \\ 0 & \Lambda \end{bmatrix}, \quad D_r = \begin{bmatrix} 1 & 0 \\ 0 & \Lambda \end{bmatrix}, \tag{2.40}$$

where all the diagonal entries of Λ are positive. Λ is to be determined as part of the design, but until then we let it be the identity matrix. We partition the scaled system as

$$\begin{bmatrix} z \\ y \end{bmatrix} = \begin{bmatrix} D_l G_{11} D_r^{-1} & D_l G_{12} \\ G_{21} D_r^{-1} & G_{22} \end{bmatrix} \begin{bmatrix} w \\ u \end{bmatrix}. \tag{2.41}$$

We also introduce the notation

$$\mathcal{F}(G, K) = G_{11} + G_{12}(I - KG_{22})^{-1} K G_{21}. \tag{2.42}$$

For our purpose, an H_∞ controller K for the scaled system is defined by the property that the closed loop system $\mathcal{F}(G,K)$ is exponentially stable and

$$\sup_{w\in L^2(0,\infty;W),w\neq 0} \frac{\|D_l\mathcal{F}(G,K)D_r^{-1}w\|_2}{\|w\|_2} < \gamma \tag{2.43}$$

for the pre-specified positive number γ where D_l and D_r are of the form (2.40).

Given that the perturbations Δ_i are normalized according to (2.39), and that W_r and W_p are chosen so that an acceptable tracking error is expressed by the inequality

$$\|z_1\|_2 \leq \|w_1\|_2 \tag{2.44}$$

for every L^2 signal W_1, then a satisfactory H_∞ controller is one that yields (2.43) with $\gamma \leq 1$, for some diagonal matrix Λ of scaling parameters. This characterization of a satisfactory H_∞ controller is closely related to the robust performance test that is the subject of section 2.4.5. Once the uncertainty structure and frequency weights have been specified, the search for an H_∞ controller is an iterative process, using the following steps which will be described in further detail below:

1. Construct an H_∞ control law using algebraic Riccati equation (ARE) formulae.

2. Improve the set of scaling parameters by solving a linear matrix inequality (LMI).

3. Reduce the controller order using Hankel norm approximation.

We have typically carried out these steps in the order 1-2-1-2-1-3. The aim of these steps is thus to obtain an H_∞ controller with $\gamma \leq 1$. If the smallest possible γ is larger than 1, we can choose to relax the robustness requirements by decreasing the magnitude of W_2, W_3, W_4, W_5 in some cricical frequency band. Alternatively, we can relax the performance requirements by specidying a lower cut-off frequency of W_1 or by reducing some entries of W_p.

In the following we give a detailed description of each of the steps 1-3.

1. An H_∞ control law is found using the ARE formulae in Glover and Doyle[28]. Under some technical assumptions (see appendix A.1) which are satisfied with our system formulation these formulae result in an H_∞ controller for a given $\gamma > 0$ and a given pair of scaling matrices D_l and D_r if such a controller exists. The dynamic order of the controller is equal to the dynamic order of the system, including frequency weights.

2. The purpose of scaling the inputs w and outputs z is to make the H_∞ problem solvable for a smaller value of γ. The use of a diagonal scaling matrix does not affect the inequality (2.39), and therefore the robustness issue of the control problem does not change. Let now

$$\frac{d\phi}{dt} = \bar{A}\phi + \bar{B}w \tag{2.45}$$

$$z = \bar{C}\phi + \bar{D}w \tag{2.46}$$

be a state space realization of the closed loop system $\mathcal{F}(G,K)$. The following condition can be derived as a scaled version of the so-called bounded real lemma, see Boyd et al.[11]. Given $\gamma > 0$, if there exists a symmetric positive definite matrix S and a diagonal positive definite matrix T satisfying the LMI

$$\left[\begin{array}{cc} \bar{A}'S + S\bar{A} & S\bar{B} \\ \bar{B}'S & -\gamma \left[\begin{array}{cc} 1 & 0 \\ 0 & T \end{array} \right] \end{array} \right] + \gamma^{-1} \left[\begin{array}{c} \bar{C}' \\ \bar{D}' \end{array} \right] \left[\begin{array}{cc} I_9 & 0 \\ 0 & T \end{array} \right] \left[\begin{array}{cc} \bar{D} & \bar{C} \end{array} \right] < 0 \qquad (2.47)$$

then K is an H_∞ controller for the scaled system, where the scaling matrices are obtained by taking $\Lambda = T^{1/2}$. This condition was used for improving the set of scaling parameters.

It turned out that the algorithm for solving the LMI (2.47) required more computer memory than there was available. We therefore tried to reduce the dimension of the closed loop system by Hankel norm approximation prior to solving the LMI. However, this approximation turned out to be too rough, and progress was unsatisfactory. As an alternative approach we reduced the number of perturbations using an ad-hoc approach before applying the Hankel norm approximation. This allowed us to use a higher order of the Hankel norm approximation of the closed loop system, and further progress in selecting appropriate scaling parameters was made. This ad-hoc procedure is described in section 3.5.

The iteration of items 1 and 2, between finding an H_∞ controller K and a pair of scaling matrices D_l and D_r is known as D-K iteration, although it is more common to let D_l and D_r be frequency dependent in order to obtain flexibility across frequencies and use an algorithm based on μ analysis to find these, see Packard and Doyle[48], and Balas et al.[33]. Unfortunately, the use of frequency dependent scaling matrices leads to a significant increase in the order of the scaled plant, and this would be potentially problematic in our case.

3. Since the dynamic order of the controller given by the ARE formulae is too high for practical implementation, we consider here the problem of finding an H_∞ controller of lower order. The algorithm for seeking the reduced order controller is less direct than in the case of the full-order controller. Even if there exists an H_∞ controller with a given γ-value and of a given order, there is no guarantee that we will find such one. The idea of the algorithm is that the reduced order controller $\hat{K}$ should perform roughly like the full order controller K in the H_∞ norm. We therefore consider first

$$\begin{aligned} &\|D_l\mathcal{F}(G,\hat{K})D_r^{-1} - D_l\mathcal{F}(G,K)D_r^{-1}\|_\infty \\ &\quad = \|D_lG_{12}(I-\hat{K}G_{22})^{-1}\hat{K}G_{21}D_r^{-1} - D_lG_{12}(I-KG_{22})^{-1}KG_{21}D_r^{-1}\|_\infty. \end{aligned}$$

Unfortunately, the reduced order controller $\hat{K}$ appears in this expression in a non linear fashion. By calculating

$$\left.\frac{d}{d\alpha}\right|_{\alpha=0} D_l\mathcal{F}(G,K+\alpha(\hat{K}-K))D_r^{-1}$$

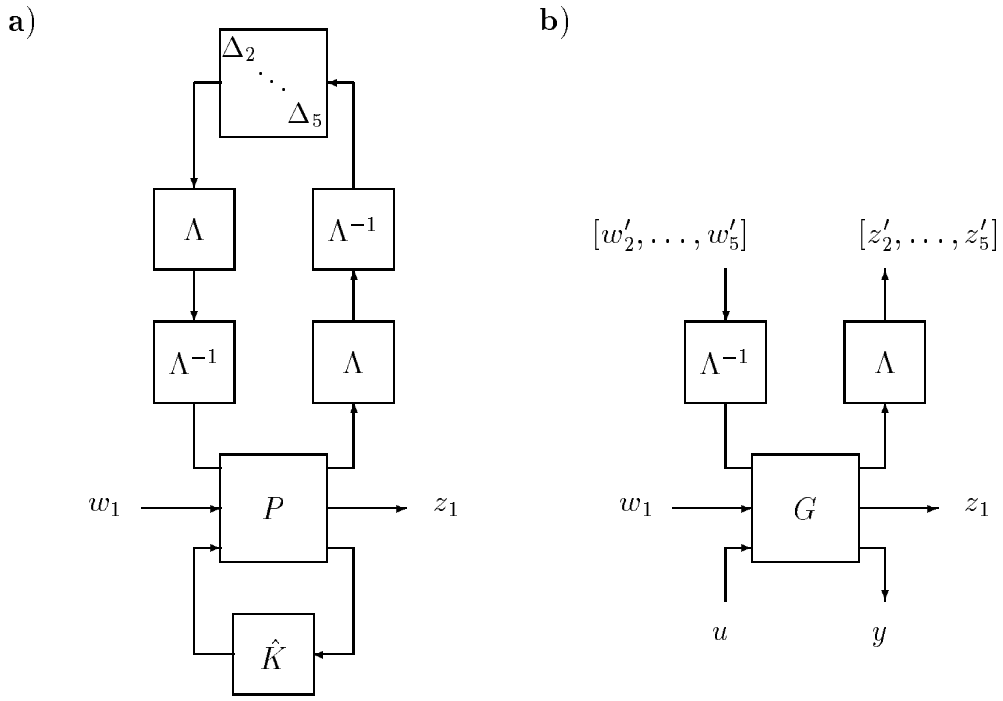

Figure 2.7: **a)** Diagram for the robust performance test with the enhanced, infinite dimensional plant P, perturbations $\Delta_2, \ldots, \Delta_5$, scaling matrix Λ, reference signal w_1, tracking error z_1, and reduced order controller $\hat{K}$. **b)** Corresponding scaled plant considered in the H_∞ synthesis.

$$= \quad D_l G_{12}(I - KG_{22})^{-1}(\hat{K} - K)(I - G_{22}K)^{-1}G_{21}D_r^{-1}, \qquad (2.48)$$

we find the approximation

$$\begin{aligned} &\|D_l\mathcal{F}(G, \hat{K})D_r^{-1} - D_l\mathcal{F}(G, K)D_r^{-1}\|_\infty \\ &\quad \approx \quad \|D_l G_{12}(I - KG_{22})^{-1}(\hat{K} - K)(I - G_{22}K)^{-1}G_{21}D_r^{-1}\|_\infty, \end{aligned} \qquad (2.49)$$

which is of first order in $\hat{K} - K$. The idea of using a first order approximation is well established, and was suggested for example in Andersson and Liu[1]. The search for a $\hat{K}$ of a pre-specified order making (2.49) small is carried out using frequency weighted Hankel norm approximation, using the algorithm given in Zhou et al.[63, th. 19.9, lem. 19.11], and Lancaster and Tismenetsky[42, sec. 12.3].

2.4.5 Robust Performance Test

Prior to applying the controller to the physical plant, extensive simulations is the best test available. However, the H_∞ method comprises a more theoretical test, the robust performance test. The robust performance test that we use

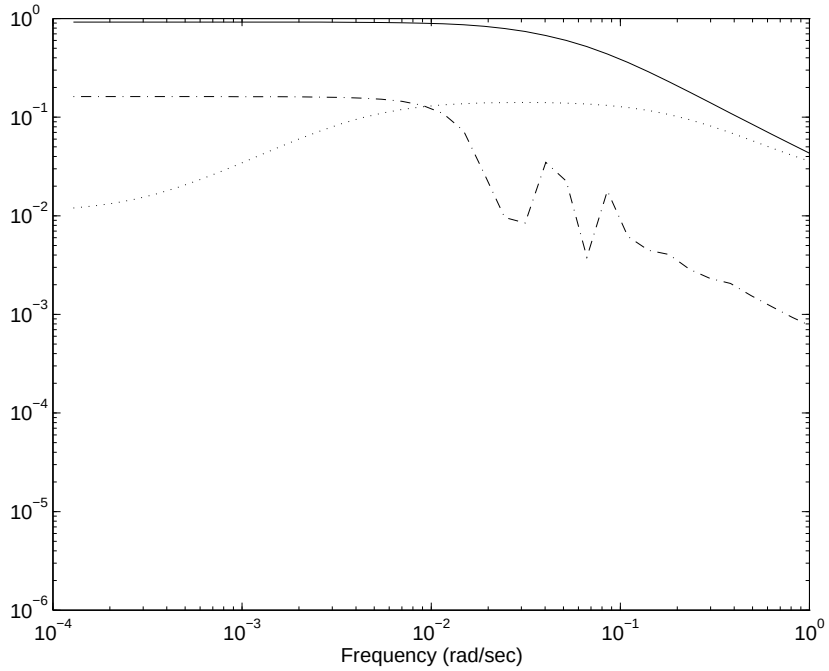

Figure 2.8: Transfer functions related to the ith upper tank and the ith lower tank: $(-)$ magnitude of $(s+a_3^i)^{-1}a_3^i e^{-sT_E^i}\Theta_{ii}(s)$, $(\cdot\cdot)$ frequency weight used in test, $(-\cdot)$ perturbation caused by parameter variation, where c_1 and a_5 are altered by 10 pct.

was developed for finite dimensional systems see e.g. Packard and Doyle[48] or Zhou et al.[63]. The test is expressed by the following lemma, which gives a sufficient condition for robust performance of the system shown in figure 2.4, in the case where all subsystems, including the perturbations Δ_i, are linear, time invariant and finite dimensional. The test involves scaling matrices similar to the ones used in the synthesis, except that we can here let them be complex and frequency dependent. Put

$$\hat{\Lambda}(\omega) = \begin{bmatrix} \hat{\lambda}_1(\omega) & & \\ & \ddots & \\ & & \hat{\lambda}_{29}(\omega) \end{bmatrix}, \quad \hat{D}_\ell(\omega) = \begin{bmatrix} I_9 & \\ & \hat{\Lambda}(\omega) \end{bmatrix}, \quad \hat{D}_r(\omega) = \begin{bmatrix} 1 & \\ & \hat{\Lambda}(\omega) \end{bmatrix}. \tag{2.50}$$

Lemma 1 *Consider the system shown in figure 2.4 where the H_∞ control law $u = K[y_1, y_2]$ has been applied. Assume that the closed loop system $\mathcal{F}(G,K)$ satisfies the condition*

$$\sup_{\omega\in\mathbb{R}} \inf_{\hat{\Lambda}(\omega)} \bar{\sigma}\left(\hat{D}_\ell(\omega)\mathcal{F}(G,K)(i\omega)\hat{D}_r(\omega)^{-1}\right) \leq \gamma \tag{2.51}$$

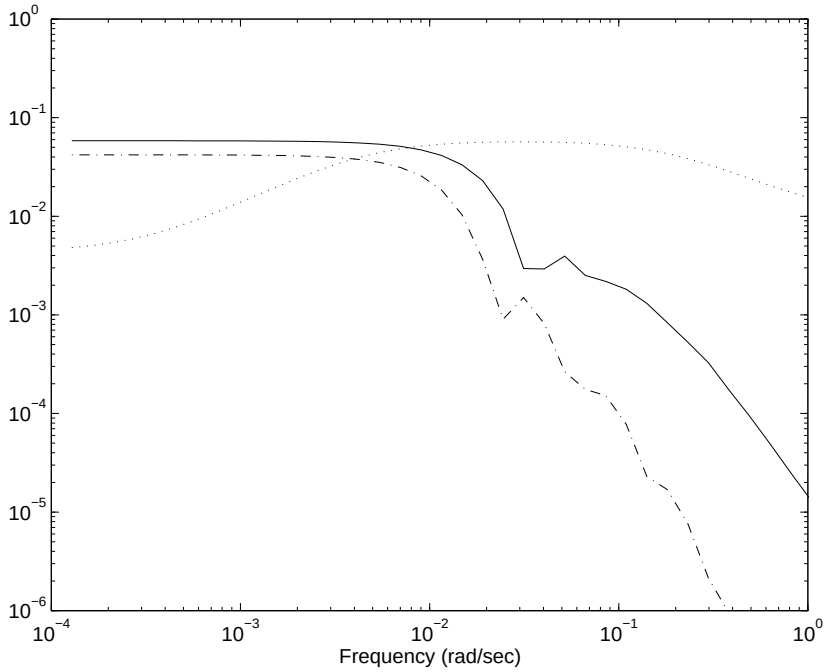

Figure 2.9: Transfer functions related to the $(i-1)$st upper tank and the ith lower tank: $(-)$ magnitude of $(s+a_3^i)^{-1}a_3^i e^{-sT_E^i}\Theta_{i,i-1}(s)$, $(\cdot\cdot)$ frequency weight used in test, $(-\cdot)$ perturbation caused by parameter variation, where c_1 and a_5 are altered by 10 pct.

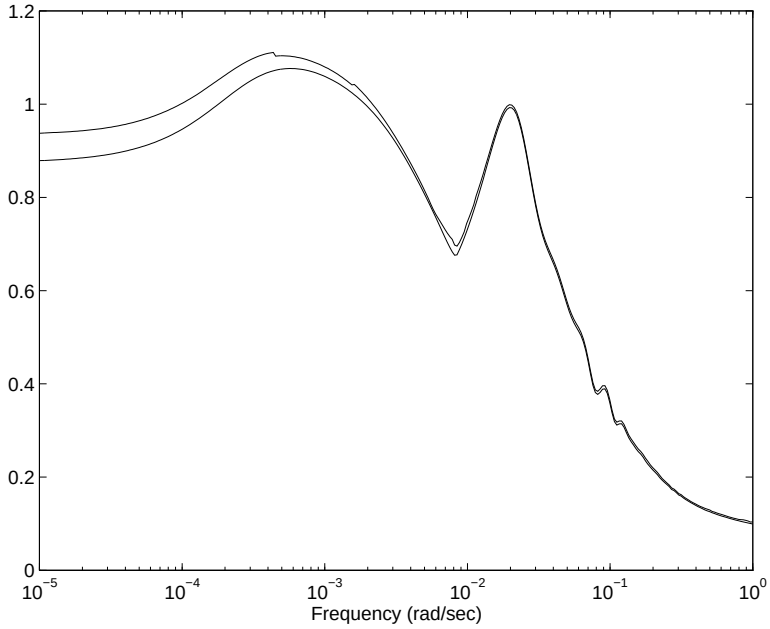

Figure 2.10: Robust performance test for the linear distributed parameter system controlled by the 16th order controller, using frequency dependent scaling matrices: upper and lower bounds for μ.

where $\hat{\Lambda}, \hat{D}_\ell, \hat{D}_r$ *are as defined in (2.50) and* $\bar{\sigma}$ *denotes the largest singular value. Assume furthermore that the perturbations satisfy* $\|\Delta_i\|_\infty < \frac{1}{\gamma}$. *Then the perturbed system is exponentially stable, and there holds*

$$\|z_1\|_2 \leq \gamma \|w_1\|_2 \tag{2.52}$$

for every L^2 *input signal* w_1.

The value of $\bar{\sigma}(\cdot)$ in (2.51) is in the literature called an upper bound for μ. For the precise definition and interpretation of μ, the reader is referred to Packard and Doyle[48]. The lower bound for μ, likewise show in figure 2.10, has the interpretation that, the closer the two bounds are together, the more precise is the information that the test gives about how well the controller handles linear, time invariant perturbations.

We use this test for the case where the system as well as the perturbations are exponentially stable Pritchard-Salamon systems (see appendix A.5) and where all input and output signals have values in finite dimensional spaces. This can be justified by combining arguments from Zhou et al.[63, sec 11.3] with robustness results for infinite dimensional systems, see e.g. Curtain and Zwart[18, corr. 7.2.2]. The substantial leap of faith that we make in this test is thus to assume that the modeling errors are adequately represented by the linear, time invariant systems $W_i \Delta_i$.

The full-order controller of section 2.4.4 is designed so that the robust performance test is satisfied for the finite dimensional nominal plant. However, we have used controller order reduction, and furthermore, we consider the infinite dimensional system as a more accurate model. It therefore makes sense to carry out this test separately. The test is carried out in frequency domain, so we use the transfer function of the infinite dimensional system, enhanced with frequency weights, and controlled by the reduced order controller $\hat{K}$ of section 2.4.4. Fortunately, the test is computationally simpler than the synthesis algorithms, and this is what allows us to let the scaling matrices depend on frequency. With this increased flexibility across frequencies, we can specify a relatively larger magnitude of modeling errors at high frequencies than we did in the synthesis.

The decision of using constant scaling matrices in the synthesis and frequency dependent ones in the robust performance test was based on the computational feasibility of the two alternatives. The use of frequency dependent scaling matrices guarantees robustness against linear time invariant perturbation systems which is qualitatively a very restricted class of perturbations. However, in the finite dimensional case, Poolla and Tikku[50] gave a result concerning slowly varying perturbation systems.

2.5 Numerical Results

The controller synthesis was implemented in Matlab[34]. Tasks like Hankel norm approximation and solving the H_∞ problem were carried out using the commercial toolbox [33], while the linear matrix inequality (2.47) was solved using the non commercial toolbox [24]. The computer platform was a workstation with 96 MB of memory. Additional memory would have been an advantage in the solution of the linear matrix inequality, but on the other hand the algorithm is of high complexity with respect to memory requirements, which means that the amount of additional memory required for obtaining significant progress may be very large. Simulations were implemented in the C language.

Two of the components of the tracking error were modified in order to make the controller behave better. The third and fifth components (see figure 2.2) of the output vector which is intended to represent the beer temperature profile in the tunnel were chosen as a weighted average of the glass temperature and beer temperature rather than simply the beer temperature, for the following reason: When simulating step responses it was observed that the control signals of the fifth heat exchanger had a short peak time and a very high peak value in the beginning, but eventually took negative values, which is an unrealistic situation. Also the glass temperature showed an overshoot. On the other hand the steady state error was not negligible. It turned out that there was a trade-off between obtaining small steady state tracking error and a short peak time of the control signal, and it turned out to be possible to adjust this trade-off. In

order to make the control signal behave more nicely, the idea was to force the glass temperatures to exhibit less overshoot. The means to obtain this was to let the third and fifth components of the tracking error contain a contribution from the glass temperature as well. Notice that these components of the tracking error represent temperatures at the end of the fourth zone and somewhat in the middle of the fifth zone of the tunnel, respectively, see figure 2.2. The background for choosing this procedure is the well known property of H_∞ controllers that they often show only little overshoot in the to-be-controlled variables during a step response. Now, it can be argued that, the temperatures of sprinkled water are already part of the to-be-controlled output of the H_∞ problem, because of the perturbations Δ_4 and Δ_5, but it turns out that this does not prevent the overshoot behavior, because of the scaling parameters λ_i.

The order of the controller was chosen sufficiently small so that the controller became numerically tractable. An adequate criterium turned out to be that poles of a magnitude significantly larger than that of the others should be removed. On the other hand, the order of the controller was chosen high enough so that the sacrifice of the robust performance property of the full order controller was not too large. We here accepted an increase of the γ value of 5 pct. relative to the γ value of the full order controller.

Ideally, the upper bound for μ shown in figure 2.10 should have the maximum value 1, but a slightly larger value is not terrible. In fact, insisting on a maximum value of 1 makes the iterative design procedure much more tedious when controller order reduction comes into play with its not easily predictive performance. Also the shift between designing for the finite dimensional plant and testing for the infinite dimensional plant makes it more difficult to make sure that this maximum value is close to 1.

An important tool in every one of the steps described in section 2.4.4 was Hankel norm approximation. Problem size was problematic in every step, but satisfactory results were obtained by reducing the order of the relevant systems using Hankel norm approximation, which in the case of solving the LMI (2.47) was combined with the method described in section 3.5.

A remark about problem size: The tunnel dynamics were first reduced to the order 128 using the modified average approximation, and then to the order 50 using Hankel norm approximation. Combined with the remaining dynamics this led to an overall system, including frequency weights, of the order 139. This system was reduced to the order 75 before applying the Riccati equation formulae, leading to a controller of the order 75. This controller was ultimately reduced to the order 16. When solving the LMI (2.47), the closed loop system of the order 75+75=150 with 30 inputs and 38 outputs was first reduced to a system with 18 inputs and 26 outputs using the procedure of section 3.5. This system was then reduced to a system of the order 27 using Hankel norm approximation. Thus the LMI was solved for a system of the order 27, with 18 inputs and 26 outputs and 17 scaling parameters.

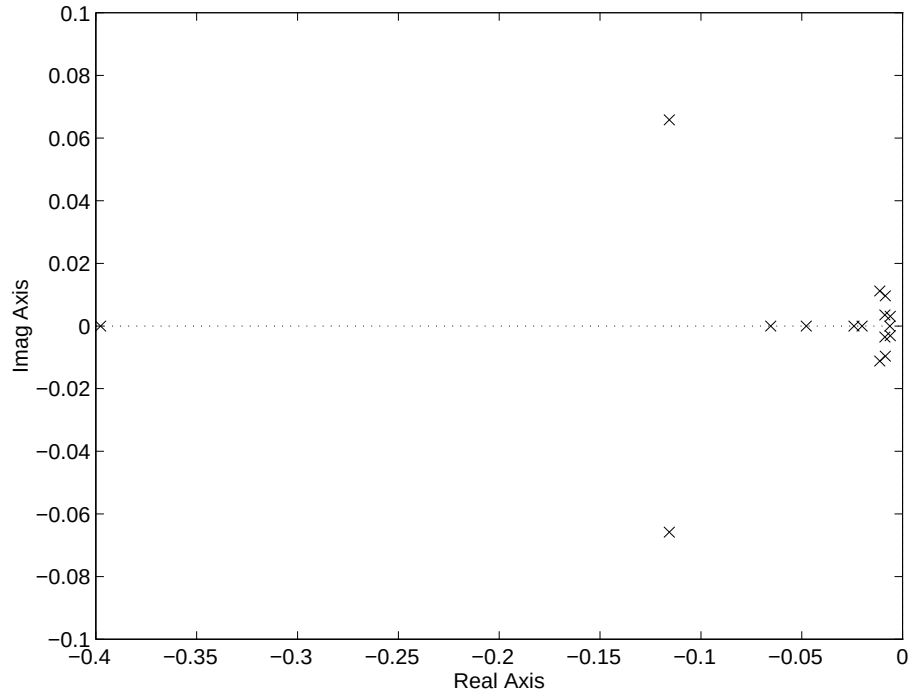

Figure 2.11: Poles of the 16th order controller.

Usually, when using Padé approximation of time delays for the purpose of controller design one should bear in mind that they produce zeros in the right half plane. Fortunately, in our case it seemed that these zeros were so far away from the origin, and the system so well damped, that these zeros did not have a significant damaging influence on the design.

2.5.1 Simulations

Simulations were carried out using a numerical implementation that is more accurate than the one used in the controller synthesis. For the discretization in time we used a fourth order Runge-Kutta method, see Lambert[41]. The delay in (2.15) and (2.17) was implemented using the second order Padé approximation

$$e^{-sT} \approx \frac{12 - 6sT + (sT)^2}{12 + 6sT + (sT)^2}. \tag{2.53}$$

The heat exchanger dynamics (2.16) was replaced by its nonlinear counterpart, see (2.5). The initial value of the temperature profile of equation (2.13) was approximated by average values, and the numerical integration was carried out by combining the method of characteristics and the Runge-Kutta method, see appendix A.3 for details.

The simulations are all step responses, since this is a standard way of demonstrating the properties of a controller, although a step response with zero initial

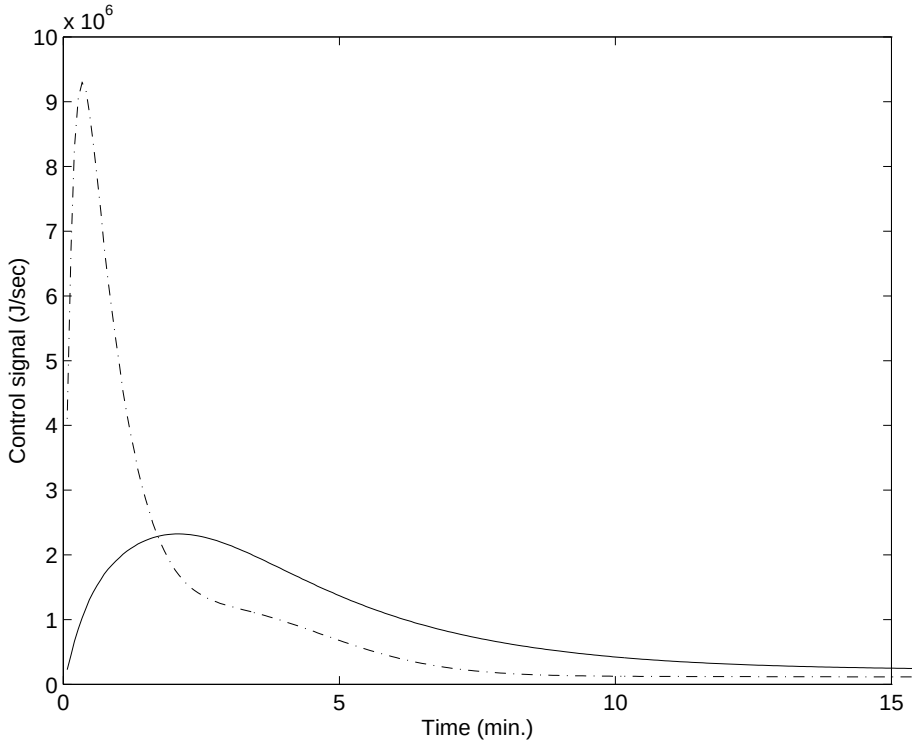

Figure 2.12: Step responses for the control input signal, with 16th order controller. $(-)$ Step response for 4th heat exchanger. $(-\cdot)$ Step response for 5th heat exchanger.

condition is clearly unrealistic in the present application. What would be realistic is the problem of reaching the desired temperature profile, starting from another profile that is close to the desired one. However, we find that a step response starting from zero initial condition does demonstrate some intrinsic characteristics of the controller, like robustness and the peak time of the control signal in the case of a step change in the reference signal. Figure 2.12 shows that the control signal has a large overshoot in the beginning, where the peak is found at $t = 20$ seconds for the 5th heat exchanger and at $t = 125$ seconds for the 4th heat exchanger. Figure 2.14 shows that also the temperatures in the upper tanks exhibit an overshoot. Figure 2.13 shows the absence of overshoot in the most important temperature, namely the beer temperature in the last subinterval of zone 5 (cf. figure 2.2). The fact that the step responses behave like it could be expected from a stable, linear system shows good robustness against the nonlinearity in the heat exchanger dynamics (cf. equation (2.5)). The steady state error in this simulation was 0.1 °C, see section 3.2 for a futher remark about this matter.

When regarding the step response of the beer temperature in figure 2.13, it is useful to bear in mind that the time that it takes for each bottle of beer to pass a single zone is approximately four minutes. The step response of figure 2.13 has a characteristic bulge at approximately four minutes. In figure 2.14 the temperature in the fifth upper tank has a peak after approximately one minute,

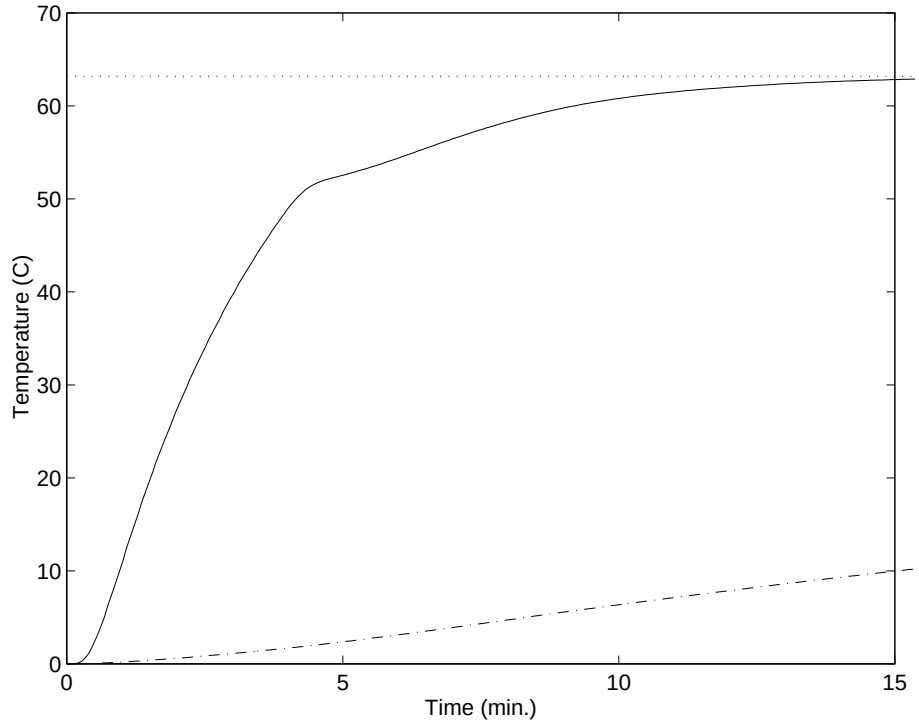

Figure 2.13: Step responses for the 6th component of beer temperature profile (see figure 2.2). $(-)$ Step response with 16th order controller. $(-\cdot)$ Step response with open loop control. $(\cdot\cdot)$ reference temperature.

and it seems that the influence from the fourth zone is effective about four minutes later when another peak is shown.

Figure 2.15 demonstrates the robustness of the controller. When altering two of the parameters by 10 pct., the performance requirement of maximum 1 °C deviation from the desired temperature in steady state was still satisfied. This observation is striking in view of the Bode plots of figures 2.8 and 2.9 where it is shown that this deviation of parameter values leads to a modeling error which is much larger than what was accounted for in the robust performance test.

2.6 Discussion

The continuous time linear control law derived in this section is not necessarily ready for implementation. For implementation using a digital computer, a discrete time control law is needed, and we have not adressed this issue. The dynamics of the system are very slow, so this should not give rise to any problems. Another issue that we have not adressed is that a control engineer might prefer to operate the heat exchangers in on-off mode, and whether or not our control law can be converted to a succesful control law of that type would have to be tested in simulations.

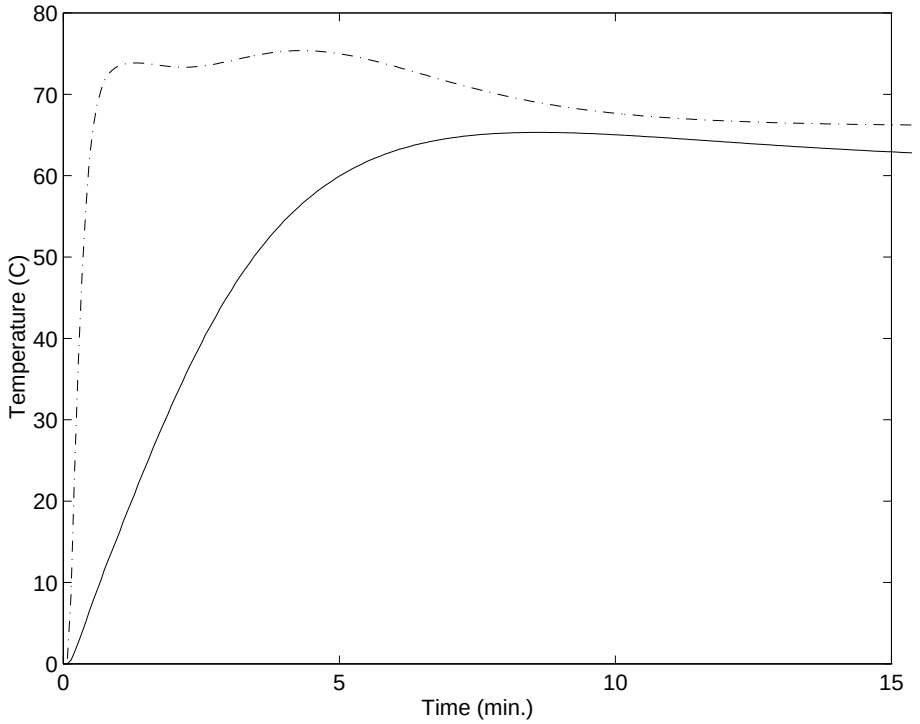

Figure 2.14: Step responses for temperatures in the upper tanks, with 16th order controller. $(-)$ Step response for 4th upper tank. $(-\cdot)$ Step response for 5th upper tank.

In the step response, the control signal of the 5th heat exchanger had a very large peak value. First of all, this probably means that reproducing the stepresponse on the physical plant is unrealistic. On the other hand, the large peak value of the control signal suggests that the control law might be suitable for tracking moderate changes in the reference signal.

A possible alternative to our aproach is to model the whole plant in discrete time from the beginning, given that the input signals are piecewise constant, according to a pre-specified sample time. The transport of the conveyor belt could be modeled in discrete time by a pure shift, and the remaining dynamics of our continuous time model could be translated to discrete time using standard methods, see e.g. Friedland[23]. In this way the model of the transport of bottles would be more precise than the one produced by the continuous time, finite dimensional approximation of the transport equation, at least at sampling instants. A problem related to this approach is that in our example, with eight subdivisions per zone like in the continuous-time approximation, this implies a sample time of approximately thirty seconds. Using model reduction techniques it should be possible to reduce this sample time somewhat, but it does nevertheless seem inevitable that this type of purely discrete time modeling would lead to a controller that reacts considerately slower than the one obtained from the continuous time modeling. However, the system dynamics are well damped, so

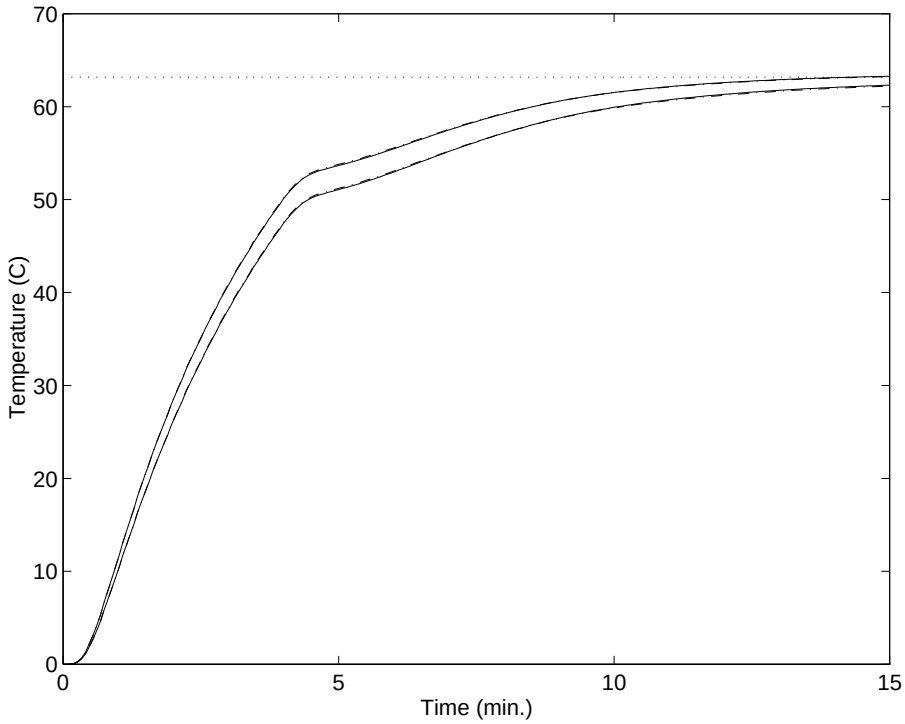

Figure 2.15: Step responses for the 6th component of beer temperature profile (see figure 2.2). $(-/-\cdot)$ Various step respones with 16th order controller where the parameters c_1 and a_5^i are altered by 10 pct., relative to the nominal value. $(\cdot\cdot)$ Reference temperature.

we are not in the position to give a qualified judgement about which modeling approach will result in the better controller.

The question that is probably the most interesting to ask is, how does the controller developed in this chapter compare with a PI-based control strategy. Unfortunately, we are not in the position to make this comparison.

A number of techniques from the H_∞ method were used in the controller synthesis. One purpose of this thesis is to demonstrate the usefulness of these methods, and therefore it was disappointing to realize that the high complexity of the numerical algorithms turned out to be a severe problem. In our case, the remedy was ad-hoc modifications of the standard algorithms.

It is characteristic for the methods that computer algorithms play a large role in the synthesis. The trial-and-error part of the synthesis was mainly concentrated on selecting frequency weights for the design. This trial-and-error part was on the other hand rather time consuming, which raises the question, whether this type of design is recommendable if the fast development of a control system is an issue. The description of the design process does identify a strategy for a controller design, but the choices that must be made when adjusting the weighting systems by trial-and-error are not always logical, in particular as the algorithm does not handle every combination of frequency weights equally well, because of the lack of flexibility across frequency of the scaling procedure.

Another interesting question is, whether it is really necessary to choose a controller of an order as high as 16. The answer to this question is clearly no. A lower order controller could be obtained by the same procedure, but with different weighting systems, and the price would be to settle for a less robust controller with a poorer tracking performance. By means of simulations it was demonstrated that the 16th order controller is potentially much more robust than what could be expected from the specified frequency weights. Therefore it might be a good idea in a further development to require less robustness in order to obtain a lower order controller.

Chapter 3

More Details on the Controller Design

In the previous chapter the procedure used for the design of a controller was presented. In the present chapter we give some further details concerning the analysis of the model, and we also describe an ad-hoc method that was used for reducing the problem size at one point of the synthesis.

3.1 The Distributed Parameter System

We base the control synthesis on the formulation of a semigroup control system which has the form

$$\frac{d\xi}{dt}(t) = A\xi(t) + Bu(t), \quad \xi(0) = \xi_0 \tag{3.1}$$

where A is the infinitesimal generator of a strongly continuous semigroup on a separable Hilbert space H and B is a linear operator defined on the input space U, which is a separable Hilbert space. In the controller synthesis problem also an output signal y with values in a separable Hilbert space Y is specified, and we can write

$$y(t) = C\xi(t) + Du(t) \tag{3.2}$$

where C is the output operator and D is the feed-through operator.

We have here intentionally omitted the precise assumptions on B, C, D, except that they are linear. The simplest case is when these operators are bounded with respect to H, i.e. $B \in \mathcal{L}(U,H)$, $C \in \mathcal{L}(H,Y)$, $D \in \mathcal{L}(U,Y)$. Background material on this class of systems can be found in Curtain and Zwart[18]. In the more general situation where B and C are not both bounded with respect to H, the system is said to have unbounded input and/or output operators. We shall here refer to results for such systems without going into details.

In this section we will show that the linear model of the pasteurization plant can actually be written in this formulation, and then take advantage of this formulation to calculate transfer functions.

Let us first look at the state operator of the transport equation (2.13)-(2.14). We use the notation

$$\Sigma = \begin{bmatrix} -c_1 - c_2 & c_2 \\ c_3 & -c_3 \end{bmatrix}. \tag{3.3}$$

Define the operator A by

$$(Aw)(t,x) = \left(-v\frac{\partial w}{\partial x} + \Sigma w\right)(t,x) \tag{3.4}$$

$$\begin{aligned} D(A) = \{&w \in (L^2([x_0,x_m]))^2 \text{ such that } \frac{\partial w}{\partial x} \in (L^2([x_0,x_m]))^2, \\ &w(t,x_0) = 0 \text{ and } w \text{ is absolutely continuous }\}. \end{aligned} \tag{3.5}$$

In lemma 2 we shall state some useful properties of the operator A.

Lemma 2 *Let A be the operator defined in (3.4)-(3.5). Then*

1. *A is the infinitesimal generator of a strongly continuous semigroup $S(t)$ on $(L^2([x_0,x_m]))^2$ and there holds*

$$\|S(t)\| \leq e^{t|c_2-c_3|/4}. \tag{3.6}$$

2. *The semigroup $S(t)$ is nilpotent.*

3. *The spectrum of A is empty.*

Proof It is enough to show that the perturbed system operator $A - I|c_2 - c_3|/4$ generates a strongly continuous contractive semigroup, and for this we use the Lumer-Philips theorem, see Pazy[49, th.4.3]. We will first show that $A - (|c_2 - c_3|/4)I$ is dissipative, which follows if,

$$\forall w \in D(A): \ \mathrm{Re}\langle w, (A - \frac{1}{4}|c_2 - c_3|I)w\rangle_{(L^2([x_0,x_m]))^2} \leq 0. \tag{3.7}$$

We find

$$\begin{aligned} &\langle w, (A - (|c_2 - c_3|/4)I)w\rangle_{(L^2([x_0,x_m]))^2} \\ &= \frac{-v}{2}|w(x_m)|^2 + \left\langle w, \left(\frac{1}{2}(\Sigma + \Sigma') - \frac{1}{4}|c_2 - c_3|I\right) w\right\rangle_{(L^2([x_0,x_m]))^2}. \end{aligned} \tag{3.8}$$

The first term on the right hand side of (3.8) is clearly negative semi definite, and for this to be true also for the real part of the second term, it is sufficient that

the eigenvalues of $(\Sigma+\Sigma')/2 + I|c_2-c_3|/4$ are non positive. The corresponding characteristic polynomial is

$$\begin{aligned}
&\begin{vmatrix} -c_1-c_2-\frac{1}{4}|c_2-c_3|-\lambda & \frac{1}{2}(c_2+c_3) \\ \frac{1}{2}(c_2+c_3) & -c_3-\frac{1}{4}|c_2-c_3|-\lambda \end{vmatrix} \\
&= \left(\lambda+\frac{1}{2}\left(c_1+c_2+c_3+\frac{|c_2-c_3|}{2}\right)\right)^2 - \frac{1}{4}\left(c_1+c_2+c_3+\frac{|c_2-c_3|}{2}\right)^2 \\
&\quad +\frac{1}{16}|c_2-c_3|^2+\frac{1}{4}(c_1+c_2+c_3-|c_2-c_3|)|c_2-c_3|+c_1c_3, \qquad (3.9)
\end{aligned}$$

so the eigenvalues are negative. It remains to show that

$$R(I-(A-(|c_2-c_3|/4)I)) = (L^2([x_0,x_m]))^2, \qquad (3.10)$$

i.e. $\forall f \in (L^2([x_0,x_m]))^2, \exists w \in D(A)$ such that $(1+|c_2-c_3|/4)w - Aw = f$. Indeed, for every $f \in (L^2([x_0,x_m]))^2$, w given by

$$w(x) = \frac{1}{v}\int_{x_0}^{x} e^{\frac{x-s}{v}(\Sigma-(1+|c_2-c_3|/4)I)} f(s)ds \qquad (3.11)$$

is in $D(A)$ and $((1+|c_2-c_3|/4)I-A)w = f$. According to the Lumer-Philips theorem it now follows that A is the infinitesimal generator of a strongly continuous semigroup satisfying (3.6).

2. The Cauchy problem

$$\begin{aligned}
\frac{\partial w}{\partial t} &= -v\frac{\partial w}{\partial x} + \Sigma w, \quad (t,x) \in]0,\infty[\times]x_0,x_m[&& (3.12)\\
w(t,0) &= 0, \qquad t \in]0,\infty[&& (3.13)\\
w(0,x) &= w_0(x), \qquad x \in]x_0,x_m[&& (3.14)
\end{aligned}$$

has the explicit solution

$$w(t,x) = e^{\Sigma t} w_0(x-vt)H(x-x_0-tv), \qquad (3.15)$$

where H denotes the Heaviside step function. For every initial condition w_0 this solution is zero for $t > (x_m-x_0)/v$, and since (3.15) can be written as

$$w(t,x) = (S(t)w_0)(x), \qquad (3.16)$$

we conclude that the semigroup $S(t)$ is nilpotent.

3. (follows [19].) For the spectra $\sigma(A)$ and $\sigma(S(t))$ we have (see [19, p.264])

$$e^{\sigma(A)t} \subset \sigma(S(t)). \qquad (3.17)$$

For the spectral radius r_ρ of $S(t)$, $t > 0$ we have

$$r_\rho(S(t)) = \lim_{n\to\infty} \|(S(t))^n\|^{1/n}. \qquad (3.18)$$

Since $S(t)$ is nilpotent, the spectral radius of $S(t)$ is zero, and we conclude that the spectrum of A is empty. □

The inequality (3.6) implies that the Laplace transform is well defined at least for $\mathrm{Re}(s) > |c_2 - c_3|/4$. After Laplace transform the transport equation (2.13)-(2.14) leads to

$$\begin{aligned} v\frac{\partial \hat{\tau}_1}{\partial x}(s,x) &= \begin{bmatrix} -c_1 - c_2 - s & c_2 \\ c_3 & -c_3 - s \end{bmatrix} \hat{\tau}_1(s,x) + c_1 \sum_{i=1}^{8} \begin{bmatrix} \chi^i(x) \\ 0 \end{bmatrix} \hat{\tau}_5^i(s) \\ \hat{\tau}_1(s,x_0) &= 0, \end{aligned} \tag{3.19}$$

where χ^i denotes the characteristic function of the interval (x_{i-1}, x_i).

The following observations allow us to calculate the relevant transfer functions explicitely. The eigenvalues of Σ are real and given by $(-c_1 - c_2 - c_3 \pm c_4)/2$, where

$$c_4 = \sqrt{(c_1 + c_2 + c_3)^2 - 4c_1c_3}. \tag{3.20}$$

It can be shown that c_4 is a real number, and furthermore there holds the following inequalities:

$$c_4 > |c_1 + c_2 - c_3| \quad \text{and} \quad c_4 > |c_2 + c_3 - c_1| \quad \text{and} \quad c_4 < c_1 + c_2 + c_3. \tag{3.21}$$

A diagonalization of Σ is given by

$$\Gamma^{-1}\Sigma\Gamma = \begin{bmatrix} -\frac{1}{2}(c_1 + c_2 + c_3 - c_4) & 0 \\ 0 & -\frac{1}{2}(c_1 + c_2 + c_3 + c_4) \end{bmatrix} \tag{3.22}$$

where

$$\Gamma = \begin{bmatrix} -c_2 & -c_2 \\ \frac{1}{2}(-c_1 - c_2 + c_3 - c_4) & \frac{1}{2}(-c_1 - c_2 + c_3 + c_4) \end{bmatrix} \tag{3.23}$$

$$\Gamma^{-1} = \frac{1}{c_2c_4} \begin{bmatrix} \frac{1}{2}(c_1 + c_2 - c_3 - c_4) & -c_2 \\ \frac{1}{2}(-c_1 - c_2 + c_3 - c_4) & c_2 \end{bmatrix}. \tag{3.24}$$

Each entry of the transfer matrices describing the input-output relations of the tunnel is related to only a single component of $\hat{\tau}_5$. We therefore calculate, for each $i = 1 \ldots 8$,

$$\begin{aligned} \hat{\tau}_1(s,x) &= (sI - A)^{-1} \begin{bmatrix} c_1\chi^i \\ 0 \end{bmatrix}(x)\hat{\tau}_5^i(s) \\ &= \frac{1}{v}\int_{x_0}^{x} \Gamma \begin{bmatrix} e^{-(c_1+c_2+c_3-c_4)(x-y)/2v} & 0 \\ 0 & e^{-(c_1+c_2+c_3+c_4)(x-y)/2v} \end{bmatrix} \Gamma^{-1} \\ &\qquad e^{-s(x-y)/v} \begin{bmatrix} c_1\chi^i(x) \\ 0 \end{bmatrix} \hat{\tau}_5^i(s)dy. \end{aligned} \tag{3.25}$$

For $x \leq x_{i-1}$, (3.25) leads to $\hat{\tau}_1(s,x) = 0$. For $x_{i-1} < x \leq x_i$ we find

$$\begin{aligned}
&\left[\begin{array}{cc} 1 & 0 \end{array}\right] \hat{\tau}_1(s,x) \\
&= \left[\frac{c_1(-c_1-c_2+c_3+c_4)}{(c_1+c_2+c_3-c_4+2s)c_4}\left(1-e^{-(c_1+c_2+c_3-c_4+2s)(x-x_{i-1})/2v}\right)\right. \\
&\quad \left.+\frac{c_1(c_1+c_2-c_3+c_4)}{(c_1+c_2+c_3+c_4+2s)c_4}\left(1-e^{-(c_1+c_2+c_3+c_4+2s)(x-x_{i-1})/2v}\right)\right] \hat{\tau}_5^i(s)
\end{aligned} \tag{3.26}$$

and

$$\begin{aligned}
&\left[\begin{array}{cc} 0 & 1 \end{array}\right] \hat{\tau}_1(s,x) \\
&= \left[\frac{2c_1c_3}{c_4(c_1+c_2+c_3-c_4+2s)}\left(1-e^{-(c_1+c_2+c_3-c_4+2s)(x-x_{i-1})/2v}\right)\right. \\
&\quad \left.-\frac{2c_1c_3}{c_4(c_1+c_2+c_3+c_4+2s)}\left(1-e^{-(c_1+c_2+c_3+c_4+2s)(x-x_{i-1})/2v}\right)\right] \hat{\tau}_5^i(s)
\end{aligned} \tag{3.27}$$

According to (2.22) we can now calculate

$$\begin{aligned}
&\Theta_{ii}(s)\hat{\tau}_5^i(s) \\
&= a_4^i(x_i-x_{i-1})\hat{\tau}_5^i(s) + a_5^i\int_{x_{i-1}}^{x_i}\left[\begin{array}{cc} 1 & 0 \end{array}\right]\hat{\tau}_1(s,x)ds \\
&= a_5^i\frac{c_1(-c_1-c_2+c_3+c_4)}{(c_1+c_2+c_3-c_4+2s)c_4}\left(x_i-x_{i-1}-\frac{2v(1-\zeta^s(x_i-x_{i-1}))}{c_1+c_2+c_3-c_4+2s}\right)\hat{\tau}_5^i(s) \\
&\quad + a_5^i\frac{c_1(c_1+c_2-c_3+c_4)}{(c_1+c_2+c_3+c_4+2s)c_4}\left(x_i-x_{i-1}-\frac{2v(1-\eta^s(x_i-x_{i-1}))}{c_1+c_2+c_3+c_4+2s}\right)\hat{\tau}_5^i(s) \\
&\quad + a_4^i(x_i-x_{i-1})\hat{\tau}_5^i(s),
\end{aligned} \tag{3.28}$$

which gives us (2.28). Likewise, we calculate

$$\Pi_{ji}(s)\hat{\tau}_5^i(s) = \frac{1}{\xi}\int_{x_{i-1}}^{x_i}\left[\begin{array}{cc} 0 & 1 \end{array}\right]\hat{\tau}_1(s,x)ds \tag{3.29}$$

in order to obtain $\Pi_{ji}(s)$ in the case that the jth component of the tracking error is calculated over an interval in the ith zone, leading to (2.30). For $x_i < x$, (3.25) leads to

$$\begin{aligned}
&\left[\begin{array}{cc} 1 & 0 \end{array}\right] \hat{\tau}_1(s,x) \\
&= \left[\frac{c_1(-c_1-c_2+c_3+c_4)}{(c_1+c_2+c_3-c_4+2s)c_4}\right. \\
&\quad \left(e^{-(c_1+c_2+c_3-c_4+2s)(x-x_i)/2v} - e^{-(c_1+c_2+c_3-c_4+2s)(x-x_{i-1})/2v}\right) \\
&\quad + \frac{c_1(c_1+c_2-c_3+c_4)}{(c_1+c_2+c_3+c_4+2s)c_4} \\
&\quad \left.\left(e^{-(c_1+c_2+c_3+c_4+2s)(x-x_i)/2v} - e^{-(c_1+c_2+c_3+c_4+2s)(x-x_{i-1})/2v}\right)\right] \hat{\tau}_5^i(s)
\end{aligned} \tag{3.30}$$

and

$$\begin{aligned}
&\left[\begin{array}{cc} 0 & 1 \end{array}\right] \hat{\tau}_1(s,x) \\
&= \left[\frac{2c_1c_3}{c_4(c_1+c_2+c_3-c_4+2s)} \right. \\
&\quad \left(e^{-(c_1+c_2+c_3-c_4+2s)(x-x_i)/2v} - e^{-(c_1+c_2+c_3-c_4+2s)(x-x_{i-1})/2v}\right) \\
&\quad - \frac{2c_1c_3}{c_4(c_1+c_2+c_3+c_4+2s)} \\
&\quad \left.\left(e^{-(c_1+c_2+c_3+c_4+2s)(x-x_i)/2v} - e^{-(c_1+c_2+c_3+c_4+2s)(x-x_{i-1})/2v}\right)\right] \hat{\tau}_5^i(s),
\end{aligned} \tag{3.31}$$

leading to $\Theta_{ji}(s)$ and $\Pi_{ji}(s)$ given by (2.27) and (2.29), respectively.

For the linear system made up by the interconnection structure shown in figure 2.4 the technical problems with respect to well posedness are relatively easy to handle. We have chosen to use here the class of Pritchard-Salamon systems (see appendix A.5) in order to make sure that the overall system is well posed, and furthermore it allows us to appeal to certain robustness results. This class has the nice property that two Pritchard-Salamon systems in cascade is again a Pritchard-Salamon system, and the same is true for the sum of two such systems. It contains linear systems on the state space form (3.1)-(3.2) with bounded input and output operators, as well as systems with some degree of unboundedness in the input and output operators. For background material, see Pritchard and Salamon[52], Curtain et al.[16], Curtain[13] and Van Keulen[59].

The linear model (2.13)-(2.17) is divided into four subsystems, and we here refer to these by their transfer functions. The systems

$$(sI + a_2)^{-1} a_2 \; e^{-sT_D} \tag{3.32}$$

$$(sI + a_3)^{-1} a_3 \; e^{-sT_E} \tag{3.33}$$

have state space realizations as Pritchard-Salamon systems, see Van Keulen[59, ex.2.8] for an example that contains as a special case a realization of (3.32) where the delay is placed after the first order system. A realization in the Pritchard-Salamon class where the delay is placed first can then be constructed using a duality argument, see Van Keulen[59, theorem 2.17]. The finite dimensional system

$$(sI + a_1)^{-1} b \tag{3.34}$$

is also of Pritchard-Salamon type. Finally, the system with the transfer matrix

$$\left[\begin{array}{c} \Theta(s) \\ \Pi(s) \end{array}\right] \tag{3.35}$$

is also in the Pritchard-Salamon class, since the input and output operators are bounded, see (2.13), (2.22), (2.23).

The system has an internal feedback, where the loop transfer function is given by

$$\Phi(s) := (sI + a_2)^{-1} a_2 e^{-sT_D} a_6 (sI + a_3)^{-1} a_3 e^{-sT_E} \Theta(s). \tag{3.36}$$

For the system to be well posed with this feedback, we must make sure that $I - \Phi(\infty)$ is invertible. This is indeed the case, since $\Phi(\infty) = 0$.

The last property that we will show about the system is exponential stability, i.e. the existence of positive constants M, α such that

$$\|S(t)\| \leq Me^{-\alpha t}, \tag{3.37}$$

where $S(t)$ is the semigroup generated by the system operator. First, notice that the systems (3.32), (3.34),(3.33) are clearly exponentially stable. This is also the case for the system (3.35), since the semigroup of this system is nilpotent.

It remains to show that also the interconnection of these subsystems makes up an exponentially stable system. Using the small gain theorem, see Curtain and Zwart[18, cor.7.2.2], it here suffices to show that the loop (3.36) has the property

$$\|\Phi(s)\|_\infty < 1. \tag{3.38}$$

It is not hard to see that there holds

$$\|(sI + a_2)^{-1} a_2 e^{-sT_D} a_6 (sI + a_3)^{-1} a_3 e^{-sT_E}\|_\infty = 1. \tag{3.39}$$

Thus, using the submultiplicaty property of the $\|\cdot\|_\infty$ norm, it remains to show that

$$\|\Theta(s)\|_\infty < 1. \tag{3.40}$$

We show this property under the assumption that all the zones are exactly alike. Under this assumption the special structure of our system means that it suffices to show that the Euclidian norm of the first column of $\Theta(s)$ is smaller than one for all $s \in \overline{\mathbb{C}^+}$. We know that $\Theta(s)$ is the transfer function of an exponentially stable system, and therefore the maximum of $\|\Theta(s)\|$ in $\overline{\mathbb{C}^+}$ is attained on the imaginary axis. That $|\Theta_{11}(s)|$ attains its maximum in $s = 0$ is seen by considering (3.101), where it is clear that all three terms of $\Theta_{11}(0)$ are positive, and that $|\Theta_{11}(\hat{i}\omega)|$ is not increased by taking $\omega \neq 0$. To see that also $|\Theta_{21}(s)|$ attains its maximum in $s = 0$ we first carry out the following calculation with $\alpha > 0$,

$$\begin{aligned} &\int_{x_{i-1}+h}^{x_i+h} \int_{x_{i-1}}^{x_i} e^{-(\alpha+s)(x-y)/v} dy dx \qquad (3.41)\\ &= \int_{x_{i-1}}^{x_i} \int_{x_{i-1}+h}^{x_i+h} e^{-(\alpha+s)(x-y)/v} dx dy \\ &= e^{-(\alpha+s)h/v} \int_{x_{i-1}}^{x_i} \int_{x_{i-1}-y}^{x_i-y} e^{-(\alpha+s)\tau/v} d\tau dy \end{aligned}$$

$$= e^{-(\alpha+s)h/v}\left(\int_{-(x_i-x_{i-1})}^{0}\int_{x_i-\tau}^{x_i} e^{-(\alpha+s)\tau/v}dyd\tau + \int_{0}^{x_i-x_{i-1}}\int_{x_{i-1}}^{x_i-\tau} e^{-(\alpha+s)\tau/v}dyd\tau\right)$$

$$= e^{-(\alpha+s)h/v}\int_0^{x_i-x_{i-1}}(x_i - x_{i-s} - \tau)\cosh((\alpha+s)\tau/v)d\tau. \quad (3.42)$$

Notice that we can write

$$\Theta_{21}(s) = \frac{a_5^i c_1(-c_1-c_2+c_3+c_4)}{2vc_4}\int_{x_1}^{x_2}\int_{x_0}^{x_1} e^{-(c_1+c_2+c_3-c_4+2s)(x-y)/2v}dydx$$
$$+\frac{a_5^i c_1(c_1+c_2-c_3+c_4)}{2vc_4}\int_{x_1}^{x_2}\int_{x_0}^{x_1} e^{-(c_1+c_2+c_3+c_4+2s)(x-y)/2v}dydx \quad (3.43)$$

We can put $h = x_1 - x_0$ and use (3.42) to obtain

$$\Theta_{21}(\hat{i}\omega)$$
$$= \frac{a_5^i c_1(-c_1-c_2+c_3+c_4)}{2vc_4}e^{-(c_1+c_2+c_3-c_4+2\hat{i}\omega)(x_1-x_0)/v} \quad (3.44)$$
$$\int_0^{x_i-x_{i-1}}(x_i - x_{i-1} - \tau)\cosh(-(c_1+c_2+c_3-c_4+2\hat{i}\omega)\tau/2v)d\tau$$
$$+\frac{a_5^i c_1(c_1+c_2-c_3+c_4)}{2vc_4}e^{-(c_1+c_2+c_3+c_4+2\hat{i}\omega)(x_1-x_0)/v}$$
$$\int_0^{x_i-x_{i-1}}(x_i - x_{i-1} - \tau)\cosh(-(c_1+c_2+c_3+c_4+2\hat{i}\omega)\tau/2v)d\tau$$

It is now easy to see that also $|\Theta_{21}(\hat{i}\omega)|$ attains its maximum at $\omega = 0$. The same is of course true for $|\Theta_{31}(\hat{i}\omega)|$, etc. For $s = 0$ we find, using (2.28), (2.4), (2.25), (2.26)

$$|\Theta_{11}(0)| = 1 - \frac{a_5^1 c_1(-c_1-c_2+c_3+c_4)}{(c_1+c_2+c_3-c_4)c_4}\int_{x_0}^{x_1}\zeta^0(x_1-y)dy \quad (3.45)$$
$$-\frac{a_5^1 c_1(c_1+c_2-c_3+c_4)}{(c_1+c_2+c_3+c_4)c_4}\int_{x_0}^{x_1}\eta^0(x_1-y)dy$$

and, using (2.27), we find for $j > 1$

$$|\Theta_{j1}(0)|$$
$$= \frac{a_5^1 c_1(-c_1-c_2+c_3+c_4)}{(c_1+c_2+c_3-c_4)c_4}\int_{x_0}^{x_1}\left(\zeta^0(x_{j-1}-y) - \zeta^0(x_j-y)\right)dy \quad (3.46)$$
$$+\frac{a_5^1 c_1(c_1+c_2-c_3+c_4)}{(c_1+c_2+c_3+c_4)c_4}\int_{x_0}^{x_1}\left(\eta^0(x_{j-1}-y) - \eta^0(x_j-y)\right)dy.$$

Now, with the assumption that the zones are exactly alike, we have $a_5^1 = \cdots = a_5^8$, and we obtain

$$\sum_{j=1}^{8}|\Theta_{j1}(0)| = 1 - \frac{a_5^1 c_1(-c_1-c_2+c_3+c_4)}{(c_1+c_2+c_3-c_4)c_4}\int_{x_0}^{x_1}\zeta^0(x_8-y)dy$$

$$-\frac{a_5^1 c_1(c_1+c_2-c_3+c_4)}{(c_1+c_2+c_3+c_4)c_4}\int_{x_0}^{x_1}\eta^0(x_8-y)dy \qquad (3.47)$$

which, by (3.21), is clearly smaller than 1. We are now in the position to establish the estimate

$$\|\Theta(s)\|_\infty = |\Theta_{\cdot 1}(0)|_2 \leq \sum_{j=1}^{8}|\Theta_{j1}(0)| < 1 \qquad (3.48)$$

from which the exponential stability follows.

3.2 More Details on Frequency Weights

In this section we give a more detailed description of the process of choosing frequency weights in the design, to complement the description in section 2.4.2

The first choice of weighting systems should be based on the anticipated model uncertainties and pre-specified performance requirements. These selected weights may not lead to a suitable controller, but a nice feature of the H_∞ method is that it provides some constructive indications concerning this feasibility matter even before carrying out simulations.

The adjustment of the frequency weights was done by trial-and-error, and as the main indicators of the required adjustments we used a singular value plot and the worst case perturbation in steady state. The singular value plot shows whether robust performance is obtained with the present controller and for the present set of frequency weights. The peak of this plot determines the critical frequency, at which the largest singular value of the close loop transfer matrix should be smaller than 1.

The worst case perturbation calculated in frequency zero is useful in order to determine whether the worst case perturbation in the design is relevant for the physical plant. Ideally the worst case perturbation should be (block-) diagonal, but in practice the main concern is to make sure that it is not excessively dominated by entries outside this diagonal, otherwise the worst case schenario is irrelevant for the plant. The scaling matrix Λ was introduced in order to avoid such a situation, but it can happen that the effect of scaling is inadequate. In that case the remedy can be to adjust (diminish) the magnitude of some of the weighting systems so that the algorithms are able to find a scaling matrix Λ such that the off-diagonal domination is diminished.

It seems to be debatable, whether or not it is necessary to take the perturbation Δ_5 into account in the H_∞ synthesis algorithm. Once the controller is applied, Δ_5 will be affecting only the tracking error. Thus, neither the dynamics of the nominal system, nor the measured output y is affected by Δ_5. It therefore seems plausible to presume that including Δ_5 and choosing the performance weight W_p to match a tracking error of 1°C will lead to roughly the same H_∞ controller as the alternative, omitting Δ_5 and choosing W_p according to a smaller

tracking error. This simplification would allow us to remove w_5 and z_5 in section 2.4.4, and thereby reduce the dimension of Λ. Since the number of perturbations is critical when selecting the scaling parameters Λ, it was of course interesting to compare the two alternatives. As it happens, we obtained the better results by including Δ_5, in the following respect: A priori, the H_∞ synthesis algorithm may or may not result in a controller that yields zero tracking error in steady state for the nominal system. Indeed, obtaining this desirable property is in our formulation not a design objective, and there is no reason to assume that it is obtained automatically. For our problem it turned out that, zero tracking error in steady state was nearly obtained when Δ_5 was considered also in the synthesis, while it was clearly not obtained when Δ_5 was omitted in the H_∞ synthesis algorithms.

3.3 Discretizing the Transport Equation

In this section we derive the approximation leading to a real rational transfer matrix to represent the tunnel dynamics in the H_∞ synthesis algorithms.

The first step in the approximation of the transport equation (2.13)-(2.14) is to partition each zone into subintervals of lenght h and approximate $\tau_1(t,x)$ by average values over each of these intervals. These average values are used as state variables for a finite dimensional system, and we shall in the following derive the dynamics for these such that the resulting real-rational transfer matrix fits the non rational transfer matrices $\Theta(s)$ and $\Pi(s)$ up to a first order approximation at low frequencies. For the sake of simple notation we let $x_0 = 0$ and we consider the nth subinterval $[(n-1)h, nh]$, assuming that it is contained in the ith zone $[x_{i-1}, x_i]$. We use the notation

$$\hat{\tau}_{1,n}(s) = \frac{1}{h}\int_{(n-1)h}^{nh} \hat{\tau}_1(s,x)dx \tag{3.49}$$

$$\Sigma = \begin{bmatrix} -c_1 - c_2 & c_2 \\ c_3 & -c_3 \end{bmatrix}. \tag{3.50}$$

After taking the Laplace transform, the transport equation (2.13) leads to the relations

$$\begin{aligned} \hat{\tau}_1(s,nh) &= e^{(\Sigma - sI)h/v}\hat{\tau}_1(s,(n-1)h) \\ &\quad + (\Sigma - sI)^{-1}\left(e^{(\Sigma-sI)h/v} - I\right)\begin{bmatrix} c_1 \\ 0 \end{bmatrix}\hat{\tau}_5^i(s) \qquad (3.51) \\ \hat{\tau}_{1,n}(s) &= \frac{v}{h}(\Sigma - sI)^{-1}\left(e^{(\Sigma-sI)h/v} - I\right)\hat{\tau}_1(s,(n-1)h) \\ &\quad +(\Sigma - sI)^{-1}\left(\frac{v}{h}(\Sigma - sI)^{-1}\left(e^{(\Sigma-sI)h/v}\right) - I\right)\begin{bmatrix} c_1 \\ 0 \end{bmatrix}\hat{\tau}_5^i(s) \qquad (3.52) \\ \hat{\tau}_{1,n}(s) &= (sI - \Sigma)^{-1} \end{aligned}$$

$$\left(-\frac{v}{h}\hat{\tau}_1(s,nh)+\frac{v}{h}\hat{\tau}_1(s,(n-1)h)+\begin{bmatrix} c_1 \\ 0 \end{bmatrix}\hat{\tau}_5^i(s)\right). \qquad (3.53)$$

The combination of (3.51) and (3.52) leads to

$$\begin{aligned}\hat{\tau}_1(s,nh) &= \hat{\tau}_{1,n}(s)+\left(e^{(\Sigma-sI)h/v}-\frac{v}{h}(\Sigma-sI)^{-1}+\frac{v}{h}(\Sigma-sI)^{-1}\right)\\ &\cdot\left(\hat{\tau}_1(s,(n-1)h)+(\Sigma-sI)^{-1}\begin{bmatrix} c_1 \\ 0 \end{bmatrix}\hat{\tau}_5^i(s)\right). \qquad (3.54)\end{aligned}$$

Using the notation

$$M=e^{\Sigma h/v}-\frac{v}{h}\Sigma^{-1}e^{\Sigma h/v}+\frac{v}{h}\Sigma^{-1} \qquad (3.55)$$

we replace (3.54) by the approximation

$$\hat{\tau}(s,nh)\approx\hat{\tau}_{1,n}(s)+M\left(\hat{\tau}_1(s,(n-1)h)+\Sigma^{-1}\begin{bmatrix} c_1 \\ 0 \end{bmatrix}\hat{\tau}_5^i(s)\right). \qquad (3.56)$$

By subsequently inserting (3.56) into (3.53) we obtain a finite dimensional system given by matrices (A^N,B^N,C^N,D^N) for approximation the transfer matrix $[\Theta'(s)\ \ \Pi'(s)]'$. We let p denote the number of subdivisions per zone. The zones have equal length so that there are $8p$ intervals of length h along the tunnel. The matrices of the approximation

$$\begin{bmatrix} \Theta^N(s) \\ \Pi^N(s) \end{bmatrix}=D^N+C^N(sI-A^N)^{-1}B^N \qquad (3.57)$$

are the following.

$$A^N=\begin{bmatrix} \Sigma-\frac{v}{h}I & 0 & & \dots & 0 \\ \frac{v}{h}(I-M) & \Sigma-\frac{v}{h}I & 0 & & \\ \frac{v}{h}(I-M)M & \frac{v}{h}(I-M) & \Sigma-\frac{v}{h}I & 0 & \vdots \\ \vdots & & & \ddots & \\ \frac{v}{h}(I-M)M^{8p-2} & \dots & \dots & & \end{bmatrix} \qquad (3.58)$$

$$B^N=\hat{B}(I_8\otimes\chi)c_1 \qquad (3.59)$$

where $\otimes$ denotes the Kronecker product, and $\chi\in\mathbb{R}^{2p\times 1}$ is given by

$$\chi=\begin{bmatrix} 1 & 0 & 1 & 0 & \cdots & 1 & 0 \end{bmatrix}' \qquad (3.60)$$

and

$$\hat{B}=\begin{bmatrix} I-\frac{v}{h}M\Sigma^{-1} & 0 & & \dots & 0 \\ \frac{v}{h}(I-M)M\Sigma^{-1} & I-\frac{v}{h}M\Sigma^{-1} & 0 & & \\ \frac{v}{h}(I-M)M^2\Sigma^{-1} & \frac{v}{h}(I-M)M\Sigma^{-1} & I-\frac{v}{h}M\Sigma^{-1} & 0 & \vdots \\ \vdots & & & \ddots & \\ \frac{v}{h}(I-M)M^{8p-1}\Sigma^{-1} & \dots & \dots & & \end{bmatrix} \qquad (3.61)$$

$$C^N = \begin{bmatrix} C^{N,\Theta} \\ C^{N,\Pi} \end{bmatrix} \tag{3.62}$$

where

$$C^{N,\Theta} = a_5 h (I_8 \otimes \chi') \tag{3.63}$$

$$C^{N,\Pi} = \begin{bmatrix} \dots & 1 & \dots & \ddots & \dots & \dots \\ \dots & \dots & 1 & \dots & \dots & \dots \\ \vdots & \vdots & \vdots & \vdots & \vdots & \vdots \\ \dots & \dots & \dots & \dots & \dots & 1 \end{bmatrix} \tag{3.64}$$

and where $C^{N,\Pi} \in \mathbb{R}^{9\times 16p}$ has in each row a single nonzero entry, with the value 1, according to the distribution of intervals over which the beer temperature is controlled. With $p = 8$ subdivisions per zone, we have chosen to let the entry 1 occur in the columns $\{32, 54, 64, 70, 76, 80, 84, 96, 128\}$ respectively. The feed-through matrix is

$$D^N = \begin{bmatrix} \operatorname{diag}\{a_4^i(x_i - x_{i-1})\} \\ 0 \end{bmatrix}. \tag{3.65}$$

3.4 Some Properties of the Approximation

As mentioned in section 2.3, The main property of the rational transfer matrix obtained using the approximation (2.36) is that the non rational transfer matrix $[\Theta'\ \Pi']'$ is matched exactly in steady state. This property is proven in the present section, and we also give an asymptotic estimate of the approximation error, pointwise in the frequency s. We will in the following consider the entries of the type (2.28). The remaining three types of entries, (2.27),(2.29), (2.30), can be described in a similar manner.

The entry $\Theta_{ii}(s)$ concerns the temperatures right above and below the ith zone. Letting the discretization intervals covering the ith zone be indexed by $U^i = \{p_\ell, \dots, p_u\}$, we can rewrite (2.28) as

$$\begin{aligned} \Theta_{ii}(s) &= a_4^i(x_i - x_{i-1}) \\ &\quad + \sum_{q\in U^i} h a_5^i \begin{bmatrix} 1 \\ 0 \end{bmatrix}' \Gamma \left(\Psi(s) + \sum_{\substack{p\in U^i \\ p<q}} \Xi(s)\Upsilon(s)^{q-p-1}\Omega(s) \right) \Gamma^{-1} \begin{bmatrix} c_1 \\ 0 \end{bmatrix} \end{aligned} \tag{3.66}$$

where

$$\Psi(s) = \begin{bmatrix} \frac{(s+\alpha)h - \left(1-e^{-(\alpha+s)h/v}\right)v}{(s+\alpha)^2 h} & 0 \\ 0 & \frac{(s+\beta)h - \left(1-e^{-(\beta+s)h/v}\right)v}{(s+\beta)^2 h} \end{bmatrix} \tag{3.67}$$

$$\Xi(s) = \begin{bmatrix} \frac{\left(1-e^{-(s+\alpha)h/v}\right)v}{(s+\alpha)h} & 0 \\ 0 & \frac{\left(1-e^{-(s+\beta)h/v}\right)v}{(s+\beta)h} \end{bmatrix} \tag{3.68}$$

$$\Upsilon(s) = \begin{bmatrix} e^{-(\alpha+s)h/v} & 0 \\ 0 & e^{-(\beta+s)h/v} \end{bmatrix} \tag{3.69}$$

$$\Omega(s) = \begin{bmatrix} \frac{1-e^{-(s+\alpha)h/v}}{s+\alpha} & 0 \\ 0 & \frac{1-e^{-(s+\beta)h/v}}{s+\beta} \end{bmatrix} \tag{3.70}$$

and where

$$\alpha = \frac{c_1 + c_2 + c_3 - c_4}{2} \tag{3.71}$$

$$\beta = \frac{c_1 + c_2 + c_3 + c_4}{2}. \tag{3.72}$$

On the other hand, the finite dimensional approximation results in a rational transfer function for approximating this entry, given by

$$\Theta^N_{ii}(s) = a^i_4(x_i - x_{i-1}) + \sum_{q\in U^i} h a^i_5 \begin{bmatrix} 1 \\ 0 \end{bmatrix}' \Gamma \left(\Psi^N(s) + \sum_{\substack{p\in U^i \\ p<q}} \Xi^N(s)\Upsilon^N(s)^{q-p-1}\Omega^N(s) \right) \Gamma^{-1} \begin{bmatrix} c_1 \\ 0 \end{bmatrix} \tag{3.73}$$

where

$$\Psi^N(s) = \begin{bmatrix} \frac{\alpha h + \left(\left(1+\frac{v}{\alpha h}\right)e^{-\alpha h/v} - \frac{v}{\alpha h}\right)v}{(v+(s+\alpha)h)\alpha} & 0 \\ 0 & \frac{\beta h + \left(\left(1+\frac{v}{\beta h}\right)e^{-\beta h/v} - \frac{v}{\beta h}\right)v}{(v+(s+\beta)h)\beta} \end{bmatrix} \tag{3.74}$$

$$\Xi^N(s) = \begin{bmatrix} \frac{\left(1-e^{-\alpha h/v}\right)\left(1+\frac{v}{\alpha h}\right)v}{v+(s+\alpha)h} & 0 \\ 0 & \frac{\left(1-e^{-\beta h/v}\right)\left(1+\frac{v}{\beta h}\right)v}{v+(s+\beta)h} \end{bmatrix} \tag{3.75}$$

$$\Upsilon^N(s) = \begin{bmatrix} \frac{\left(\alpha h + v - ve^{\alpha h/v}\right)\frac{s}{\alpha} + \alpha h + v}{v+(s+\alpha)h} e^{-\alpha h/v} & 0 \\ 0 & \frac{\left(\beta h + v - ve^{\beta h/v}\right)\frac{s}{\beta} + \beta h + v}{v+(s+\beta)h} e^{-\beta h/v} \end{bmatrix} \tag{3.76}$$

$$\Omega^N(s) = \begin{bmatrix} \frac{\alpha h + \left(\frac{v}{\alpha h} - \left(1+\frac{v}{\alpha h}\right)e^{-\alpha h/v}\right)(s+\alpha)h}{(v+(s+\alpha)h)\alpha} & 0 \\ 0 & \frac{\beta h + \left(\frac{v}{\beta h} - \left(1+\frac{v}{\beta h}\right)e^{-\beta h/v}\right)(s+\beta)h}{(v+(s+\beta)h)\beta} \end{bmatrix} \tag{3.77}$$

It is not difficult to see that $\Theta_{ii}(0) - \Theta^N_{ii}(0) = 0$. We will not show that the approximation converges in L_∞ norm but merely consider the error pointwise in s for $s \in \bar{\mathbb{C}}_+$. As the grid is refined and $h \to 0$ we have the following asymptotic properties:

$$\frac{\Psi(s) - \Psi^N(s)}{h^2} \to \frac{s}{3v^2}$$

$$
\begin{aligned}
\frac{\Xi(s)-\Xi^N(s)}{h} &\to \frac{s}{2v} \\
\frac{\Upsilon(s)-\Upsilon^N(s)}{h^2} &\to \frac{-s(s+\alpha)}{2v^2} \\
h\sum_{q\in U^i}\sum_{\substack{p\in U^i\\ p<q}}\left(\Upsilon(s)-\Upsilon^N(s)\right)^{q-p-1} &\to x_i - x_{i-1} \\
\frac{\Omega(s)-\Omega^N(s)}{h^3} &\to \frac{-s(s+\alpha)}{3v^3} \\
\frac{\Psi(s)}{h} &\to \frac{1}{2v} \\
\Xi(s) &\to 1 \\
h^2\sum_{q\in U^i}\sum_{\substack{p\in U^i\\ p<q}}\left(\Upsilon(s)\right)^{q-p-1} &\to \frac{v(x_i-x_{i-1})}{s+\alpha} - \frac{v^2(1-e^{-(s+\alpha)(x_i-x_{i-1})/v})}{(s+\alpha)^2} \\
\frac{\Omega(s)}{h} &\to \frac{1}{v} \\
\frac{\Psi^N(s)}{h} &\to \frac{1}{2v} \\
\Xi^N(s) &\to 1 \\
h^2\sum_{q\in U^i}\sum_{\substack{p\in U^i\\ p<q}}\left(\Upsilon^N(s)\right)^{q-p-1} &\to \frac{v(x_i-x_{i-1})}{s+\alpha} - \frac{v^2(1-e^{-(s+\alpha)(x_i-x_{i-1})/v})}{(s+\alpha)^2} \\
\frac{\Omega^N(s)}{h} &\to \frac{1}{v}
\end{aligned}
$$

The approximation error can be written as

$$
\begin{aligned}
\Theta_{ii}(s)-\Theta_{ii}^N(s) &= ha_5^i \begin{bmatrix} 1 \\ 0 \end{bmatrix}' \Gamma \Bigg(\sum_{q\in U^i}\left(\Psi(s)-\Psi^N(s)\right) \\
&\quad + \sum_{q\in U^i}\sum_{\substack{p\in U^i\\ p<q}}\left(\Xi(s)-\Xi^N(s)\right)\Upsilon(s)^{q-p-1}\Omega(s) \\
&\quad + \sum_{q\in U^i}\sum_{\substack{p\in U^i\\ p<q}}\Xi^N(s)\left(\Upsilon(s)-\Upsilon^N(s)\right)^{q-p-1}\Omega(s) \qquad (3.78) \\
&\quad + \sum_{q\in U^i}\sum_{\substack{p\in U^i\\ p<q}}\Xi^N(s)\Upsilon^N(s)^{q-p-1}\left(\Omega(s)-\Omega^N(s)\right)\Bigg)\Gamma^{-1}\begin{bmatrix} c_1 \\ 0 \end{bmatrix}.
\end{aligned}
$$

This allows us to conclude that the approximation error behaves like $constant \cdot h$ as the grid is refined.

3.5 Scaling Parameters for a Reduced Number of Uncertainties

We now describe the procedure of reducing the number of perturbation components. The idea is to reduce the number of inputs and outputs of the plant in such a way that there is some hope that this will induce a situation where the set of scaling parameters Λ that are suitable for the reduced plant will also be suitable for the original plant, when some of the parameters are used for several inputs and outputs of the original plant.

We consider the perturbation Δ_3 (cf. figure 2.4). We will reduce $\Delta_3 = \text{diag}(\Delta_{3,1}, \ldots, \Delta_{3,8})$ to the perturbation $\tilde{\Delta}_3 = \text{diag}(\tilde{\Delta}_{3,1}, \ldots, \tilde{\Delta}_{3,6})$, so that three components $\Delta_{3,1}, \Delta_{3,2}, \Delta_{3,3}$ are replaced by one single component $\tilde{\Delta}_{3,1}$. This means that in the H_∞ problem the disturbance input w and the to-be-controlled input z are each reduced by two components.

Assume that an H_∞ controller K has been found for the plant G, and denote the closed loop system by $M = \mathcal{F}(G, K)$. Choose a critical frequency ω_0, and let $\Delta(i\omega_0)$ be a destabilizing perturbation[1] of minimal norm at this frequency, defined as a complex matrix of minimal induced Euclidian norm that makes

$$\det(I - \Delta(i\omega_0)M(i\omega_0)) = 0. \tag{3.79}$$

Assume that $\Delta(\omega_0)$ is written on the form

$$\Delta(i\omega_0) = \phi\psi' \tag{3.80}$$

where

$$\phi = [\phi_1, \ldots, \phi_{2,5}, \phi_{3,1}, \phi_{3,2}, \phi_{3,3}, \phi_{3,4}, \ldots, \phi_{5,8}]' \tag{3.81}$$

$$\psi = [\psi_{1,1}, \ldots, \psi_{2,5}, \psi_{3,1}, \psi_{3,2}, \psi_{3,3}, \psi_{3,4}, \ldots, \psi_{5,8}]' \tag{3.82}$$

where ϕ and ψ have 30 and 38 components respectively, indexed according to the indices of w and z in section 2.4.4. This assumption is without loss of generality, see Zhou et al.[63, cp.11].

We construct $\tilde{\Delta}$ from $\Delta(i\omega_0)$ by replacing three columns by one single column and three rows by one row, in the following manner,

$$\tilde{\Delta} = \tilde{\phi}\tilde{\psi}' \tag{3.83}$$

where

$$\tilde{\phi} = [\phi_1, \ldots, \phi_{2,5}, \sqrt{|\phi_{3,1}|^2 + |\phi_{3,2}|^2 + |\phi_{3,3}|^2}, \phi_{3,4}, \ldots, \phi_{5,8}]' \tag{3.84}$$

$$= [\tilde{\phi}_1, \ldots, \tilde{\phi}_{2,5}, \tilde{\phi}_{3,1}, \tilde{\phi}_{3,2}, \ldots, \tilde{\phi}_{5,8}]' \tag{3.85}$$

$$\tilde{\psi} = [\psi_{1,1}, \ldots, \psi_{2,5}, \sqrt{|\psi_{3,1}|^2 + |\psi_{3,2}|^2 + |\psi_{3,3}|^2}, \psi_{3,4}, \ldots, \psi_{5,8}]' \tag{3.86}$$

$$= [\tilde{\psi}_{1,1}, \ldots, \tilde{\psi}_{2,5}, \tilde{\psi}_{3,1}, \tilde{\psi}_{3,2}, \ldots, \tilde{\psi}_{5,8}]'. \tag{3.87}$$

[1] The term 'destabilizing' is not to be taken literally, see Packard and Doyle[48]

Thus we obtain the property $\|\tilde{\Delta}\| = \|\Delta(i\omega_0)\|$.

Define

$$\Pi_\phi = \begin{bmatrix} I & 0 & 0 \\ 0 & \frac{1}{\tilde{\phi}_{3,1}} \begin{bmatrix} \phi_{3,1} \\ \phi_{3,2} \\ \phi_{3,3} \end{bmatrix} & 0 \\ 0 & 0 & I \end{bmatrix}, \quad \Pi_\psi = \begin{bmatrix} I & 0 & 0 \\ 0 & \frac{1}{\tilde{\psi}_{3,1}} \begin{bmatrix} \psi_{3,1} & \psi_{3,2} & \psi_{3,3} \end{bmatrix} & 0 \\ 0 & 0 & I \end{bmatrix} \tag{3.88}$$

where I denotes the identity matrix in appropriate dimension so that there holds $\phi = \Pi_\phi \tilde{\phi}$, $\Pi_\phi^* \phi = \tilde{\phi}$, $\psi' = \tilde{\psi}' \Pi_\psi$, $\psi' \Pi_\psi^* = \tilde{\psi}'$. We also define

$$\tilde{M} = \Pi_\psi M \Pi_\phi. \tag{3.89}$$

We now show that $\tilde{\Delta}$ is a smallest destabilizing perturbation for $\tilde{M}$. $\tilde{\Delta}$ is destabilizing, since there holds

$$\begin{aligned} 0 &= \det(I - \phi\psi' M(i\omega_0)) = 1 - \psi' M(i\omega_0)\phi \\ &= 1 - \tilde{\psi}' \Pi_\psi M(i\omega_0) \Pi_\phi \tilde{\phi} = 1 - \tilde{\psi}' \tilde{M} \tilde{\phi} = \det(I - \tilde{\phi}\tilde{\psi}' \tilde{M}). \end{aligned} \tag{3.90}$$

It is also of minimal norm. Suppose not, then there exists $\bar{\Delta}$ which is destabilizing for $\tilde{M}$ and with $\|\bar{\Delta}\| < \|\tilde{\Delta}\|$. Consequently, (3.90) would imply that $\Pi_\phi \bar{\Delta} \Pi_\psi$ is destabilizing for $M(i\omega_0)$. But then there would hold

$$\|\Pi_\phi \bar{\Delta} \Pi_\psi\| \leq \|\Pi_\phi\| \|\bar{\Delta}\| \|\Pi_\psi\| < \|\tilde{\Delta}\| = \|\Delta(i\omega_0)\|, \tag{3.91}$$

which contradicts the assumption that $\Delta(i\omega_0)$ is of minimal norm.

In order to exploit the above observations, we would like to let $\tilde{M}$ represent the reduced closed loop system at frequency ω_0. However, the algorithm for improving the scaling parameters is based on the LMI (2.47), where it is assumed that the system matrices are real. Define therefore $\tilde{w}$ and $\tilde{z}$ by the relations

$$\begin{bmatrix} w_{3,1} \\ w_{3,2} \\ w_{3,3} \end{bmatrix} = \begin{bmatrix} \pm|\phi_{3,1}| \\ \pm|\phi_{3,2}| \\ \pm|\phi_{3,3}| \end{bmatrix} \frac{1}{\tilde{\phi}_{3,1}} \tilde{w}_{3,1} \tag{3.92}$$

$$\tilde{z}_{3,1} = \frac{1+\epsilon}{\tilde{\psi}_{3,1}} \begin{bmatrix} \pm|\psi_{3,1}| & \pm|\psi_{3,2}| & \pm|\psi_{3,3}| \end{bmatrix} \begin{bmatrix} z_{3,1} \\ z_{3,2} \\ z_{3,3} \end{bmatrix}, \tag{3.93}$$

where the sign is chosen so that the complex vectors $[\phi_{3,1},\ \phi_{3,2},\ \phi_{3,3}]$, $[\psi_{3,1},\ \psi_{3,2},\ \psi_{3,3}]$ are matched as well as possible. As an attempt to imitate the destabilization scenario made up by $\tilde{M}$ and $\tilde{\Delta}$, we modify the closed looop system so that $\tilde{w}_{3,1}$ and $\tilde{z}_{3,1}$ are replacing $[w_{3,1}, w_{3,2}, w_{3,3}]'$ and $[z_{3,1}, z_{3,2}, z_{3,3}]'$, respectively. The parameter ϵ is to be chosen in a heuristic manner.

We chose the critical frequency ω_0 close to the origin, and in the formula (3.93) we chose ϵ to be, for example, 0.025 or 0.05. The adjustment of ϵ was carried out based on knowledge of the destabilizing perturbation at the critical frequency. A destabilizing perturbation of of minimal norm of the type (3.80) is provided by the toolbox [33]. With an adequate set of scaling parameters, and assuming that the critical frequency ω_0 is essential for the control problem, the magnitudes of the entries of this perturbation should have a reasonably homogenous distribution. A given pattern of the entries of $\Delta(\omega_0)$ may indicate, say, that the scaling parameters have been chosen for a plant where the signal $\tilde{z}_{3,1}$ has too little weight, compared to the situation of the plant for which the H_∞ controller is designed, and in this case ϵ should be increased.

The procedure described above is based on the naive idea that a small modification of the closed loop system based on the destabilization scenario at a single critical frequency will give an adequate representation of the closed loop system with respect to the selection of scaling parameters using an LMI. Another weak point of the procedure is that, in the formulae (3.92) and (3.93) important information about the phase is lost. A natural consequence of these shortcomings is that the class of control problems for which this procedure is succesful, is rather restricted. It is clear that this procedure accentuates the lack of flexibility across frequencies that appears when the H_∞ problem is scaled using constant scaling parameters. However, the results obtained for the current case study are encouraging, at least for this type of problems.

3.6 Zeros in the Right Half Plane

It is well known that the presence of zeros in the right half plane imposes limitations on what can be achieved with a feedback design, see e.g. Doyle et al.[20] and references therein. On the other hand, for multiple-input-multiple-output systems the presense of such zeros is often less severe than it is for single-input-single-output systems. Nevertheless we show in this section that $\Theta(s)$ has no zeros in the right half plane.

Our design strategy is to base the actual synthesis algorithm on a finite dimensional system and afterwards carry out the robust performance test for the infinite dimensional system. With this strategy there is a catch to be taken into account. If the infinite dimensional plant has a zero that is not shared by the finite dimensional counterpart, then it may happen that the design limitaions imposed by this zero are not recognized by the synthesis algorithm.

Our system is exponentially stable, and so are all of the subsystems that we use for building the system. For a given transfer matrix we can therefore define the zeros in the right half plane to be those $s \in \overline{\mathbb{C}^+}$ where the transfer matrix loses rank, see e.g. Curtain and Zwart[18, def.7.2.18].

Some of the subsystems have diagonal transfer matrix and the diagonal entries

are first order systems which clearly do not contribute with any zeros, and neither does the time delay in the pipes that take the water to the upper tanks. Therefore the zeros must stem from the transfer matrices $\Theta(s)$ and $\Pi(s)$ if there are any. An interpretation of the possible damage caused by such zeros are that, for example, a zero of $\Theta(s)$ may prevent disturbance signals at certain frequencies from travelling to the measure output y. On the other hand, a zero of $\Pi(s)$ may cause a limitation of the tracking ability of the system.

One way of seeking a quantification of such limitations is to consider the closed loop system

$$G_{11} + G_{12}K(I - G_{22}K)^{-1}G_{21}. \tag{3.94}$$

If $G_{21}(s)$ has a zero s_0 in the right half plane, then there exists a vector w_0 such that

$$(G_{12}(s_0)K(s_0)(I - G_{22}(s_0)K(s_0))^{-1}G_{21}(s_0))w_0 = 0. \tag{3.95}$$

This would imply that

$$\begin{aligned} &\|G_{11} + G_{12}K(I - G_{22}K)^{-1}G_{21}\|_\infty && (3.96)\\ &= \sup_{s\in\overline{\mathbb{C}^+}} \|G_{11}(s) + G_{12}(s)K(s)(I - G_{22}(s)K(s))^{-1}G_{21}(s)\| && (3.97)\\ &\geq \frac{\|G_{11}(s_0)w_0\|}{\|w_0\|}, && (3.98)\end{aligned}$$

regardless of the controller K. Disregarding the uncertainty frequency weights, $G_{21}(s)$ has a zero in s_0 if and only if $\Theta(s)$ does.

We will now show that $\Theta(s)$ has no right half plane zeros. It is a quadratic, lower triangular matrix, so the zeros can be determined by simply examining each of the diagonal entries. The task is thus to show that the function

$$\begin{aligned}\Theta_{ii}(s) &= a_5^i \frac{c_1(-c_1-c_2+c_3+c_4)}{(c_1+c_2+c_3-c_4+2s)c_4}\left(x_i - x_{i-1} - \frac{2v(1-\zeta^s(x_i-x_{i-1}))}{c_1+c_2+c_3-c_4+2s}\right)\\ &\quad + a_5^i \frac{c_1(c_1+c_2-c_3+c_4)}{(c_1+c_2+c_3+c_4+2s)c_4}\left(x_i - x_{i-1} - \frac{2v(1-\eta^s(x_i-x_{i-1}))}{c_1+c_2+c_3+c_4+2s}\right)\\ &\quad + (x_i - x_{i-1})a_4^{ii}\end{aligned}$$

has no zeros in the right half plane. To begin with we carry out the following useful calculation, with $\alpha > 0$,

$$\begin{aligned}\int_{x_{i-1}}^{x_i}\int_{x_{i-1}}^{x} e^{-(\alpha+s)(x-y)/v}dydx &= \int_{x_{i-1}}^{x_i}\int_{y}^{x_i} e^{-(\alpha+s)(x-y)/v}dxdy && (3.99)\\ &= \int_{x_{i-1}}^{x_i}\int_{0}^{x_i-y} e^{-(\alpha+s)\tau/v}d\tau dy\\ &= \int_{0}^{x_i-x_{i-1}}\int_{x_{i-1}}^{x_i-\tau} e^{-(\alpha+s)\tau/v}dyd\tau\\ &= \int_{0}^{x_i-x_{i-1}}(x_i - x_{i-1} - \tau)e^{-(\alpha+s)\tau/v}d\tau,\end{aligned}$$

where we have used the substitution $\tau = x - y$. It is not hard to see that changing the order of integration is justified. Notice that we can write

$$\begin{aligned}\Theta_{ii}(s) &= \frac{a_5^i c_1(-c_1 - c_2 + c_3 + c_4)}{2vc_4} \int_{x_{i-1}}^{x_i} \int_{x_{i-1}}^{x} e^{-(c_1+c_2+c_3-c_4+2s)(x-y)/2v} dy dx \\ &+ \frac{a_5^i c_1(c_1 + c_2 - c_3 + c_4)}{2vc_4} \int_{x_{i-1}}^{x_i} \int_{x_{i-1}}^{x} e^{-(c_1+c_2+c_3+c_4+2s)(x-y)/2v} dy dx \\ &+ a_4^i(x_i - x_{i-1}). \end{aligned} \tag{3.100}$$

We now write $s = \sigma + \hat{i}\omega$, where $\hat{i}$ denotes the imaginary unit and $\sigma \geq 0$. Combining (3.99) and (3.100) we obtain

$$\begin{aligned}\Theta_{ii}(\sigma + \hat{i}\omega) &= \frac{a_5^i c_1(-c_1 - c_2 + c_3 + c_4)}{2vc_4} \\ &\int_0^{x_i - x_{i-1}} (x_i - x_{i-1} - \tau) e^{-(c_1+c_2+c_3-c_4+2\sigma)\tau/2v} e^{-\hat{i}\omega\tau/v} d\tau \\ &+ \frac{a_5^i c_1(c_1 + c_2 - c_3 + c_4)}{2vc_4} \\ &\int_0^{x_i - x_{i-1}} (x_i - x_{i-1} - \tau) e^{-(c_1+c_2+c_3+c_4+2\sigma)\tau/2v} e^{-\hat{i}\omega\tau/v} d\tau \\ &+ a_4^i(x_i - x_{i-1}). \end{aligned} \tag{3.101}$$

Let us consider the imaginary part of the expression (3.101), assuming that $\sigma \geq 0, \omega > 0$. Notice that it can be shown that $c_4 > |c_1 + c_2 - c_3|$ and $c_4 < c_1 + c_2 + c_3$. The expression $(x_i - x_{i-1} - \tau)e^{-(c_1+c_2+c_3-c_4+2\sigma)\tau/2v}$ is a decreasing function of τ, $0 < \tau < x_i - x_{i-1}$, whence it is clear that the first term has strictly negative imaginary part. A similar argument applies to the second term, and since the third term is real, it is clear that (3.101) has strictly negative imaginary part when $\sigma \geq 0, \omega > 0$. For $\sigma \geq 0, \omega < 0$ the above argument can be repeated but with the change that the imaginary parts in (3.101) are strictly positive. For $\omega = 0$ all of the three terms of (3.101) are real and strictly positive. This allows us to conclude that $\Theta(s)$ has no zeros in the closed right half plane.

Chapter 4

H_∞-Control of Linear Systems with Almost Periodic Inputs

4.1 Introduction

Recently, Shaked and de Souza[57] obtained formulas for a two-degrees-of-freedom design of an H_∞ controller where à priori knowledge of future values of the tracking trajectory and the forcing terms could be taken into account. This feature was new compared to earlier approaches based on casting the tracking problem into a standard H_∞ format. The standard problem approach involves representing the reference signal by an unknown disturbance signal, and it is likely that this leads to a conservative design in cases where the reference signal is actually known in advance.

The result of Shaked and de Souza was formulated for finite-horizon tracking problems and for finite-dimensional, time-varying systems. The result presented in the present chapter is an infinite-horizon analogue of their result for infinite-dimensional time-invariant systems, and at the same time it allows for a richer class of inputs. One motivation for considering infinite-horizon problems is that the formulas for the controller involve algebraic Riccati equations instead of Riccati differential equations. This means that the controller is easier to implement, and, in particular, controller order reduction algorithms are available. A motivation for considering an infinite-dimensional setting for H_∞-tracking is that certain applications are most naturally modelled in this setting (see e.g. Banks et al.[5]).

Our approach is different from the usual infinite-horizon approach in that we do not specify the initial condition, but we assume that the signals are defined on the whole real axis. A special feature is the rich class of input signals we allow, namely a class of generalized almost periodic functions. Roughly speaking, we consider signals with a square summable spectrum, where the frequencies can be arbitrary real numbers. This class contains the periodic functions as a subset.

Notice that these input signals are excluded from the L^2 class of inputs that are usually considered in H_∞ problems, and also from the class of sinusoids considered in the most common frequency domain interpretation.

Control problems with periodic inputs are interesting mainly for three reasons. Firstly, one can choose to formulate a finite-horizon tracking problem as a periodic problem in order to obtain algebraic Riccati equations and consequently, a simpler control law. Secondly, some control problems are naturally formulated as periodic control problems, see Guardabassi et al.[31] for some examples and see Banks et al.[5] for a case study of a problem with a periodic forcing term. Thirdly, a periodic setup allows you to track signals that do not tend asymptotically to zero.

Unfortunately, a theory formulated for periodic signals also has its limitations; it does not cover situations in which there occur, for example, two periodic forcing terms of different periods. The reason is that the space of periodic functions lacks an important structural property: it is not a vector space. For instance, the sum of two periodic functions is not a periodic function, unless the ratio of their periods is rational. This illustrates the need for a function space that generalizes the concept of periodic functions in such a way that it has the vector space property. Almost periodic functions (see Bohr[8], Corduneanu[12], Levitan and Zhikov[45]), do form such a space.

When formulating a tracking problem on infinite time interval where the tracking trajectory does not asymptote to zero, one often faces the difficulty that the usual cost function is not finite. This is the case in the LQ problem and in the regular H_∞-problem. In the LQ case several authors (e.g. Anderson and Moore[2], Banks et al.[6], Da Prato and Ichikawa [51]) have suggested to remedy this by considering an average cost function, and for the H_∞ case we will in this chapter use the same idea. In the case of almost periodic inputs, the average cost function is particularly interesting, since it can be written in terms of an inner product on the space of almost periodic functions. The completion of this inner product space produces the appropriate Hilbert space of generalized almost periodic functions. The use of signals from this Hilbert space as input signals for semigroup control systems has been studied in some detail in Jacob et al.[36].

4.2 Preliminaries

We shall be concerned with almost periodic functions with values in a Hilbert space. Background material for this can be found in Corduneanu[12], Levitan and Zhikov[45]. In the literature one finds three different definitions of almost periodic functions. Probably the most intuitive definition is the original one by H. Bohr, where the concept of a period is replaced by an almost period. When adapted to Hilbert space valued functions, this definition reads as follows.

Definition 3 *Let H be a separable Hilbert space, and let $f(\cdot)$ be a continuous function of $t \in \mathbb{R}$ with values in H. f is said to be* almost periodic *and belong to $AP(H)$ if, for any number $\varepsilon > 0$, one can find a number $l(\varepsilon) > 0$ such that any interval on the real line of length $l(\varepsilon)$ contains at least one point τ with the property that*

$$\|f(t+\tau) - f(t)\|_H < \varepsilon \quad \forall t \in \mathbb{R}.$$

In this case τ is called an ε-almost period *of $f(t)$.*

Notice that in the case that $f(\cdot)$ is a continuous, periodic function, one can take ε arbitrarily small, $l(\varepsilon)$ should be larger than the period of the function, and τ can be chosen to be equal to the period.

Some basic properties of $f \in AP(H)$ are that $\|f(t)\|_H$ is uniformly bounded on the real axis and that $f(t)$ is continuous uniformly in t. Furthermore, $AP(H)$ is a Banach space when equipped with the norm

$$\sup_{t \in \mathbb{R}} \|f(t)\|_H.$$

If $f \in AP(H)$, then $f(t) \in H$ is defined pointwise in t. Next we define an abstract space where this is not the case. For quadratic control problems concerning almost periodic functions it is convenient to work with

$$\langle f, g \rangle_{ap} := \lim_{T \to \infty} \frac{1}{T} \int_0^T \langle f(t), g(t) \rangle_H dt, \tag{4.1}$$

which is an inner product on $AP(H)$. It is well known that the appropriate way of handling H_∞ control problems in the time domain is to consider each signal as an element in a Hilbert space. For our purpose, we consider the Hilbert space $AP_2(H)$, defined as follows.

Definition 4 *The completion of $AP(H)$ with respect to the inner product $\langle \cdot, \cdot \rangle_{ap}$ is denoted by $AP_2(H)$.*

This idea was used for LQ control problems in Da Prato and Ichikawa [51]. This Hilbert space has the advantage that it generalizes the concept of almost periodic functions to functions that are not necessarily continuous. A disadvantage of the space $AP_2(H)$ is that it contains some elements that cannot be represented by functions in a natural way, see Jacob et al.[36], and Riesz and Sz-Nagy[53]. To cope with this situation we do the following: Every element of $AP_2(H)$ is characterized by a Cauchy sequence of almost periodic functions. For some of the elements this Cauchy sequence converges to an almost periodic function, and in this case we let this function represent the element. In the other cases we let the element be represented by a Cauchy sequence of almost periodic functions, and for such elements we obtain the properties that we need by continuous extension and

limit arguments. Even the norm of such elements is defined by a limit argument. Background material for this type of arguments can be found in Kreyszig[39].

The space $AP_2(H)$ is closely related to a space of generalized almost periodic functions introduced by A.S. Besicovitch, and is usually in the literature called the space of Besicovitch-almost periodic functions. The interested reader may consult Besicovitch[7] and Bohr and Følner[9] for details. For an alternative characterization of the space $AP_2(H)$, see e.g. Shubin[58].

In the analysis of almost periodic functions an important role is played by a generalized Fourier transform. For $f \in AP(H)$, consider the Bohr transform (cf. Levitan and Zhikov[45])

$$a_f(\lambda) = \lim_{T\to\infty} \frac{1}{T} \int_0^T f(t) e^{-i\lambda t} dt \ , \quad \lambda \in \mathbb{R}. \tag{4.2}$$

For every $\lambda \in \mathbb{R}$, $a_f(\lambda) \in H$ is well defined, and the set $\{\lambda \in \mathbb{R} \mid a_f(\lambda) \neq 0\}$ is countable. Furthermore, we have the Parseval relation

$$\|f\|_{ap}^2 = \sum_{\lambda\in\mathbb{R}} \|a_f(\lambda)\|_H^2, \tag{4.3}$$

where $\|\cdot\|_{ap}$ is the norm induced by the inner product (4.1).

For our mathematical analysis it turns out to be convenient to work with trigonometric polynomials of the type

$$P_N(t) = \sum_{k=1}^{N} a_k e^{i\lambda_k t} \ , \quad a_k \in H, \ \lambda_k \in \mathbb{R}, \ N \in \mathbb{N}. \tag{4.4}$$

We denote the space of such trigonometric polynomials by $TP(H)$. Trigonometric polynomials are natural for approximating almost periodic functions. Approximation in the norm $\|\cdot\|_{ap}$ is obtained directly from the Bohr transform $a_f(\lambda)$ so that in this sense we may write

$$f(t) \sim \sum_{\lambda\in\mathbb{R}} a_f(\lambda) e^{i\lambda t}. \tag{4.5}$$

Approximation uniformly on the real line can be obtained by using the Bohr transform in connection with a special summation method (cf. Levitan and Zhikov[45]). Given an arbitrary series of the form

$$\sum_{k=1}^{\infty} a_k e^{i\lambda_k t} \ , \quad a_k \in H, \ \lambda_k \in \mathbb{R},$$

it can be very hard to determine whether it converges to a function. However, if it is known how the series was constructed, then the question of convergence does sometimes have a simple answer. For example, as mentioned above, a trigonometric series obtained from an almost periodic function using the Bohr transform converges in the quadratic mean.

Example 5 To illustrate that the space $AP_2(H)$ contains elements that should not be considered as functions, consider the sequence $\{f_n\}$ in $AP(\mathbb{R})$ given by

$$f_n(t) = \sum_{k=1}^{n} \frac{2}{k} \cos \frac{t}{k} = \sum_{k=1}^{n} \frac{1}{k} \left(e^{it/k} + e^{-it/k} \right).$$

By calculating

$$\|f_n - f_m\|_{ap} = \sum_{k=m+1}^{n} \frac{2}{k^2}, \quad \text{with } n > m,$$

we find that $\{f_n\}$ is a Cauchy sequence in $AP_2(\mathbb{R})$, and therefore it converges in this space. Notice now that $f_n(t)$ does not converge in any point t, and neither does f_n converge in the topology of $L^1_{loc}(0, \infty; \mathbb{R})$. □

It can be shown (see e.g. Jacob et al.[36]), that the space $AP_2(H)$ may formally be represented by trigonometric series such that $\sum_{k=1}^{\infty} \|a_k\|_H^2 < \infty$. Using trigonometric polynomials that may be viewed as truncated trigonometric series, we carry out the mathematical analysis in such a way that we do not have to resolve the question of whether such a series converges to a function.

4.3 Main Results

We consider infinite-dimensional systems of the form

$$\dot{x} = Ax + B_1 w + B_2 u + B_3 r, \quad t \in \mathbb{R} \tag{4.6}$$

$$z = C_1 x + D_{12} u + D_{13} r \tag{4.7}$$

$$y = C_2 x + D_{21} w \tag{4.8}$$

where $x(t) \in H$ is the state, $u(t) \in U$ is the control, $w(t) \in W$ is the unknown disturbance, $z(t) \in Z$ is the to-be-controlled output, $y(t) \in Y$ is the measured output, and $r(t) \in R$ is a known external signal. H, U, W, Z, Y and R are all real separable Hilbert spaces. We assume that A generates a strongly continuous semigroup $S(t)$ on H, and $B_1, B_2, B_3, C_1, C_2, D_{12}, D_{13}, D_{21}$ are bounded operators, i.e. $B_1 \in \mathcal{L}(W, H)$, $C_1 \in \mathcal{L}(H, Z)$, $D_{12} \in \mathcal{L}(U, Z)$, etc. In the tracking problem that can be considered in this setting, the trajectory to be tracked is $-D_{13}r$, and $B_3 r$ is an external forcing term. Thus $B_3 r$ is a known external forcing term, while $B_1 w$ is an unknown external forcing term. For background material on infinite-dimensional linear systems, see Curtain and Zwart[18].

The input signals are considered in the following spaces: $w \in AP_2(W)$, $u \in AP_2(U)$ and $r \in AP_2(R)$. In the abstract setup it is thus not assumed that the input signals are defined pointwise in t, nor almost everywhere, so the results should be understood in terms of approximating, almost periodic functions. The

solutions to (4.6) that we consider are, with $w \in AP(W)$, $u \in AP(U)$ and $r \in AP(R)$, of the form

$$x(t) = \int_{-\infty}^{t} S(t-\tau)[B_1 w(\tau) + B_2 u(\tau) + B_3 r(\tau)]d\tau. \tag{4.9}$$

If the semigroup $S(t)$ is exponentially stable, then this convolution integral defines an almost periodic function $x(\cdot)$. In the case that the system is merely exponentially stabilizable, the convolution integral still makes sense for some control signals $u(\cdot)$.

The result resembles the standard H_∞ result, in that the criterion for the existence of an admissible controller is given in terms of Riccati equations. However, the usual disturbance attenuation bound is replaced by the inequality

$$\|z\|_{ap}^2 \leq \gamma^2 \|w\|_{ap}^2 + J^0, \tag{4.10}$$

where $J^0 \in \mathbb{R}$ depends on the signal r and on the stabilizing solution to the (control) Riccati equation. As it will appear from the proof, J^0 is determined as the value of a game, where the controller plays against nature.

4.3.1 The State Feedback Result

Here we consider the special case where $C_2 = I$ and $D_{21} = 0$. The standard regularity assumption is (cf. van Keulen et al.[60])

H 1

1. There exists an $\varepsilon > 0$ such that for all $(\omega, x, u) \in \mathbb{R} \times D(A) \times U$ satisfying $\hat{\imath}\omega x = Ax + B_2 u$, there holds $\|C_1 x + D_{12} u\|_Z^2 \geq \varepsilon \|x\|_H^2$
2. $D_{12}^* D_{12}$ is coercive.

To simplify the notation we define

$$V_1 = (D_{12}^* D_{12})^{-1} \tag{4.11}$$

$$F_\infty = V_1(B_2^* P + D_{12}^* C_1). \tag{4.12}$$

Proposition 6 *Consider the system (4.6)-(4.7). Suppose that H1 holds, and that $r \in AP_2(R)$ is an à priori known signal. With $0 < \gamma$ and $0 \leq P = P^* \in \mathcal{L}(H)$, and*

$$\tilde{A} := A - B_2 F_\infty + \gamma^{-2} B_1 B_1^* P, \tag{4.13}$$

the following statements are equivalent:

1. *P satisfies*

$$\begin{aligned} 0 = {} & \langle (A - B_2 V_1 D_{12}^* C_1)x, Py\rangle_H + \langle Px, (A - B_2 V_1 D_{12}^* C_1)y\rangle_H \\ & + \langle P(\gamma^{-2} B_1 B_1^* - B_2 V_1 B_2^*)Px, y\rangle_H + \langle C_1^*(I - D_{12} V_1 D_{12}^*)C_1 x, y\rangle_H \end{aligned} \tag{4.14}$$

for all $x, y \in D(A)$, and $\tilde{A}$ generates an exponentially stable semigroup $S_{\tilde{A}}(t)$.

2. *There exists an exponentially stabilizing state-feedback control law such that there holds*

$$\|z\|_{ap}^2 \leq \gamma^2 \|w\|_{ap}^2 + J^0 \qquad \forall w \in AP_2(W), \tag{4.15}$$

where

$$J^0 = \|D_{13} r\|_{ap}^2 + \gamma^{-2} \|B_1^* \theta\|_{ap}^2 - \|V_1^{1/2}(B_2^* \theta + D_{12}^* D_{13} r)\|_{ap}^2 + 2\langle \theta, B_3 r \rangle_{ap}, \tag{4.16}$$

where $\theta \in AP_2(H)$ is given by

$$\theta(t) = -\int_t^\infty S_{\tilde{A}}^*(\tau - t)[F_\infty^* D_{12}^* D_{13} - P B_3 - C_1^* D_{13}] r(\tau) d\tau, \tag{4.17}$$

and such that in the special case that $r = 0$, there exists $\varepsilon > 0$ such that

$$\|z\|_{ap}^2 \leq (\gamma^2 - \varepsilon)\|w\|_{ap}^2 \qquad \forall w \in AP_2(W). \tag{4.18}$$

Such a control law is given by

$$u = -F_\infty x - V_1(D_{12}^* D_{13} r + B_2^* \theta). \tag{4.19}$$

We refer to the solution $P \geq 0$ such that $S_{\tilde{A}}(t)$ is exponentially stable as the stabilizing solution to the Riccati equation.

Remark 7 For an arbitrary $r \in AP_2(H)$, the convolution integral (4.17) is not necessarily well defined in the usual sense. In this case the convolution integral must be understood in the extended sense defined by lemma 14. □

4.3.2 The Measurement Feedback Result

Here we consider the case where the control law is to be based on disturbance-corrupted measurements. We introduce an additional standard regularity assumption on the system, see van Keulen[59, p.131].

H 2

1. *There exists an $\varepsilon > 0$ such that for all $(\omega, x, y) \in \mathbb{R} \times D(A) \times Y$ satisfying $\hat{i}\omega x = A^* x + C_2^* y$, there holds $\|B_1^* x + D_{21}^* y\|_W^2 \geq \varepsilon \|x\|_H^2$*
2. *$D_{21} D_{21}^*$ is coercive.*

To simplify the notation we introduce

$$V_2 = (D_{21} D_{21}^*)^{-1}. \tag{4.20}$$

Proposition 8 *Consider the system (4.6)-(4.8). Suppose that H1 and H2 hold, and that $r \in AP_2(R)$ is an à priori known signal. With $0 < \gamma$, $0 \leq P = P^* \in \mathcal{L}(H)$ and $0 \leq Q = Q^* \in \mathcal{L}(H)$, the following statements are equivalent:*

1. *Q satisfies*

$$\begin{aligned} 0 &= \langle (A^* - C_2^* V_2 D_{21} B_1^*)x, Qy\rangle_H + \langle Qx, (A^* - C_2^* V_2 D_{21} B_1^*)y\rangle_H \\ &\quad + \langle Q(\gamma^{-2} C_1^* C_1 - C_2^* V_2 C_2)Qx, y\rangle_H + \langle B_1(I - D_{21}^* V_2 D_{21}) B_1^* x, y\rangle_H \end{aligned} \tag{4.21}$$

for all $x, y \in D(A)$, and

$$A^* - C_2^* V_2 (C_2 Q + D_{21} B_1^*) + \gamma^{-2} C_1^* C_1 Q \tag{4.22}$$

generates an exponentially stable semigroup. Furthermore, item 1 of proposition 6 holds, and P and Q satisfy the coupling condition

$$r_\sigma(PQ) < \gamma^2, \tag{4.23}$$

where r_σ denotes the spectral radius.

2. *There exists an exponentially stabilizing measurement-feedback control law such that there holds*

$$\|z\|_{ap}^2 \leq \gamma^2 \|w\|_{ap}^2 + J^0 \qquad \forall w \in AP_2(W) \tag{4.24}$$

where J^0 is given by (4.16), and in the special case that $r = 0$, there exists $\varepsilon > 0$ such that

$$\|z\|_{ap}^2 \leq (\gamma^2 - \varepsilon)\|w\|_{ap}^2. \tag{4.25}$$

Such a control law is given by

$$u = -F_\infty \hat{x} - V_1 (D_{12}^* D_{13} r + B_2^* \theta) \tag{4.26}$$

where θ is defined by (4.17) and $\hat{x}$ is given by

$$\begin{aligned} \hat{x}(t) &= \int_{-\infty}^{t} S_{\tilde{A} - L C_F}(t-\tau)[Ly(\tau) + (\gamma^{-2}(B_1 - LD_{21})B_1^* - B_2 V_1 B_2^*)\theta(\tau) \\ &\quad + (B_3 - B_2 V_1 D_{12}^* D_{13}) r(\tau)] d\tau \end{aligned} \tag{4.27}$$

where

$$C_F = C_2 + \gamma^{-2} D_{21} B_1^* P \tag{4.28}$$

$$L = (I - \gamma^{-2} QP)^{-1}(QC_2^* + B_1 D_{21}^*) V_2. \tag{4.29}$$

Remark 9 For an arbitrary $r \in AP_2(H)$, the convolution integral (4.27) is not necessarily well defined in the usual sense. In this case the convolution integral must be understood in the extended sense defined by lemma 14. □

4.3.3 Loop-shifting

For completeness of the measurement feedback result we will in this section consider systems of the more general type

$$\begin{aligned} \dot{x} &= Ax + B_1 w + B_2 u + B_3 r \ , \quad t \in \mathbb{R} && (4.30)\\ z &= C_1 x + D_{11} w + D_{12} u + D_{13} r && (4.31)\\ y &= C_2 x + D_{21} w + D_{22} u + D_{23} r, && (4.32) \end{aligned}$$

where, as before, all input and output operators are bounded. The idea is to use the well-known loop-shifting formulas from Safonov et al.[55], Green and Limebeer[30, section 4.6]. The presence of B_3, D_{13}, D_{23} is handled by a simple modification of these transformations.

Assuming that the conditions (4.44)-(4.45) are satisfied, there exists a static feedback R_∞ such that

$$\| D_{11} + D_{12} R_\infty (I - D_{22} R_\infty)^{-1} D_{21} \|_{\mathcal{L}(W,Z)} < \gamma. \tag{4.33}$$

Assuming that such an R_∞ has been constructed, it is applied to the plant as shown in figure 4.1, and this leads to the transformations

$$\begin{aligned} \bar{A} &= A + B_2 (I - R_\infty D_{22})^{-1} R_\infty C_2 \\ \bar{B}_1 &= B_1 + B_2 (I - R_\infty D_{22})^{-1} R_\infty D_{21} \\ \bar{B}_2 &= B_2 (I - R_\infty D_{22})^{-1} \\ \bar{B}_3 &= B_3 + B_2 (I - R_\infty D_{22})^{-1} R_\infty D_{23} \\ \bar{C}_1 &= C_1 + D_{12} (I - R_\infty D_{22})^{-1} R_\infty C_2 \\ \bar{C}_2 &= (I - D_{22} R_\infty)^{-1} C_2 \\ \bar{D}_{11} &= D_{11} + D_{12} (I - R_\infty D_{22})^{-1} R_\infty D_{21} \\ \bar{D}_{12} &= D_{12} (I - R_\infty D_{22})^{-1} \\ \bar{D}_{13} &= D_{13} + D_{12} (I - R_\infty D_{22})^{-1} R_\infty D_{23} \\ \bar{D}_{21} &= (I - D_{22} R_\infty)^{-1} D_{21} \\ \bar{D}_{22} &= D_{22} (I - R_\infty D_{22})^{-1} \\ \bar{D}_{23} &= (I - D_{22} R_\infty)^{-1} D_{23}. \end{aligned} \tag{4.34}$$

Next we introduce the transformation Θ as shown in figure 4.1, where

$$\Theta = \begin{bmatrix} \Theta_{11} & \Theta_{12} \\ \Theta_{21} & \Theta_{22} \end{bmatrix} = \gamma^{-1} \begin{bmatrix} \gamma^{-1} \bar{D}_{11} & (I - \gamma^{-2} \bar{D}_{11} \bar{D}_{11}^*)^{\frac{1}{2}} \\ -(I - \gamma^{-2} \bar{D}_{11}^* \bar{D}_{11})^{\frac{1}{2}} & \gamma^{-1} \bar{D}_{11}^* \end{bmatrix},$$

leading to the transformations

$$\hat{A} = \bar{A} + \bar{B}_1 (\gamma^2 I - \bar{D}_{11}^* \bar{D}_{11})^{-1} \bar{D}_{11}^* \bar{C}_1$$

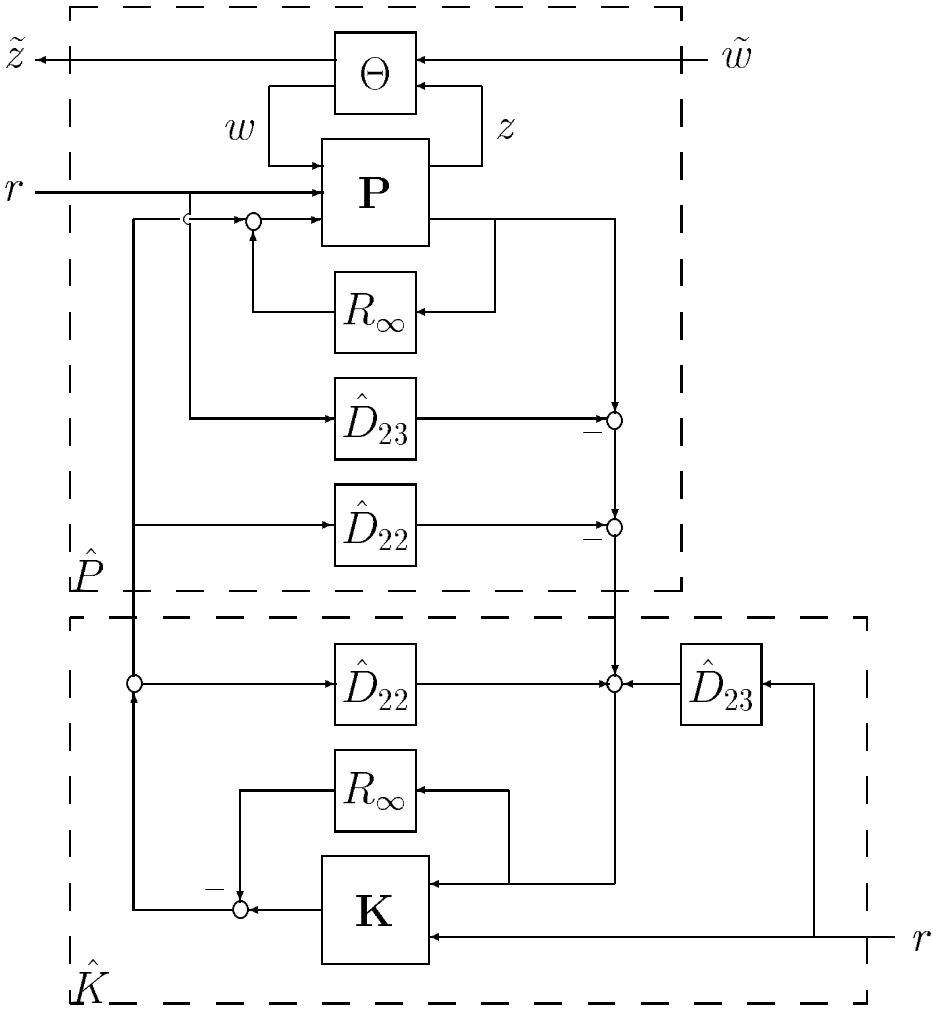

Figure 4.1: Loop-shifting transformations.

$$
\begin{aligned}
\hat{B}_1 &= -\bar{B}_1(\gamma^2 I - \bar{D}_{11}^*\bar{D}_{11})^{-\frac{1}{2}} \\
\hat{B}_2 &= \bar{B}_2 + \bar{B}_1(\gamma^2 I - \bar{D}_{11}^*\bar{D}_{11})^{-1}\bar{D}_{11}^*\bar{D}_{12} \\
\hat{B}_3 &= \bar{B}_3 + \bar{B}_1(\gamma^2 I - \bar{D}_{11}^*\bar{D}_{11})^{-1}\bar{D}_{11}^*\bar{D}_{13} \\
\hat{C}_1 &= (\gamma^2 I - \bar{D}_{11}\bar{D}_{11}^*)^{-\frac{1}{2}}\bar{C}_1 \\
\hat{C}_2 &= \bar{C}_2 + \bar{D}_{21}(\gamma^2 I - \bar{D}_{11}^*\bar{D}_{11})^{-1}\bar{D}_{11}^*\bar{C}_1 \\
\hat{D}_{12} &= (\gamma^2 I - \bar{D}_{11}\bar{D}_{11}^*)^{-\frac{1}{2}}\bar{D}_{12} \\
\hat{D}_{13} &= (\gamma^2 I - \bar{D}_{11}\bar{D}_{11}^*)^{-\frac{1}{2}}\bar{D}_{13} \\
\hat{D}_{21} &= -\bar{D}_{21}(\gamma^2 I - \bar{D}_{11}^*\bar{D}_{11})^{-\frac{1}{2}} \\
\hat{D}_{22} &= \bar{D}_{22} + \bar{D}_{21}(\gamma^2 I - \bar{D}_{11}^*\bar{D}_{11})^{-1}\bar{D}_{11}^*\bar{D}_{12} \\
\hat{D}_{23} &= \bar{D}_{23} + \bar{D}_{21}(\gamma^2 I - \bar{D}_{11}^*\bar{D}_{11})^{-1}\bar{D}_{11}^*\bar{D}_{13}.
\end{aligned} \tag{4.35}
$$

Finally, the feed-through operators $\hat{D}_{22}$ and $\hat{D}_{23}$ are eliminated as shown in figure 4.1. This leads to the transformed plant $\hat{\mathbf{P}}$, which has the form

$$\dot{\bar{x}} = \hat{A}\bar{x} + \hat{B}_1\bar{w} + \hat{B}_2\bar{u} + \hat{B}_3 r \ , \quad t \in \mathbb{R} \tag{4.36}$$

$$\bar{z} = \hat{C}_1\bar{x} + \hat{D}_{12}\bar{u} + \hat{D}_{13} r \tag{4.37}$$

$$\bar{y} = \hat{C}_2\bar{x} + \hat{D}_{21}\bar{w}. \tag{4.38}$$

In the following proposition we give a criterion for the existence of a controller that solves an H_∞ problem of the same type as in section 4.3.2. In order to shorten the notation we define, assuming that (4.44) and (4.45) hold,

$$\mathcal{V}_1 = \begin{bmatrix} D_{11}^*D_{11} - \gamma^2 I & D_{11}^*D_{12} \\ D_{12}^*D_{11} & D_{12}^*D_{12} \end{bmatrix}^{-1} \ ; \quad \mathcal{V}_2 = \begin{bmatrix} D_{11}D_{11}^* - \gamma^2 I & D_{11}D_{21}^* \\ D_{21}D_{11}^* & D_{21}D_{21}^* \end{bmatrix}^{-1}.$$

We also introduce the Riccati equation

$$
\begin{aligned}
0 = \ & \langle(\hat{A} - \hat{B}_2\hat{V}_1\hat{D}_{12}^*\hat{C}_1)x, \tilde{P}y\rangle_H + \langle\tilde{P}x, (\hat{A} - \hat{B}_2\hat{V}_1\hat{D}_{12}^*\hat{C}_1)y\rangle_H \\
& + \langle\tilde{P}(\gamma^2\hat{B}_1\hat{B}_1^* - \hat{B}_2\hat{V}_1\hat{B}_2^*)\tilde{P}x, y\rangle_H + \langle\hat{C}_1^*(I - \hat{D}_{12}\hat{V}_1\hat{D}_{12}^*)\hat{C}_1 x, y\rangle_H,
\end{aligned} \tag{4.39}
$$

where

$$\hat{V}_1 = (\hat{D}_{12}^*\hat{D}_{12})^{-1}. \tag{4.40}$$

Proposition 10 *Consider the system (4.30)-(4.32). Suppose that H1 and H2 hold, and that $r \in AP_2(R)$ is an à priori known signal. Given $\gamma > 0$, there exists an exponentially stabilizing output-feedback control law such that there holds*

$$\|z\|_{ap}^2 \leq \gamma^2\|w\|_{ap}^2 + \gamma^2\hat{J}^0 \ , \qquad \forall w \in AP_2(W), \tag{4.41}$$

where

$$\hat{J}^0 = \|\hat{D}_{13}r\|_{ap}^2 + \gamma^2\|\hat{B}_1^*\hat{\theta}\|_{ap}^2 - \|\hat{V}_1^{1/2}(\hat{B}_2^*\hat{\theta} + \hat{D}_{12}^*\hat{D}_{13}r)\|_{ap}^2 + 2\langle\hat{\theta}, \hat{B}_3 r\rangle_{ap}, \tag{4.42}$$

and where $\hat{\theta} \in AP_2(H)$ *is given by*

$$\begin{aligned}\hat{\theta}(t) &= -\int_t^\infty S^*_{\hat{A}-\hat{B}_2\hat{V}_1(\hat{B}_2^*\tilde{P}+\hat{D}_{12}^*\hat{C}_1)+\gamma^2\hat{B}_1\hat{B}_1^*\tilde{P}}(\tau-t) \\ &\quad [(\tilde{P}\hat{B}_2+\hat{C}_1^*\hat{D}_{12})\hat{V}_1\hat{D}_{12}^*\hat{D}_{13}-\tilde{P}\hat{B}_3-\hat{C}_1^*\hat{D}_{13}]r(\tau)d\tau, \qquad (4.43)\end{aligned}$$

if and only if the following four conditions are satisfied.

1. *There exists a* $\delta > 0$ *such that*

$$\gamma^2 I - D_{11}^*(I - D_{12}(D_{12}^*D_{12})^{-1}D_{12}^*)D_{11} > \delta I \qquad (4.44)$$

$$\gamma^2 I - D_{11}(I - D_{21}^*(D_{21}D_{21}^*)^{-1}D_{21})D_{11}^* > \delta I. \qquad (4.45)$$

2. *There exists* $0 \le \mathcal{X} = \mathcal{X}^* \in \mathcal{L}(H)$ *satisfying*

$$\begin{aligned}0 = \langle \mathcal{X}x, (A - \begin{bmatrix} B_1 & B_2 \end{bmatrix} \mathcal{V}_1 \begin{bmatrix} D_{11}^*C_1 \\ D_{12}^*C_1 \end{bmatrix})y\rangle_H \qquad (4.46)\\ +\langle (A - \begin{bmatrix} B_1 & B_2 \end{bmatrix} \mathcal{V}_1 \begin{bmatrix} D_{11}^*C_1 \\ D_{12}^*C_1 \end{bmatrix})x, \mathcal{X}y\rangle_H \\ -\langle \mathcal{X}\begin{bmatrix} B_1 & B_2 \end{bmatrix} \mathcal{V}_1 \begin{bmatrix} B_1^* \\ B_2^* \end{bmatrix}\mathcal{X}x, y\rangle_H \\ +\langle (I - \begin{bmatrix} D_{11} & D_{12} \end{bmatrix} \mathcal{V}_1 \begin{bmatrix} D_{11}^* \\ D_{12}^* \end{bmatrix})C_1x, C_1y\rangle_Y\end{aligned}$$

   for all $x, y \in D(A)$*, such that*

$$A - \begin{bmatrix} B_1 & B_2 \end{bmatrix} \mathcal{V}_1 \begin{bmatrix} D_{11}^*C_1 + B_1^*\mathcal{X} \\ D_{12}^*C_1 + B_2^*\mathcal{X} \end{bmatrix}$$

   generates an exponentially stable semigroup.

3. *There exists* $0 \le \mathcal{Y} = \mathcal{Y}^* \in \mathcal{L}(H)$ *satisfying*

$$\begin{aligned}0 = \langle \mathcal{Y}x, (A^* - \begin{bmatrix} C_1^* & C_2^* \end{bmatrix} \mathcal{V}_2 \begin{bmatrix} D_{11}B_1^* \\ D_{21}B_1^* \end{bmatrix})y\rangle_H \qquad (4.47)\\ +\langle A^* - \begin{bmatrix} C_1^* & C_2^* \end{bmatrix} \mathcal{V}_2 \begin{bmatrix} D_{11}B_1^* \\ D_{21}B_1^* \end{bmatrix})x, \mathcal{Y}y\rangle_H \\ -\langle \mathcal{Y}\begin{bmatrix} C_1^* & C_2^* \end{bmatrix} \mathcal{V}_2 \begin{bmatrix} C_1 \\ C_2 \end{bmatrix}\mathcal{Y}x, y\rangle_H \\ +\langle (I - \begin{bmatrix} D_{11}^* & D_{21}^* \end{bmatrix} \mathcal{V}_2 \begin{bmatrix} D_{11} \\ D_{21} \end{bmatrix})B_1^*x, B_1^*y\rangle_U\end{aligned}$$

   for all $x, y \in D(A^*)$*, such that*

$$A^* - \begin{bmatrix} C_1^* & C_2^* \end{bmatrix} \mathcal{V}_2 \begin{bmatrix} D_{11}B_1^* + C_1\mathcal{Y} \\ D_{21}B_1^* + C_2\mathcal{Y} \end{bmatrix}$$

   generates an exponentially stable semigroup.

4. $\mathcal{X}$ and $\mathcal{Y}$ given above satisfy

$$r_\sigma(\mathcal{X}\mathcal{Y}) < \gamma^2$$

where r_σ denotes the spectral radius.

Remark 11 Concerning $\hat{\theta}$ defined by (4.43), see remark 7. □

The controller $\mathbf{K}$ can be obtained using proposition 8 in the following way: The formulas (4.26), (4.27) are modified in such a way that throughout proposition 8 one is to replace γ by γ^{-1}, A by $\hat{A}$, B_1 by $\hat{B}_1$, etc, leading to the controller $\hat{\mathbf{K}}$. This controller is modified by introducing feed-through operators and linear fractional transformations according to figure 4.1, so that $\hat{\mathbf{K}}$ is transformed into the controller $\mathbf{K}$. If we make the partitioning $\hat{\mathbf{K}} = [\hat{\mathbf{K}}_{11} \quad \hat{\mathbf{K}}_{12}]$, we can write the control law as

$$u = \mathbf{K}\begin{bmatrix} y \\ r \end{bmatrix} = (I + \hat{\mathbf{K}}_{11}\hat{D}_{22})^{-1}(\hat{\mathbf{K}}_{11}(y - \hat{D}_{23}r) + \hat{\mathbf{K}}_{12}r) + R_\infty y. \tag{4.48}$$

4.4 Proofs

Before proceeding to the actual proofs we need to state some lemmas.

Lemma 12 *Assume that $S(t)$ is an exponentially stable semigroup. With $f \in AP(H)$, y given by*

$$y(t) = \int_{-\infty}^{t} S(t-\tau)f(\tau)d\tau \tag{4.49}$$

is in $AP(H)$.

Proof See Jacob et al.[36], Da Prato and Ichikawa[51]. □

The following perturbation result is a small extension of a well known result.

Lemma 13 *Assume that $S(t)$ is a strongly continuous semigroup on H with generator A. Consider the system*

$$\dot{x} = Ax + Bu + f,$$

where $B \in \mathcal{L}(U,H)$, $f \in AP(H)$. With $F \in \mathcal{L}(H,U)$, assume that $A + BF$ generates an exponentially stable semigroup $S_{A+BF}(t)$. Then there holds uniformly in t

$$\int_{-\infty}^{t} S(t-\tau)[BFx(\tau) + f(\tau)]d\tau = \int_{-\infty}^{t} S_{A+BF}(t-\tau)f(\tau)d\tau. \tag{4.50}$$

Proof From a well known perturbation result (see e.g. [59, lemma 2.14]) it follows that

$$\int_T^t S(t-\tau)[BFx(\tau)+f(\tau)]d\tau = \int_T^t S_{A+BF}(t-\tau)f(\tau)d\tau$$

for every T, t, where $T < t$. Using the exponential stability of $S_{A+BF}(t)$ we let $T \to -\infty$, and the lemma follows immediately. □

The next lemma defines an extension of the concept of mild solution to the space $AP_2(H)$.

Lemma 14 *Assume that $S(t)$ is an exponentially stable semigroup. Consider the linear mapping $\Phi : f \in AP(H) \to y \in AP(H)$ given by the convolution integral*

$$y(t) = \int_{-\infty}^t S(t-\tau)f(\tau)d\tau. \tag{4.51}$$

This mapping has a unique continuous extension in $\mathcal{L}(AP_2(H))$.

Proof See Jacob et al.[36]. □

Remark 15 We will occasionally write a convolution integral involving an input signal in a space of the type AP_2. In cases for which this convolution integral does not make sense in the usual way, it is to be understood in the extended sense defined by lemma 14. □

In the sufficiency proof of the state feedback result it is useful to differentiate functions, and therefore we need a space of smooth, almost periodic functions; this role will be played by $TP(H)$.

Lemma 16 *The space $TP(H)$ of trigonometric polynomials, with values in H, is dense in $AP_2(H)$.*

Proof Using the Bohr transform, an arbitrary almost periodic function can be approximated by trigonometric polynomials in the norm $\|\cdot\|_{ap}$, and by the definition of $AP_2(H)$ we know that $AP(H)$ is dense in this space. Therefore $TP(H)$ is dense in $AP_2(H)$. □

Lemma 17 *Assume that $f \in TP(H)$, and that $S(t)$ is an exponentially stable semigroup. Then y given by the expression (4.49) is in $TP(H)$. Furthermore, $\frac{dy}{dt} = Ay + f$.*

Proof See Jacob et al.[36]. □

The next lemma serves to establish the connection between our problem and the H_∞ standard problem.

Lemma 18 *Consider the exponentially stable C_0 semigroup $S(t)$ on H and $B \in \mathcal{L}(\mathcal{W}, \mathcal{H})$, $C \in \mathcal{L}(H, Z)$, $D \in \mathcal{L}(W, Z)$. The following statements are equivalent.*

1. *For arbitrary $w_2 \in L^2(0, \infty; W)$ and z_2 given by*

$$z_2(t) = Dw_2(t) + C \int_0^t S(t-\tau) B w_2(\tau) d\tau, \tag{4.52}$$

$z_2 \in L^2(0, \infty; Z)$ and there holds

$$\sup_{w_2 \neq 0} \frac{\|z_2\|_2}{\|w_2\|_2} < \gamma. \tag{4.53}$$

2. *For arbitrary $w \in AP_2(W)$ and z given by*

$$z(t) = Dw(t) + C \int_{-\infty}^t S(t-\tau) B w(\tau) d\tau, \tag{4.54}$$

$z \in AP_2(H)$ and there holds

$$\sup_{w \neq 0} \frac{\|z\|_{ap}}{\|w\|_{ap}} < \gamma. \tag{4.55}$$

Remark 19 Notice that the convolution integral in (4.54) is to be understood in the extended sense defined by lemma 14. □

Proof Notice first that since $S(t)$ is exponentially stable and B, C, D are bounded, the transfer function $G \in H_\infty(\mathcal{L}(W, Z))$ given by

$$G(s) := D + C(sI - A)^{-1} B$$

is well defined and holomorphic in the closed right half plane $\overline{\mathbb{C}^+}$.

1.⇒2. Since $S(t)$ is exponentially stable it is known (see e.g.[59],theorem 3.4) that (4.53) is equivalent to

$$\sup_{\lambda \in \mathbb{R}} \|G(\hat{i}\lambda)\|_{\mathcal{L}(W,Z)} < \gamma. \tag{4.56}$$

Now consider an arbitrary signal $w \in TP(W)$, which can be written as

$$w(t) = \sum_{k=1}^{N} a_k e^{\hat{i}\lambda_k t} \ , \quad a_k \in W, \ \lambda_k \in \mathbb{R}, \ N \in \mathbb{N}. \tag{4.57}$$

With z defined as in (4.54), we obtain (see [36])

$$\begin{aligned} \|z\|_{ap}^2 &= \sum_{k=1}^{N} \|G(\hat{i}\lambda_k)a_k\|_W^2 \\ &\leq \sup_{\lambda\in\mathbb{R}} \|G(\hat{i}\lambda)\|_{\mathcal{L}(W,Z)}^2 \sum_{k=1}^{N} \|a_k\|_W^2 \\ &= \sup_{\lambda\in\mathbb{R}} \|G(\hat{i}\lambda)\|_{\mathcal{L}(W,Z)}^2 \|w\|_{ap}^2. \end{aligned} \tag{4.58}$$

The inequality (4.58) holds uniformly for every $w \in TP(W)$. The linear input-output map (4.54), which is well defined for $w \in TP(W)$, therefore has an extension in $\mathcal{L}(AP_2(W), AP_2(Z))$, see Kreyszig[39, theorem 2.7-11], and the norm of this operator is bounded by $\|G\|_\infty$. Thus (4.56) implies that for $w \in AP_2(W)$, there holds

$$\sup_{w\neq 0} \frac{\|z\|_{ap}^2}{\|w\|_{ap}^2} \leq \sup_{\lambda\in\mathbb{R}} \|G(i\lambda)\|_{\mathcal{L}(W,Z)}^2 < \gamma^2.$$

2.⇒1. Let $\xi > 0$ be given. Because of the exponential stability of G there exists a $\bar{\lambda} \in \mathbb{R}$ such that

$$\left| \sup_{\lambda\in\mathbb{R}} \|G(\hat{i}\lambda)\|_{\mathcal{L}(W,Z)} - \|G(\hat{i}\bar{\lambda})\|_{\mathcal{L}(W,Z)} \right| \leq \frac{\xi}{2}$$

and an $\bar{a} \in W$ such that

$$\left| \sup_{a\neq 0} \frac{\|G(\hat{i}\bar{\lambda})a\|_Z}{\|a\|_W} - \frac{\|G(\hat{i}\bar{\lambda})\bar{a}\|_Z}{\|\bar{a}\|_W} \right| \leq \frac{\xi}{2},$$

whence by the triangle inequality,

$$\left| \sup_{\lambda\in\mathbb{R}} \|G(\hat{i}\lambda)\|_{\mathcal{L}(W,Z)} - \frac{\|G(\hat{i}\bar{\lambda})\bar{a}\|_Z}{\|\bar{a}\|_W} \right| \leq \xi. \tag{4.59}$$

Now choose $\bar{w} \in AP_2(W)$ given by

$$\bar{w}(t) = \bar{a}e^{\hat{i}\bar{\lambda}t}$$

and let $\bar{z}$ be defined via (4.54). From (4.55) it follows that there exists $\delta > 0$ such that

$$\frac{\|G(\hat{i}\bar{\lambda})\bar{a}\|_Z}{\|\bar{a}\|_W} = \frac{\|\bar{z}\|_{ap}}{\|\bar{w}\|_{ap}} \leq \gamma - \delta. \tag{4.60}$$

We can now use (4.59) and (4.60) together with the triangle inequality to obtain

$$\sup_{\lambda\in\mathbb{R}} \|G(\hat{i}\lambda)\|_{\mathcal{L}(W,Z)} \leq \gamma - \delta + \xi,$$

and finally, since the above arguments can be repeated with ξ arbitrarily small, and since δ can be chosen independently of ξ, we deduce that

$$\sup_{\lambda \in \mathbb{R}} \|G(\hat{i}\lambda)\|_{\mathcal{L}(W,Z)} < \gamma.$$

This implies that $\|G\|_\infty < \gamma$, which is known to be equivalent to (4.53), since $S(t)$ is exponentially stable. □

4.4.1 Proof of the State Feedback Result

Sufficiency. 1.⇒ 2. Assume that there exists $P = P^* \geq 0$ satisfying the algebraic Riccati equation (4.14) such that $\tilde{A}$ given by (4.13) generates an exponentially stable semigroup $S_{\tilde{A}}(t)$. We will work with the average cost function

$$J(r,u,w) := \lim_{T\to\infty} \frac{1}{T} \int_0^T \{\|z\|_Z^2 - \gamma^2 \|w\|_W^2\} dt = \|z\|_{ap}^2 - \gamma^2 \|w\|_{ap}^2, \tag{4.61}$$

assuming that (4.6)-(4.7) hold. The first step is to determine a saddle point of $J(r,u,w)$ with respect to the variables u and w, in the case where r, u, w are trigonometric polynomials. The control law of this saddle point leads to the inequality (4.68). The second step is to extend (4.68) to hold also for the larger class of input signals, namely $w \in AP_2(W)$, $r \in AP_2(R)$. The third step is to specialize to the case $r = 0$ and obtain the inequality (4.18).

In the first step we assume that $w \in TP(W)$ and $r \in TP(R)$. Because of the exponential stability of $S_{\tilde{A}}(t)$, it follows from lemma 17 that $\theta(\cdot)$ given by (4.17) is in $TP(H)$, and that

$$\dot{\theta} = -\tilde{A}^*\theta + [F_\infty^* D_{12}^* D_{13} - PB_3 - C_1^* D_{13}]r. \tag{4.62}$$

As the space of admissible controls we take

$$\mathcal{U}_{ad} = \{u \in TP(U) \text{ such that } x \in TP(H)\}. \tag{4.63}$$

Let us first show that $\mathcal{U}_{ad}$ is non empty. Define

$$\hat{u} = -V_1(B_2^*P + D_{12}^*C_1)x - V_1(D_{12}^*D_{13}r + B_2^*\theta).$$

We could for example choose $u = \hat{u}$; this would introduce a feedback such that the system operator would be

$$A - B_2V_1(B_2^*P + D_{12}^*C_1).$$

From van Keulen et al.[60, theorem 2.2] it follows that the semigroup $S_{A-B_2V_1(B_2^*P+D_{12}^*C_1)}$ is exponentially stable. Therefore, with $u = \hat{u}$, $x \in TP(H)$ and we conclude that $\mathcal{U}_{ad}$ is non empty.

Using lemma 17 we carry out the following differentiation:

$$\frac{d}{dt}(\langle x, Px\rangle_H + 2\langle\theta, x\rangle_H).$$

Now, using (4.6,4.7,4.12,4.14,4.62) and integrating from 0 to T, it can he shown by calculations that are nearly identical to those done by Shaked and de Souza [57] that

$$\begin{aligned} J_T(r,u,w) &:= \int_0^T \left\{\|z\|_Z^2 - \gamma^2\|w\|_W^2\right\} d\tau \\ &= \int_0^T \Big\{-\gamma^2\|w - \gamma^{-2}B_1^*(Px+\theta)\|_W^2 \\ &\quad +\|D_{12}(u + F_\infty x + V_1(D_{12}^*D_{13}r + B_2^*\theta))\|_Z^2 \\ &\quad +\|D_{13}r\|_W^2 + \gamma^{-2}\|B_1^*\theta\|_Z^2 - \|V_1^{1/2}(B_2^*\theta + D_{12}^*D_{13}r)\|_U^2 + 2\langle\theta, B_3 r\rangle_H\Big\} d\tau \\ &\quad -2\langle\theta(T), x(T)\rangle_H + 2\langle\theta(0), x(0)\rangle_H - \langle x(T), Px(T)\rangle_H + \langle x(0), Px(0)\rangle_H. \end{aligned} \tag{4.64}$$

For $u \in \mathcal{U}_{ad}$, it follows that $z \in TP(Z)$, and

$$\lim_{T\to\infty} \frac{1}{T} J_T(r,u,w)$$

exists. Now we can divide $J_T(r,u,w)$ by T and let $T \to \infty$ in order to obtain an expression for $J(r,u,w)$ which is valid for $r \in TP(R)$, $u \in \mathcal{U}_{ad}$ and $w \in TP(W)$.

$$\begin{aligned} J(r,u,w) &= \lim_{T\to\infty} \frac{1}{T} J_T(r,u,w) \\ &= -\gamma^2\|w - \gamma^{-2}B_1^*(Px+\theta)\|_{ap}^2 \\ &\quad +\|D_{12}(u + F_\infty x + V_1(D_{12}^*D_{13}r + B_2^*\theta))\|_{ap}^2 + J^0. \end{aligned} \tag{4.65}$$

Define $\hat{w} = \gamma^{-2}B_1^*(Px+\theta)$. There holds the following inequalities

$$\begin{aligned} J(r,\hat{u},w) &= -\gamma^2\|w - \gamma^{-2}B_1^*(Px+\theta)\|_{ap}^2 + J^0 \\ &\le J(r,v,w) \quad \forall v \in \mathcal{U}_{ad}\ \forall w \in TP(W), \end{aligned} \tag{4.66}$$

$$\begin{aligned} J(r,u,\hat{w}) &= \|D_{12}(u + F_\infty x + V_1(D_{12}^*D_{13}r + B_2^*\theta))\|_{ap}^2 + J^0 \\ &\ge J(r,u,\nu) \quad \forall u \in \mathcal{U}_{ad}\ \forall \nu \in TP(W). \end{aligned} \tag{4.67}$$

This shows that for fixed $r \in TP(R)$, J has a saddle point at $(r,\hat{u},\hat{w})$ with respect to $u \in \mathcal{U}_{ad}$ and $w \in TP(W)$. Notice that this saddle point is obtained using the strategy given by the Riccati equation. By considering the cost function (4.61) and the inequality (4.66), we find, when the control law $u = \hat{u}$ is applied,

$$\|z\|_{ap}^2 \le \gamma^2\|w\|_{ap}^2 + J^0 \quad \forall w \in TP(W). \tag{4.68}$$

As the second step we extend (4.68) to hold also for $w \in AP_2(W)$, $r \in AP_2(R)$, assuming that the control law $u = \hat{u}$ is applied. Using lemma 14 together with the boundedness of the input and output operators, we find that the input-output map from $(w, r) \in TP(W) \times TP(R)$ to $z \in TP(Z)$ is linear and continuous with respect to the norms of $AP_2(W)$, $AP_2(R)$ and $AP_2(Z)$. Therefore, using lemma 16, this mapping has an extension in $\mathcal{L}(AP_2(W) \times AP_2(R), AP_2(Z))$. Using the sub-additivity property of the norm $\|\cdot\|_{ap}$, we can define the continuous function

$$\Theta(w, r) = \|z\|_{ap}^2 - \gamma^2 \|w\|_{ap}^2 , \quad w \in AP_2(W),\ r \in AP_2(R). \tag{4.69}$$

Consider now the pair of signals $(w, r) \in AP_2(W) \times AP_2(R)$, where w is arbitrary, and let J^0 be defined by (4.16)-(4.17), here denoted $J^0(r)$ to stress the dependence on r. By continuity of Θ we have that

$$\Gamma = \{(\nu, \rho) \in AP_2(W) \times AP_2(R) \text{ such that } \Theta(\nu, \rho) \leq J^0(r)\} \tag{4.70}$$

is a closed set. Since $TP(W)$ and $TP(R)$ are dense in $AP_2(W)$ and $AP_2(R)$ respectively, we can to (w, r) relate a sequence of signals $\{(w_n, r_n)\}$, with $w_n \in TP(W)$ and $r_n \in TP(R)$, converging to (w, r) in the topology of $AP_2(W) \times AP_2(R)$. Furthermore, defining $J^0(r_n)$ analogously to $J^0(r)$, it can be shown that we can choose the sequence $\{r_n\}$ such that $J^0(r_n) \leq J^0(r)$ for every n. Using (4.68) we deduce that $\Theta(w_n, r_n) \leq J^0(r_n) \leq J^0(r)$ holds for every n. Since the set Γ is closed in $AP_2(W) \times AP_2(R)$, it also holds that $\Theta(w, r) \leq J^0(r) = J^0$. Since the above argument can be repeated with arbitrary $w \in AP_2(W)$, we obtain, given $r \in AP_2(R)$, the inequality

$$\|z\|_{ap}^2 - \gamma^2 \|w\|_{ap}^2 \leq J^0 \quad \forall w \in AP_2(W), \tag{4.71}$$

which was what we wanted.

As the third step we consider the special case $r = 0$. We apply the control law $u = \hat{u}$. It is known, see Van Keulen et al.[60], that this control law solves the standard H_∞ problem. By using lemma 18 we immediately obtain the inequality (4.18).

Necessity. 2.⇒ 1. It suffices to show that with $r = 0$, and under the hypothesis H1, item 1 is implied by the assumption that the control law (4.19) is exponentially stabilizing and yields the disturbance attenuation bound (4.18). Using lemma 18, this follows immediately from the analogous result for the H_∞ standard problem, see [60]. □

4.4.2 Proof of the Measurement Feedback Result

The measurement feedback result relies heavily on results from van Keulen[59]. The formulas for the controller are reminiscent of the finite-dimensional case, where the appropriate references would be Doyle et al.[21] and Limebeer et al.[46].

Sufficiency. 1.⇒ 2. We assume again that $w \in TP(W)$, $r \in TP(R)$ and $u \in \mathcal{U}_{ad}$ as defined by (4.63). We have

$$\begin{aligned} J(r,u,w) &= -\gamma^2 \|w - \gamma^{-2} B_1^*(Px+\theta)\|_{ap}^2 \\ &\quad + \|D_{12}(u + F_\infty x + V_1(D_{12}^* D_{13} r + B_2^* \theta))\|_{ap}^2 + J^0, \end{aligned} \tag{4.72}$$

where

$$x(t) = \int_{-\infty}^{t} S(t-\tau)[B_1 w(\tau) + B_2 u(\tau) + B_3 r(\tau)]d\tau. \tag{4.73}$$

To shorten the notation we define

$$\bar{r} = \gamma^{-2} B_1 B_1^* \theta + B_3 r - B_2 V_1 (D_{12}^* D_{13} r + B_2^* \theta). \tag{4.74}$$

We now aim for a shift of variables such that r and θ are substituted out. To this end we introduce

$$q = w - \gamma^{-2} B_1^*(Px+\theta) \tag{4.75}$$

$$v = u + V_1(D_{12}^* D_{13} r + B_2^* \theta) + F_\infty x \tag{4.76}$$

which gives us

$$x(t) = \int_{-\infty}^{t} S_{\tilde{A}}(t-\tau)[B_1 q(\tau) + B_2 v(\tau) + \bar{r}(\tau)]d\tau \tag{4.77}$$

$$u = -F_\infty x + v - V_1(D_{12}^* D_{13} r + B_2^* \theta). \tag{4.78}$$

We write the control as $u = \tilde{u} + u_r$, such that $\tilde{u}$ is given as a linear function of (q,v) by

$$\tilde{x}(t) = \int_{-\infty}^{t} S_{\tilde{A}}(t-\tau)[B_1 q(\tau) + B_2 v(\tau)]d\tau \tag{4.79}$$

$$\tilde{u} = -F_\infty \tilde{x} + v, \tag{4.80}$$

and u_r is given as a linear function of r by

$$\rho(t) = \int_{-\infty}^{t} S_{\tilde{A}}(t-\tau)\bar{r}(\tau)d\tau \tag{4.81}$$

$$u_r = -F_\infty \rho - V_1(D_{12}^* D_{13} r + B_2^* \theta). \tag{4.82}$$

Notice that since $S_{\tilde{A}}(t)$ is exponentially stable, both of $\tilde{u}$ and u_r are in $TP(U)$. Furthermore, we introduce

$$\tilde{y} = y - \gamma^{-2} D_{21} B_1^* \theta - C_F \rho \tag{4.83}$$

$$= C_F \tilde{x} + D_{21} q \tag{4.84}$$

and

$$\tilde{v} = (D_{12}^* D_{12})^{\frac{1}{2}} v. \tag{4.85}$$

We can now rewrite J as

$$J(r,u,w) = -\gamma^2 \|q\|_{ap}^2 + \|\tilde{v}\|_{ap}^2 + J^0 \tag{4.86}$$

where

$$\begin{aligned}
\tilde{x}(t) &= \int_{-\infty}^{t} S_{A+\gamma^2 B_1 B_1{}^* P}(t-\tau)[B_1 q(\tau) + B_2 \tilde{u}(\tau)] d\tau & (4.87)\\
\tilde{v} &= (D_{12}^* D_{12})^{\frac{1}{2}} F_\infty \tilde{x} + (D_{12}^* D_{12})^{\frac{1}{2}} \tilde{u} & (4.88)\\
\tilde{y} &= C_F \tilde{x} + D_{21} q. & (4.89)
\end{aligned}$$

Notice that the convolution integral (4.87) is well defined, although $S_{A+\gamma^{-2} B_1 B_1{}^* P}$ is not necessarily exponentially stable. This follows from the substitution (4.80) and lemma 13, leading to a convolution integral where the exponentially stable semigroup $S_{A-B_2 F_\infty}$ appears. We will now apply known results concerning the H_∞ standard problem. Introduce therefore the signals $q_2 \in L^2(0,\infty;W)$, $\tilde{u}_2 \in L^2(0,\infty;U)$ and consider

$$\begin{aligned}
\tilde{x}_2(t) &= \int_{0}^{t} S_{A+\gamma^{-2} B_1 B_1{}^* P}(t-\tau)[B_1 q_2(\tau) + B_2 \tilde{u}_2(\tau)] d\tau & (4.90)\\
\tilde{v}_2 &= (D_{12}^* D_{12})^{\frac{1}{2}} F_\infty \tilde{x}_2 + (D_{12}^* D_{12})^{\frac{1}{2}} \tilde{u}_2 & (4.91)\\
\tilde{y}_2 &= C_F \tilde{x}_2 + D_{21} q_2. & (4.92)
\end{aligned}$$

It is known (see van Keulen[59, pp.160-162]) how to construct an exponentially stabilizing causal controller $\tilde{\mathbf{K}}$ for the system (4.90)-(4.92) such that with $\tilde{u}_2 = \tilde{\mathbf{K}} \tilde{y}_2$ and $q_2 \in L^2(0,\infty;W)$,

$$\sup_{q_2 \neq 0} \frac{\|\tilde{v}_2\|_2}{\|q_2\|_2} < \gamma.$$

Now, by lemma 17 and lemma 18, the system obtained from (4.87)-(4.89) by putting $\tilde{u} = \tilde{\mathbf{K}} \tilde{y}$ maps $q \in TP(W)$ to $\tilde{v} \in TP(Z)$ such that

$$\sup_{q \neq 0} \frac{\|\tilde{v}\|_{ap}}{\|q\|_{ap}} < \gamma.$$

This shows that when the controller $\tilde{\mathbf{K}}$ is applied, we have $J(r,u,w) \leq J^0$, and therefore, with $r \in TP(R)$,

$$\|z\|_{ap}^2 \leq \gamma^2 \|w\|_{ap}^2 + J^0 \qquad \forall\, w \in TP(W). \tag{4.93}$$

The formulas for the so-called central controller, which can be deduced from van Keulen[59, theorem 5.4], read, for the system (4.87)-(4.89),

$$\begin{aligned}
x_k(t) &= \int_{-\infty}^{t} S_{\tilde{A}-LC_F}(t-\tau) L \tilde{y}(\tau) d\tau & (4.94)\\
\tilde{u} &= -F_\infty x_k. & (4.95)
\end{aligned}$$

Now, substituting back through (4.74), (4.81), (4.83) while using lemma 13 and introducing $\hat{x} = x_k + \rho$ we obtain the control law (4.26)-(4.27). In the case $r = 0$, we can use the measurement-feedback result of [59, theorem 5.4] together with lemma 18 to obtain, for some $\epsilon > 0$,

$$\|z\|_{ap}^2 \leq (\gamma^2 - \epsilon)\|w\|_{ap}^2 \qquad \forall w \in AP_2(W), \tag{4.96}$$

when the control law of (4.26)-(4.27) is applied. Finally, the inequality (4.93) needs to be extended to hold also for $r \in AP_2(R)$, $w \in AP_2(W)$. This can be done analogously to the procedure used in the state feedback case, and we therefore leave this out.

Necessity. 2.⇒ 1. It suffices to show that with $r = 0$, and under the hypothesis H1, H2, the relations (4.26), (4.27), (4.25) imply item 1. As in the state feedback case we can use lemma 18, and in this case the H_∞ standard problem result that we use can be found in van Keulen[59].

4.4.3 Proof of the Loop-shifting Result

We only give a sketch of the proof. Firstly, let us make sure that the feed-back loops of the transformed system are still well posed. For the standard problem, this question was dealt with in van Keulen[59], and since the introduction of B_3, D_{13}, D_{23} does not alter the feedback structure, we can use these results immediately.

For the special case $r = 0$, it was stated in Curtain et al[17, theorem 3] that items 1-4 are equivalent to the solvability of the γ-suboptimal H_∞ problem. Using lemma 18, we find that this shows proposition 10 in the special case $r = 0$, and at the same time this shows the necessity part. It remains to show that items 1-4 imply the existence of an exponentially stabilizing controller, such that (4.41) holds, also in the case $r \neq 0$. The presence of r clearly has no influence on the existence of an exponentially stabilizing controller. As stated in [17], the usual loop-shifting transformations, which amount to introducing Θ, R_∞, $\hat{D}_{22}$ in a fictitious manner as shown in figure 4.1, are possible, assuming that item 1 holds. By carrying out these transformations, together with the introduction of $\hat{D}_{23}$ as shown in figure 4.1, and applying proposition 8 to the transformed plant $\hat{\mathbf{P}}$, we can construct an exponentially stabilizing controller $\hat{\mathbf{K}}$ such that there holds

$$\|\tilde{z}\|_{ap}^2 \leq \gamma^{-2}\|\tilde{w}\|_{ap}^2 + \hat{J}^0. \tag{4.97}$$

Since loop-shifting is possible, it follows from proposition 8 that the Riccati criterion is not affected by the signal r. Therefore, the Riccati equation (4.39) has a stabilizing solution, provided that the Riccati equation (4.46) does and R_∞ is chosen such that (4.33) is satisfied. The explicit expression for $\hat{J}^0$ follows from the loop-shifting transformations and proposition 8. The inequality (4.41) finally

follows from the identity

$$\|z\|_{ap}^2 - \gamma^2\|w\|_{ap}^2 = \gamma^2\|\tilde{z}\|_{ap}^2 - \|\tilde{w}\|_{ap}^2. \tag{4.98}$$

4.5 Discussion

In this chapter we have presented an H_∞-type result in the case that the input signals are in a class of generalized almost periodic functions. The formulae obtained are natural extensions of a known result for finite-horizon tracking problems; however, the justification of the result was non trivial. In order to obtain a rigorous mathematical derivation of the result, we used a space of input signals where some of the signals were only defined in terms of limit arguments.

The class of input signals that was considered was specified in a rather abstract way. However, as mentioned in this chapter, if a given signal has a well defined Bohr transform (spectrum) which is a square summable sequence, then this signal may be considered as an element of our space, via the Bohr transform.

It is characteristic for the proofs of this chapter that the relation to the standard H_∞ problem was used extensively. This suggests that a number of methods used in connection with the standard H_∞ problem may be adapted without too much difficulty. We have in this chapter adapted the loop-shifting transformations, and it would be useful to adapt also controller reduction algorithms, as well as methods for problems with structured uncertainties. One possible approach to these matters can be found in chapter 5.

Chapter 5

A Two-Degrees-Of-Freedom Design

5.1 Introduction

The control law formulated in chapter 4 is not immediately applicable to a controller design when the uncertainty structure is as complex as the one encountered in chapter 2. On the other hand, the methods used in chapter 2, namely scaling and controller order reduction are relatively easy to adapt to the control law of chapter 4. This is the purpose of the present chapter.

5.2 Controller Order Reduction

We will in this section consider the problem of reducing the order of the dynamic part of the control law. We suggest to adapt well known controller reduction techniques in such a way that the inequality

$$\|z\|_{ap}^2 \leq \gamma^2 \|w\|_{ap}^2 + J^0 \tag{5.1}$$

still holds for some $\gamma > 0$. The control signal u depends dynamically on both the measured output y and the reference signal r. However, since r is known á priori, it will in many applications be acceptable to calculate the part of the control law that depends only on r, based on a high order controller. We therefore suggest to apply controller reduction with respect to the dependence on y, but to retain the order of the dynamic dependence of r.

When considering the measurement feedback control law (4.26)-(4.27), it is not immediately evident how controller order reduction should be carried out. Therefore, we choose in this section an alternative formulation of the control law which is well suited for controller reduction, namely the one shown in figure 5.1.

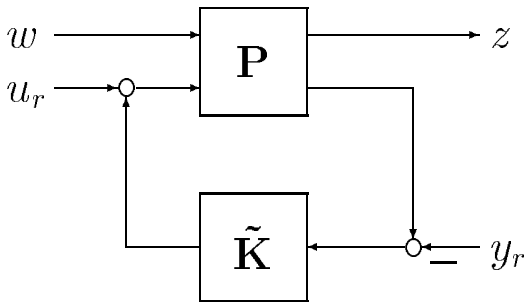

Figure 5.1: Controller structure used for controller order reduction.

The key to the controller reduction problem is to consider the system (4.87)-(4.89), which reads

$$\begin{aligned}
\tilde{x}(t) &= \int_{-\infty}^{t} S_{A+\gamma^2 B_1 B_1{}^* P}(t-\tau)[B_1 q(\tau) + B_2 \tilde{u}(\tau)]d\tau && (5.2)\\
\tilde{v} &= (D_{12}^* D_{12})^{\frac{1}{2}} F_\infty \tilde{x} + (D_{12}^* D_{12})^{\frac{1}{2}} \tilde{u} && (5.3)\\
\tilde{y} &= C_F \tilde{x} + D_{21} q, && (5.4)
\end{aligned}$$

where we have used the notation of chapter 4. By applying the controller $\tilde{u} = \tilde{K}\tilde{y}$, given by

$$\tilde{u}(t) = -F_\infty \int_{-\infty}^{t} S_{\tilde{A}-LC_F}(t-\tau) L\tilde{y}(\tau)d\tau, \qquad (5.5)$$

we obtain, as in section 4.4.2,

$$\sup_{q\neq 0} \frac{\|\tilde{v}\|_{ap}}{\|q\|_{ap}} < \gamma. \qquad (5.6)$$

The idea is to seek a controller of lower order than $\tilde{K}$ which also yields (5.6), and then carry out appropriate substitutions leading to a control law of the type shown in figure 5.1, where u_r and y_r depend only on r, and where $\tilde{K}$ is replaced by a lower order controller. Algorithms based on weighted Hankel norm approximation for seeking such a reduced order controller are available, see Zhou[62], Zhou et al.[63] and references therein. See also section 2.4.4.

With this in mind we now rewrite the control law (4.26)-(4.27) as follows,

$$\begin{aligned}
u(t) &= \tilde{u}(t) + u_r(t)\\
&= -F_\infty \int_{-\infty}^{t} S_{\tilde{A}-LC_F}(t-\tau) L(y(\tau) - y_r(\tau))d\tau + u_r(t)\\
&= (\tilde{K}(y - y_r))(t) + u_r(t) && (5.7)
\end{aligned}$$

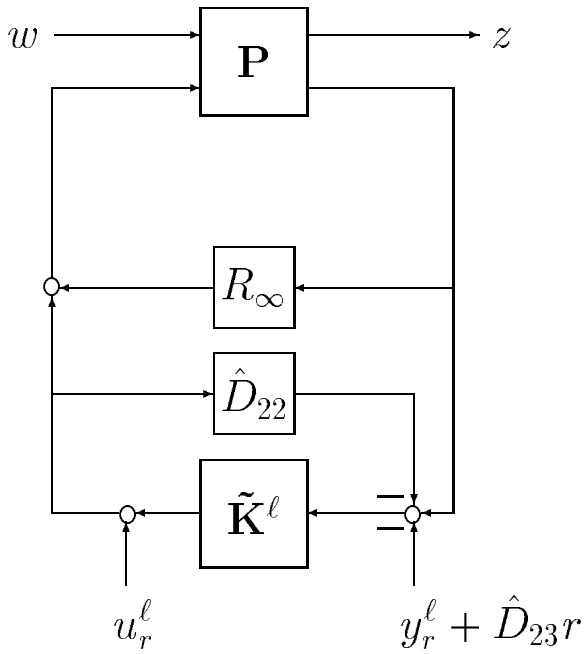

Figure 5.2: Controller structure with loop-shifting and controller order reduction.

where

$$
\begin{aligned}
y_r &= \gamma^{-2} D_{21} B_1^* \theta + C_F \rho && (5.8)\\
u_r &= -F_\infty \rho - V_1 (D_{12}^* D_{13} r + B_2^* \theta) && (5.9)\\
\rho(t) &= \int_{-\infty}^{t} S_{\tilde{A}}(t-\tau) \\
&\qquad [(B_3 - B_2 V_1 D_{12}^* D_{13}) r(\tau) + (\gamma^{-2} B_1 B_1^* - B_2 V_1 B_2^*)\theta(\tau)] d\tau && (5.10)\\
\theta(t) &= -\int_{t}^{\infty} S_{\tilde{A}}^*(\tau - t)[F_\infty^* D_{12}^* D_{13} - P B_3 - C_1^* D_{13}] r(\tau) d\tau, && (5.11)
\end{aligned}
$$

and where $\tilde{A}$, V_1, F_∞, P, C_F are defined in section 4.3.3. Notice that the control law (5.7) has the form shown in figure 5.1, and if the reference signal r is time-dependent, then so are the signals y_r and u_r.

Let now K_1 be a dynamic controller that, when applied to the system (5.2)-(5.4), yields (5.6). In practice, K_1 is to be obtained from $\tilde{K}$ using standard controller order reduction techniques. By a careful examination of the substitutions that relate the controller $\tilde{K}$ with the control law (5.7), it can be shown that if $\tilde{K}$ is replaced by a controller K_1 that likewise yields (5.6), then the inequality (5.1) still holds. Now, if we have found such a controller K_1 that is of lower order than $\tilde{K}$, then the controller order reduction was succesful.

Remark 20 The loop-shifting transformations described in section 4.3.3 can be applied also in connection with controller order reduction, using the following

procedure. The controller $\tilde{K}^\ell$ and the signals u_r^ℓ and y_r^ℓ are constructed analogously to the controller $\tilde{K}$ and the signals u_r and y_r, respectively, but with the difference that γ is replaced by γ^{-1}, A by $\hat{A}$, B_1 by $\hat{B}_1$, etc., just like it is done in the loop-shifting procedure described in section 4.3.3. The controller $\tilde{K}^\ell$ is thus constructed from the Riccati equation formula of section 4.3.3, followed by controller order reduction. The controller to be implemented is then constructed according to equation (4.48), which reads

$$u = (I + \hat{K}_{11}\hat{D}_{22})^{-1}(\hat{K}_{11}(y - \hat{D}_{23}r) + \hat{K}_{12}r) + R_\infty y. \tag{5.12}$$

With a configuration analogous to the one of figure 5.1, we can write

$$\hat{K}_{12}r = u_r^\ell - \tilde{K}^\ell y_r^\ell \tag{5.13}$$
$$\hat{K}_{11} = \tilde{K}^\ell, \tag{5.14}$$

leading to the control law

$$u = (I + \tilde{K}^\ell\hat{D}_{22})^{-1}(\tilde{K}^\ell(y - y_r^\ell - \hat{D}_{23}r) + u_r^\ell) + R_\infty y, \tag{5.15}$$

which is depicted in figure 5.2.

Remark 21 The controller structure that we have used in this section may, at first sight, seem to have a nicer structure than the the one used in the formulation of the measurement feedback result in section 4.3.2. However, it does involve an additional integration, which means that it is less appealing from a computational point of view, in the case that one does not wish to apply controller order reduction where, in addition, the reference signal is time dependent.

5.3 A Tracking Trajectory with Minimal Cost

We consider in this section the special case where the reference signal r is scalar and constant in time. The measurement feedback control law can in this case be simplified, as the dependence of the control signal on r is now static; this follows from the observation that it can be determined as the steady state solution to a particular differential equation. We consider in this section finite dimensional systems of the type

$$\dot{x} = Ax + B_1 w + B_2 u + B_3 r \tag{5.16}$$
$$z = C_1 x + D_{12} u + D_{13} r \tag{5.17}$$
$$y = C_2 x + D_{21} w, \tag{5.18}$$

We have in this section chosen to formulate the control law as in section 5.2, since in practice the control engineer will opt for a low order controller if possible.

The control law of proposition 8, section 4.3.3 can be written as

$$u = -F_\infty(x_k + \rho) - V_1(D_{12}^* D_{13} r + B_2^* \theta) \tag{5.19}$$

where

$$\begin{aligned}
x_k(t) &= \int_{-\infty}^{t} S_{\tilde{A}-LC_F}(t-\tau) L\tilde{y}(\tau) d\tau \\
&= \int_{-\infty}^{t} S_{\tilde{A}-LC_F}(t-\tau) L(y - \gamma^{-2} D_{21} B_1^* \theta - C_F \rho)(\tau) d\tau \qquad (5.20) \\
\theta(t) &= -\int_{t}^{\infty} S_{\tilde{A}^*}(\tau - t)[F_\infty^* D_{12}^* D_{13} - P B_3 - C_1^* D_{13}] r(\tau) d\tau \qquad (5.21) \\
\rho &= \int_{-\infty}^{t} S_{\tilde{A}}(t-\tau) \bar{r}(\tau) d\tau. \qquad (5.22)
\end{aligned}$$

Since r is constant in time, we have the simplifications

$$\begin{aligned}
\theta &= (\tilde{A}^*)^{-1}[F_\infty^* D_{12}^* D_{13} - P B_3 - C_1^* D_{13}] r \qquad (5.23) \\
\rho &= -\tilde{A}^{-1}(\gamma^{-2} B_1 B_1^* \theta + B_3 r - B_2 V_1 (D_{12}^* D_{13} r + B_2^* \theta)). \qquad (5.24)
\end{aligned}$$

This leads to a simplified control law given by (5.19), (5.20), (5.23), (5.24).

In some applications it is not immediately clear how to choose the tracking trajectory $-D_{13}r$. An important consideration is to make sure that it is possible to obtain a small tracking error. In the framework that we use here, this translates to making J^0 small. In the application that we consider in chapter 2, where we have chosen to control the average temperature over nine intervals along the tunnel, it could for example be appropriate to pre-specify two or three temperatures of the desired profile, while the rest of the profile could be chosen from the criterium that the profile should be easy to track.

We consider the problem of determining D_{13} such that J^0 given by (4.16) is minimized under p constraints, written as

$$\begin{aligned}
\langle \phi_1, D_{13} r \rangle_Z &= 1 \qquad (5.25) \\
&\vdots \\
\langle \phi_p, D_{13} r \rangle_Z &= 1, \qquad (5.26)
\end{aligned}$$

where $\phi_i \in Z$, the space of the to-be-controlled output. With the simplification that r is constant in time we denote $\bar{\xi} = D_{13} r$. We introduce the matrix $\Phi = [\phi_i, \ldots, \phi_p]$, so that we can write the constraint as

$$\Phi' \bar{\xi} = \begin{bmatrix} 1 \\ \vdots \\ 1 \end{bmatrix}. \tag{5.27}$$

We can write

$$\begin{aligned} J^0 &= \|D_{13}r\|_{ap}^2 + \gamma^{-2}\|B_1^*\theta\|_{ap}^2 - \|V_1^{1/2}(B_2^*\theta + D_{12}^* D_{13}r)\|_{ap}^2 + 2\langle\theta, B_3 r\rangle_{ap} \\ &= \langle D_{13}r, MD_{13}r\rangle_Z + \langle D_{13}r, NB_3 r\rangle_Z + \langle B_3 r, UB_3 r\rangle_H \end{aligned} \tag{5.28}$$

where

$$\begin{aligned} M &= I - D_{12}V_1 D_{12}^* - 2D_{12}V_1 B_2^*(\tilde{A}^*)^{-1}(F_\infty^* D_{12}^* - C_1^*) \\ &\quad +(D_{12}F_\infty - C_1)\tilde{A}^{-1}(\gamma^{-2}B_1 B_1^* - B_2 V_1 B_2^*)(\tilde{A}^*)^{-1}(F_\infty^* D_{12}^* - C_1^*) \end{aligned} \tag{5.29}$$

$$\begin{aligned} N &= 2D_{12}V_1 B_2^*(\tilde{A}^*)^{-1}P + 2(D_{12}F_\infty - C_1)\tilde{A}^{-1} \\ &\quad -2(D_{12}F_\infty - C_1)\tilde{A}^{-1}(\gamma^{-2}B_1 B_1^* - B_2 V_1 B_2^*)(\tilde{A}^*)^{-1}P \end{aligned} \tag{5.30}$$

$$U = P\tilde{A}^{-1}(\gamma^{-2}B_1 B_1^* - B_2 V_1 B_2^*)(\tilde{A}^*)^{-1}P - 2P\tilde{A}^{-1} \tag{5.31}$$

Notice that the symmetric part of M is positive semi definite because J^0 must be non-negative. Now, the task is to find $\bar{\xi}$ satisfying

$$\bar{\xi} = \arg\min_{\xi}\{\langle\xi, M\xi\rangle + \langle\xi, NB_3 r\rangle + \langle B_3 r, UB_3 r\rangle\} \tag{5.32}$$

under the constraint (5.27). This has the form of minimization of a positive semi definite quadratic functional over linear equality constraints, which is a standard problem in mathematical programming. First we calculate the derivative

$$\frac{d}{d\xi}\left(\langle\xi, M\xi\rangle + \langle\xi, NB_3 r\rangle + \langle B_3 r, UB_3 r\rangle\right) = (M + M^*)\xi + NB_3 r. \tag{5.33}$$

This gives us the following condition: $\bar{\xi}$ minimizes J^0 under the constraint (5.27), if and only if there holds

$$\langle(M + M^*)\bar{\xi} + NB_3 r, \rho - \bar{\xi}\rangle = 0 \quad \forall\rho \in \{\rho|\langle\phi_i, \rho\rangle = 1,\ i = 1\ldots p\}. \tag{5.34}$$

The condition (5.34) can also be written as

$$\langle(M + M^*)\bar{\xi} + NB_3 r, \psi\rangle = 0 \quad \forall\psi \in \{\psi|\langle\phi_i, \psi\rangle = 0,\ i = 1\ldots p\}. \tag{5.35}$$

This means that there exists a vector $\kappa = [\kappa_1, \ldots, \kappa_p]'$ of Lagrange multipliers such that

$$(M + M^*)\bar{\xi} + NB_3 r = \kappa_1\phi_1 + \cdots + \kappa_p\phi_p. \tag{5.36}$$

A solution $\bar{\xi}$ to optimality conditions of the minimization problem is now given by solving

$$\begin{bmatrix} M + M^* & -\Phi \\ \Phi' & 0 \end{bmatrix}\begin{bmatrix} \bar{\xi} \\ \kappa \end{bmatrix} = \begin{bmatrix} -NB_3 r \\ \begin{bmatrix} 1 \\ \vdots \\ 1 \end{bmatrix} \end{bmatrix} \tag{5.37}$$

with respect to $D_{13}r$ and κ.

The more general plant. Let us now consider the more general plant

$$\begin{aligned} \dot{x} &= Ax + B_1 w + B_2 u + B_3 r \ , \quad t \in \mathbb{R} && (5.38)\\ z &= C_1 x + D_{11} w + D_{12} u + D_{13} r && (5.39)\\ y &= C_2 x + D_{21} w + D_{22} u + D_{23} r, && (5.40) \end{aligned}$$

The task of finding a suitable tracking trajectory is now only slightly more complicated than before. We must here consider $\hat{J}^0$, given in (4.42). For shortening the notation, introduce

$$\begin{aligned} \mathcal{F} &= \hat{V}_1(\hat{B}_2^* \tilde{P} + \hat{D}_{12}^* \hat{C}_1) && (5.41)\\ \mathcal{A} &= \hat{A} - \hat{B}_2 \mathcal{F} + \gamma^2 \hat{B}_1 \hat{B}_1^* \tilde{P} && (5.42) \end{aligned}$$

Let us introduce

$$\begin{aligned} \hat{M} &= I - \hat{D}_{12}\hat{V}_1\hat{D}_{12}^* - 2\hat{D}_{12}\hat{V}_1\hat{B}_2^*(\mathcal{A}^*)^{-1}(\mathcal{F}^*\hat{D}_{12}^* - \hat{C}_1^*)\\ &\quad +(\hat{D}_{12}\mathcal{F} - \hat{C}_1)\mathcal{A}^{-1}(\gamma^2\hat{B}_1\hat{B}_1^* - \hat{B}_2\hat{V}_1\hat{B}_2^*)(\mathcal{A}^*)^{-1}(\mathcal{F}^*\hat{D}_{12}^* - \hat{C}_1^*) && (5.43)\\ \hat{N} &= 2\hat{D}_{12}\hat{V}_1\hat{B}_2^*(\mathcal{A}^*)^{-1}\tilde{P} + 2(\hat{D}_{12}\mathcal{F} - \hat{C}_1)\mathcal{A}^{-1}\\ &\quad - 2(\hat{D}_{12}\mathcal{F} - \hat{C}_1)\mathcal{A}^{-1}(\gamma^2\hat{B}_1\hat{B}_1^* - \hat{B}_2\hat{V}_1\hat{B}_2^*)(\mathcal{A}^*)^{-1}\tilde{P} && (5.44)\\ \hat{U} &= \tilde{P}\mathcal{A}^{-1}(\gamma^2\hat{B}_1\hat{B}_1^* - \hat{B}_2\hat{V}_1\hat{B}_2^*)(\mathcal{A}^*)^{-1}\tilde{P} - 2\tilde{P}\mathcal{A}^{-1} && (5.45) \end{aligned}$$

where $\hat{B}_1$, $\hat{B}_2$, etc. are defined as in section 4.3.3. Still considering the case where r is real and constant, we can now write

$$\hat{J}^0 = \langle \hat{D}_{13}r, \hat{M}\hat{D}_{13}r\rangle + \langle \hat{D}_{13}r, \hat{N}\hat{B}_3 r\rangle + \langle \hat{B}_3 r, \hat{U}\hat{B}_3 r\rangle. \tag{5.46}$$

In order to express $\hat{J}^0$ in terms of D_{13} rather that $\hat{D}_{13}$, we must again apply the transformations of section 4.3.3. Introduce now

$$\begin{aligned} \mathcal{M} &= (\gamma^2 I - \bar{D}_{11}\bar{D}_{11}^*)^{-\frac{1}{2}}\hat{M}(\gamma^2 I - \bar{D}_{11}\bar{D}_{11}^*)^{-\frac{1}{2}}\\ &\quad +(\gamma^2 I - \bar{D}_{11}\bar{D}_{11}^*)^{-\frac{1}{2}}\hat{N}\bar{B}_1\bar{D}_{11}^*(\gamma^2 I - \bar{D}_{11}\bar{D}_{11}^*)^{-1}\\ &\quad +(\gamma^2 I - \bar{D}_{11}\bar{D}_{11}^*)^{-1}\bar{D}_{11}\bar{B}_1^*\hat{U}\bar{B}_1\bar{D}_{11}^*(\gamma^2 I - \bar{D}_{11}\bar{D}_{11}^*)^{-1} && (5.47)\\ \mathcal{N} &= \Big[2(\gamma^2 I - \bar{D}_{11}\bar{D}_{11}^*)^{-\frac{1}{2}}\hat{M}(\gamma^2 I - \bar{D}_{11}\bar{D}_{11}^*)^{-\frac{1}{2}}\\ &\quad +(\gamma^2 I - \bar{D}_{11}\bar{D}_{11}^*)^{-\frac{1}{2}}\hat{N}\bar{B}_1(\gamma^2 I - \bar{D}_{11}^*\bar{D}_{11})^{-1}\bar{D}_{11}^*\\ &\quad +\bar{D}_{11}(\gamma^2 I - \bar{D}_{11}^*\bar{D}_{11})^{-1}\bar{B}_1^*\hat{N}^*(\gamma^2 I - \bar{D}_{11}\bar{D}_{11}^*)^{-\frac{1}{2}}\\ &\quad +2\bar{D}_{11}(\gamma^2 I - \bar{D}_{11}^*\bar{D}_{11})^{-1}\bar{B}_1^*\hat{U}\bar{B}_1(\gamma^2 I - \bar{D}_{11}^*\bar{D}_{11})^{-1}\bar{D}_{11}^*\Big]\\ &\qquad\qquad D_{12}(I - R_\infty D_{22})^{-1}R_\infty D_{23}\\ &\quad +\Big[(\gamma^2 I - \bar{D}_{11}\bar{D}_{11}^*)^{-\frac{1}{2}}\hat{N} + 2\bar{D}_{11}(\gamma^2 I - \bar{D}_{11}^*\bar{D}_{11})^{-1}\bar{B}_1^*\hat{U}\Big]\ \bar{B}_3 && (5.48)\\ \mathcal{U} &= D_{23}^* R_\infty^*(I - D_{22}^* R_\infty^*)^{-1}D_{12}^*\mathcal{M}D_{12}(I - R_\infty D_{22})^{-1}R_\infty D_{23} \end{aligned}$$

$$
\begin{aligned}
&+D_{23}^*R_\infty^*(I-D_{22}^*R_\infty^*)^{-1}D_{12}^* \\
&\quad\left[(\gamma^2 I-\bar{D}_{11}\bar{D}_{11}^*)^{-\frac{1}{2}}\hat{N}+2\bar{D}_{11}(\gamma^2 I-\bar{D}_{11}^*\bar{D}_{11})^{-1}B_1^*\hat{U}\right]\bar{B}_3 \\
&+\bar{B}_3^*\hat{U}\bar{B}_3
\end{aligned}
\tag{5.49}
$$

We can now write

$$
\hat{J}^0=\langle D_{13}r,\mathcal{M}D_{13}r\rangle+\langle D_{13}r,\mathcal{N}r\rangle+\langle r,\mathcal{U}r\rangle, \tag{5.50}
$$

and apply the minimization procedure described above. This amounts to solving

$$
\begin{bmatrix} \mathcal{M}+\mathcal{M}^* & -\Phi \\ \Phi' & 0 \end{bmatrix}\begin{bmatrix} \bar{\xi} \\ \kappa \end{bmatrix}=\begin{bmatrix} -\mathcal{N}r \\ \begin{bmatrix} 1 \\ \vdots \\ 1 \end{bmatrix} \end{bmatrix} \tag{5.51}
$$

with respect to $\bar{\xi}$ and κ and choosing D_{13} so that $D_{13}r=\bar{\xi}$.

5.4 The Scaled H_∞ Problem

The presence of structured uncertainties was in chapter 2 handled by scaling the inputs and outputs using a diagonal scaling matrix Λ. In the present section we adapt this procedure to the two-degrees-of-freedom design, for a tracking problem with a known reference signal.

We assume a perturbation structure where the perturbation system Δ is diagonal, linear, time-invariant and stable, and of the form

$$
\Delta=\begin{bmatrix} \Delta_1 & & \\ & \ddots & \\ & & \Delta_n \end{bmatrix}. \tag{5.52}
$$

We are thus assuming that each of Δ_i is a scalar system, in order to keep the notation reasonably transparent.

A situation where such a perturbation is present, and where the controller to be constructed is applied, is shown in figure 5.3 where r is a reference signal and z_p is the tracking error. The signals w_s are introduced to obtain a plant of the type (4.30)-(4.32), and we partition them as $w_s=[w_s^1,\ldots,w_s^n]'$ and $z_s=[z_s^1,\ldots,z_s^n]'$, according to the perturbation Δ. We assume that each of the Δ_i's is normalized with respect to γ so that there holds

$$
\|w_s^1\|_{ap}^2 < \gamma^{-2}\|z_s^1\|_{ap}^2 \tag{5.53}
$$

$$
\vdots
$$

$$
\|w_s^n\|_{ap}^2 < \gamma^{-2}\|z_s^n\|_{ap}^2 \tag{5.54}
$$

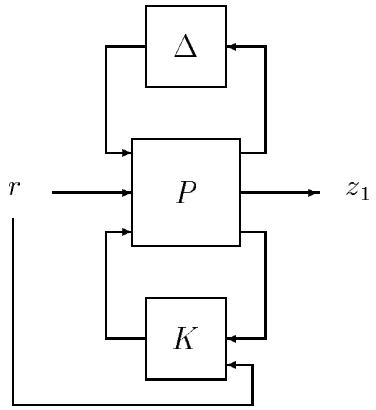

Figure 5.3:

for some $\gamma > 0$. We now give a bound on the tracking error, based on the control law given in proposition 10. Introducing the scaling matrix Λ according to the perturbation structure described above, we arrive at an H_∞ problem where the disturbance input is Λw_s, and the to-be-controlled output is given by $[z_p', (\Lambda z_s)']'$. With the controller given in proposition 10, we obtain by substituting $\|z\|_{ap}^2 = \|z_p\|_{ap}^2 + \|z_s\|_{ap}^2$ into the inequality (4.41), provided that the condition for this control law is satisfied, the inequality

$$\|z_p\|_{ap}^2 + \|z_s\|_{ap}^2 \leq \gamma^2 \|w_s\|_{ap}^2 + \gamma^2 \hat{J}^0 \tag{5.55}$$

which can also be written

$$\|z_p\|_{ap}^2 \leq \sum_{i=1}^{n} \lambda_i^2 \left(\gamma^2 \|w_s^i\|_{ap}^2 - \|z_s^i\|_{ap}^2 \right). \tag{5.56}$$

Now, using (5.53)-(5.54), we obtain

$$\|z_p\|_{ap}^2 \leq \gamma^2 \hat{J}^0. \tag{5.57}$$

We are not in the position to give a constructive method for seeking the ideal set of scaling parameters Λ. Instead we recommend to first formulate the tracking problem so that the reference signal is modelled by an unknown disturbance signal, and look for a set of scaling parameters that is suitable for this problem, using D-K iteration as it was done in section 2.4.4.

5.5 An Algorithm for the Two-degrees-of-freedom design

The type of control problems that we have in mind in this section is tracking problems where structured uncertainties are present. The techniques previously

described in this chapter are intended as an attempt to improve a controller design of the type used in chapter 2. An application of these techniques would be based on the following algorithm.

1. Design an H_∞ controller using the same procedure as in section 2.4.
2. Modify the scaled plant of the type shown in figure 2.7b in such a way that the signals, which are denoted w_1 and y_2 in figure 2.4, are removed.
3. Perform loop-shifting if necessary.
4. If needed, determine the reference profile using the technique of section 5.3.
5. Perform controller order reduction as shown in section 5.2, followed by the inverse loop-shifting procedure if necessary.

5.6 Discussion

The formulae developed in this chapter are based on those from chapter 4, which are again based on formulae obtained by Shaked and de Souza[57]. This is a natural development, since the very appealing method introduced in [57] did not at that stage take into account structured uncertainties, etc.

The way we have introduced the controller order reduction seems to be the most natural one possible. This may however not be the case for the scaling procedure, and we see no reason to claim that adopting the scaling parameters from the more standard design of chapter 2 is optimal in some sense. It would be interesting to apply the procedure developed in the present chapter to the case study of chapter 2.

Appendix A

A.1 Conditions for Solving the H_∞ Problem

The solution to the suboptimal H_∞ problem for finite dimensional systems can be found in Glover and Doyle[28]. This solution has been implemented in the toolbox [33], which we have used in section 2.5. For convenience of the reader we state here the part of the result of Glover and Doyle[28] that concerns the existence of a controller that solves the suboptimal H_∞ problem. We use here the same notation as in that paper.

Let a finite dimensional linear system be described by the state equation

$$\begin{aligned} \dot{x}(t) &= Ax(t) + B_1 w(t) + B_2 u(t), && \text{(A.1)} \\ z(t) &= C_1 x(t) + D_{11} w(t) + D_{12} u(t), && \text{(A.2)} \\ y(t) &= C_2 x(t) + D_{21} w(t) + D_{22} u(t), && \text{(A.3)} \end{aligned}$$

where $w(t) \in \mathbb{R}^{m_1}$ is the disturbance input, $u(t) \in \mathbb{R}^{m_2}$ is the control input, $z(t) \in \mathbb{R}^{p_1}$ is the to-be-controlled output, $y(t) \in \mathbb{R}^{p_2}$ is the measured output, and $x(t) \in \mathbb{R}^n$ denotes the state. The transfer matrix of this system P is denoted by

$$P(s) = \begin{bmatrix} P_{11}(s) & P_{12}(s) \\ P_{21}(s) & P_{22}(s) \end{bmatrix} = \begin{bmatrix} D_{11} & D_{12} \\ D_{21} & D_{22} \end{bmatrix} + \begin{bmatrix} C_1 \\ C_2 \end{bmatrix} (sI - A)^{-1} \begin{bmatrix} B_1 & B_2 \end{bmatrix}. \tag{A.4}$$

The controller to be designed is likewise a linear system, with the transfer matrix $K(s)$. The closed loop system is denoted by

$$\mathcal{F}(P, K) = P_{11} + P_{12} K (I - P_{22} K)^{-1} P_{21} \tag{A.5}$$

The following assumptions are made:

A1. (A, B_2, C_2) is stabilizable and detectable.

A2. rank $D_{12} = m_2$, rank $D_{21} = p_2$.

A3.

$$D_{12} = \begin{bmatrix} 0 \\ I \end{bmatrix}, \quad D_{21} = \begin{bmatrix} 0 & I \end{bmatrix} \tag{A.6}$$

and we have the partitioning

$$D_{11} = \begin{array}{c} \left[\begin{array}{cc} D_{1111} & D_{1112} \\ D_{1121} & D_{1122} \end{array} \right] \begin{array}{l} \updownarrow p_1 - m_2 \\ \updownarrow m_2 \end{array} \\ \begin{array}{cc} \leftrightarrow & \leftrightarrow \\ m_1 - p_2 & p_2 \end{array} \end{array} \tag{A.7}$$

A4. $D_{22} = 0$

A5.

$$\text{rank} \left[\begin{array}{cc} A - i\omega I & B_2 \\ C_1 & D_{12} \end{array} \right] \quad \forall \omega \in \mathbb{R} \tag{A.8}$$

A6.

$$\text{rank} \left[\begin{array}{cc} A - i\omega I & B_1 \\ C_2 & D_{21} \end{array} \right] \quad \forall \omega \in \mathbb{R} \tag{A.9}$$

Notice that **A1** is assumed to ensure the existence of a stabilizing controller. **A2** is a technical assumption which is essential for the applicability of this result, but not necessarily for the solvability of the H_∞ problem. **A3** and **A4** are assumed in order to simplify the formulae. **A5** and **A6** have roughly the same status as **A2**. Notice also that avoiding to violate assumption **A2** is in many cases a matter of formulating the control problem carefully.

Define

$$R = D_{1\cdot}^* D_{1\cdot} - \left[\begin{array}{cc} \gamma^2 I_{m_1} & 0 \\ 0 & 0 \end{array} \right] \tag{A.10}$$

where

$$D_{1\cdot} = \left[\begin{array}{cc} D_{11} & D_{12} \end{array} \right] \tag{A.11}$$

and

$$\tilde{R} = D_{\cdot 1} D_{\cdot 1}^* - \left[\begin{array}{cc} \gamma^2 I_{p_1} & 0 \\ 0 & 0 \end{array} \right] \tag{A.12}$$

where

$$D_{\cdot 1} = \left[\begin{array}{c} D_{11} \\ D_{21} \end{array} \right]. \tag{A.13}$$

We introduce the Riccati equations

$$\begin{aligned} 0 \;=\; & (A - BR^{-1}D_{1\cdot}^* C_1)^* X_\infty + X_\infty (A - BR^{-1}D_{1\cdot}^* C_1) \\ & - X_\infty (BR^{-1}B^*) X_\infty + C_1^* (I - D_{1\cdot} R^{-1} D_{1\cdot}^*) C_1 \end{aligned} \tag{A.14}$$

$$\begin{aligned} 0 \;=\; & (A^* - C^* \tilde{R}^{-1} D_{\cdot 1} B_1^*)^* Y_\infty + Y_\infty (A^* - C^* \tilde{R}^{-1} D_{\cdot 1} B_1^*) \\ & - Y_\infty (C^* \tilde{R}^{-1} C) Y_\infty + B_1 (I - D_{\cdot 1}^* \tilde{R}^{-1} D_{\cdot 1}) B_1^*. \end{aligned} \tag{A.15}$$

We are now in the position to quote part of the main theorem of Glover and Doyle[28].

Theorem 22 *For the system described by (A.1)-(A.3) and satisfying the assumptions A1-A6: There exists an internally stabilizing controller K such that*

$$\|\mathcal{F}(P,K)\|_\infty < \gamma \tag{A.16}$$

if and only if

(i) $\gamma > \max(\bar{\sigma}[D_{1111}, D_{1112}], \bar{\sigma}[D^*_{1111}, D^*_{1121}])$

(ii) *there exists X_∞ satisfying (A.14) and Y_∞ satisfying (A.15) respectively and such that $\rho(X_\infty Y_\infty) < \gamma^2$. ($\rho(\cdot)$ denotes the largest eigenvalue.)*

The part of the theorem that we have omitted are the explicit formulae for a dynamic controller K of the same order as the plant P, together with a parametrization of all rational stabilizing controllers satisfying (A.16).

A.2 Hankel Norm Approximation

Hankel norm approximation was used several times in the controller synthesis in chapter 2, and we therefore give in this appendix some remarks related to that method.

Consider the finite dimensional stable system

$$\frac{dx}{dt} = Ax + Bu \tag{A.17}$$

$$y = Cx + Du \tag{A.18}$$

where $u(t) \in \mathbb{R}^m$, $x(t) \in \mathbb{R}^n$, $y(t) \in \mathbb{R}^p$. The Hankel operator of this system relates past inputs to future outputs. We consider input signals in the space $L^2(-\infty, 0; \mathbb{R}^m)$, and we are interested in $y(t)$ only for $t > 0$. The Hankel operator that maps $u \in L^2(-\infty, 0; \mathbb{R}^m)$ to $y \in L^2(0, \infty; \mathbb{R}^p)$ is defined by

$$y(t) = \int_{-\infty}^{0} Ce^{A(t-\tau)}Bu(\tau)d\tau, \quad t > 0. \tag{A.19}$$

The Hankel norm of the system is equal to

$$\sup_{u \in L^2(-\infty,0;\mathbb{R}^m)} \frac{\sqrt{\int_0^\infty \|y(t)\|^2 dt}}{\sqrt{\int_{-\infty}^0 \|u(t)\|^2 dt}}. \tag{A.20}$$

The problem of model reduction by Hankel norm approximation is to find a system of lower order that approximates the original system in the Hankel norm. A comprehensive treatment of this technique can be found in Glover[25], and implementations are available, for example in the Matlab toolbox [33]. The method

is particularly efficient for approximation of systems when the maximum error across frequencies is an issue.

A theory for Hankel norm approximation of a class of infinite dimensional systems is available, see Glover et al.[27], but explicit formulae for such an approximation are not known in general. An exception can be found in Glover et al.[29].

A.3 Simulating the Pasteurization Plant

The numerical simulations were carried out using a combination of a Runge-Kutta method, and the method of characteristics.

The Runge-Kutta method (see Lambert[41]) is designed for simulating initial value problems of ordinary differential equations of the form

$$\frac{dy}{dt} = f(t,y)\ , \quad y(0) = y_0,\ f : \mathbb{R} \times \mathbb{R}^m \to \mathbb{R}^m. \tag{A.21}$$

For simplicity we describe here the method without error estimate. With an explicit 4 stage Runge-Kutta method is associated the Buther array

$$\begin{array}{c|cccc} c_1 & & & & \\ c_2 & a_{21} & & & \\ c_3 & a_{31} & a_{32} & & \\ c_4 & a_{41} & a_{42} & a_{43} & \\ \hline & b_1 & b_2 & b_3 & b_4. \end{array} \tag{A.22}$$

Denoting the time-discretization step by h, the method calculates $y_1, y_2, \ldots$ as the approximate solutions to the system (A.21) at the times $t_1 = h, t_2 = 2h, \ldots$. The method is defined by

$$y_{n+1} = y_n + h \sum_{i=1}^{4} b_i f(t_n + c_i h, Y_i), \tag{A.23}$$

where

$$Y_i = y_n + h \sum_{j=1}^{i-1} a_{ij} f(t_n + c_j h, Y_j). \tag{A.24}$$

This means that the right hand side $f(\cdot,\cdot)$ is in the $(n+1)$st step evaluated at the times $t_n, t_n + c_1 h, t_n + c_2 h, t_n + c_3 h$ and at the state values Y_1, Y_2, Y_3, Y_4. We have chosen to use the Runge-Kutta method with the Butcher array

$$\begin{array}{c|cccc} 0 & & & & \\ \frac{1}{2} & \frac{1}{2} & & & \\ \frac{1}{2} & \frac{1}{4} & \frac{1}{4} & & \\ 1 & 0 & -1 & 2 & \\ \hline & \frac{1}{6} & 0 & \frac{2}{3} & \frac{1}{6} \end{array} \tag{A.25}$$

which is known as England's method, except that we have omitted the error estimate provided by that method.

The idea behind using the method of characteristics for our simulation is to isolate the transport effect in such a way that the problem of simulating a partial differential equation is replaced by the problem of simulating a set of time-varying ordinary differential equation. In order to describe the principle of this method we consider the transport equation

$$\begin{aligned} \frac{\partial \phi}{\partial t}(t,x) &= -v\frac{\partial \phi}{\partial x}(t,x) + a\phi(t,x) + u(t,x)\ ,\ t>0,\ x>0 && \text{(A.26)} \\ \phi(t,0) &= 0 && \text{(A.27)} \\ \phi(0,x) &= \phi_0(x). && \text{(A.28)} \end{aligned}$$

This equation has the explicit solution

$$\phi(t,x) = e^{at}\phi_0(x-vt)H(x-vt) + \int_0^t e^{a(t-s)}u(s,x-v(t-s))H(x-v(t-s))ds \tag{A.29}$$

where $H(x) = 1$ for $x > 0$ and $H(x) = 0$ for $x < 0$. We introduce the substitution $\kappa = x - vt$ and define

$$\psi_\kappa(t) := \phi(t,x) = e^{at}\phi_0(\kappa) + \int_0^t e^{a(t-s)}u(s,\kappa+vs)H(\kappa+vs)ds. \tag{A.30}$$

There holds $\psi_\kappa(0) = \phi_0(\kappa)$, and hence

$$\psi_\kappa(t) = e^{at}\psi_\kappa(0) + \int_0^t e^{a(t-s)}u(s,\kappa+vs)H(\kappa+vs)ds. \tag{A.31}$$

For fixed κ, ψ_κ is now considered as a function of t that satisfies the ordinary differential equation

$$\begin{aligned} \frac{d\psi_\kappa}{dt}(t) &= \psi_\kappa(t) + u(t,\kappa+vt). && \text{(A.32)} \\ \psi_\kappa(0) &= \phi_0(\kappa) && \text{(A.33)} \end{aligned}$$

Clearly, simulating (A.32) and finding ϕ by the relation $\phi(t,\kappa+vt) = \psi_\kappa(t)$ is easier than simulating (A.26) directly.

The discretization in the spatial variable is carried out by approximating the initial value function ϕ_0 by average values. This means that in (A.32), the initial value $\psi_\kappa(0)$ is replaced by an average of the type

$$\frac{1}{\kappa_{i+1}-\kappa_i}\int_{\kappa_i}^{\kappa_{i+1}} \psi_\kappa(0)d\kappa. \tag{A.34}$$

In order to use the Runge-Kutta method we need to be able to evaluate the right-hand side of (A.32), where keeping track of $u(t,\kappa+vt)$ does involve a little

book-keeping. The discretization grid is chosen according to the time-step h. This means that, with the Butcher array (A.25), we need to evaluate the right-hand side of (A.32) at the times $t = 0, \frac{h}{2}, h, \frac{3h}{2}, 2h, \ldots$ and a natural choice of discretization grid is to let $\kappa_{i+1} - \kappa_i = vh/2$. The transformation between $\phi(t,x)$ and $\psi_\kappa(t)$ can be carried out in each step, but a more efficient implementation is obtained by doing this only occasionally.

The procedure described above can be applied to the transport equation (2.13). The implementation of the remaining part of the model is straightforward.

The stability constraints for England's method are roughly determined by the eigenvalues of the linearized system, see Lambert [41, sec. 5.12]. For this reason the time needed for simulating the closed loop system depends on the poles of the controller, where, for example, an eigenvalue of excessively large magnitude requires the simulation time to be proportional to the magnitude of that eigenvalue.

A.4 Minimizing a Constant Linear Fractional Transformation

In the loop-shifting procedure of section 4.3.3, the conditions for the existence of a static feedback F, minimizing

$$\|D_{11} + D_{12}F(I - D_{22}F)^{-1}D_{21}\| \tag{A.35}$$

were given. Below, we consider a standard procedure for the construction of such an F in the finite dimensional case where D_{11}, D_{12}, D_{22}, D_{21} are matrices.

Find Cholesky factors G and H such that

$$G'G = D_{12}'D_{12} \text{ and } H'H = D_{21}D_{21}'. \tag{A.36}$$

Define

$$\begin{aligned} T_{12} &= D_{12}(D_{12}'D_{12})^{-1}G' \\ T_{21} &= H(D_{21}D_{21}')^{-1}D_{21} \\ T_{11} &= D_{11} \\ Q &= GF(I - D_{22}F)^{-1}H' \\ \hat{T}_{12} &= (T_{12}')^{\perp} \\ \hat{T}_{21} &= (T_{21}^{\perp})' \end{aligned}$$

where $A^{\perp}$ denotes an ortonormal basis for the nullspace of A, i.e. $(A^{\perp})'A^{\perp} = I$ and $AA^{\perp} = 0$. Then there holds

$$\begin{bmatrix} \hat{T}_{12}' \\ T_{12}' \end{bmatrix} \begin{bmatrix} \hat{T}_{12} & T_{12} \end{bmatrix} = I \ , \quad \begin{bmatrix} \hat{T}_{21} \\ T_{21} \end{bmatrix} \begin{bmatrix} \hat{T}_{21}' & T_{21}' \end{bmatrix} = I, \tag{A.37}$$

and we can write

$$\begin{aligned}
&\|D_{11} + D_{12}F(I - D_{22}F)^{-1}D_{21}\| \\
&= \left\| T_{11} + \begin{bmatrix} \hat{T}_{12} & T_{12} \end{bmatrix} \begin{bmatrix} 0 & 0 \\ 0 & Q \end{bmatrix} \begin{bmatrix} \hat{T}_{21} \\ T_{21} \end{bmatrix} \right\| \\
&= \left\| \begin{bmatrix} \hat{T}'_{12} \\ T'_{12} \end{bmatrix} T_{11} \begin{bmatrix} \hat{T}'_{21} & T'_{21} \end{bmatrix} + \begin{bmatrix} 0 & 0 \\ 0 & Q \end{bmatrix} \right\|. \qquad \text{(A.38)}
\end{aligned}$$

Finding a matrix Q that minimizes (A.38) is a so-called four-block problem. An algorithm for solving this is explicitely described in Green and Limebeer[30, sec. 11.2]. Having found such a Q, the matrix F minimizing (A.35) can be found by the formula

$$F = (I + G^{-1}Q(H')^{-1}D_{22})^{-1}G^{-1}Q(H')^{-1}. \qquad \text{(A.39)}$$

A.5 The Pritchard-Salamon Class of Systems

For convenience of the reader, we here give the definition of the Pritchard-Salamon class of systems, where we quote Curtain et al.[17]. For background material on Hilbert spaces of the type considered below we refer to Aubin[3].

Let $\mathcal{W}$ and $\mathcal{V}$ be real separable Hilbert spaces, satisfying $\mathcal{W} \hookrightarrow \mathcal{V}$, where by $\hookrightarrow$ we mean that $\mathcal{W} \subset \mathcal{V}$ and the canoncal injection $\mathcal{W}$ is continuous and $\mathcal{W}$ is dense in $\mathcal{V}$. We consider strongly continuous semigroups $S(\cdot)$ on $\mathcal{V}$ which restrict to strongly continuous semigroups on $\mathcal{W}$. The infinitesimal generators of $S(\cdot)$ on $\mathcal{V}$ and $\mathcal{W}$ will be denoted by $A^{\mathcal{V}}$ and $A^{\mathcal{W}}$ respectively.

Definition 23 *Let $\mathcal{W}, \mathcal{V}$ and $S(\cdot)$ be as above and let U and Y be real separable Hilbert spaces.*

(i) *An operator $B \in \mathcal{L}(U, \mathcal{V})$ is called an* admissible input operator for $S(\cdot)$ *if there exist $t_1 > 0$ and $\beta > 0$ such that $\int_0^{t_1} S(t_1 - s)Bu(s)ds \in \mathcal{W}$ and*

$$\left\| \int_0^{t_1} S(t_1 - s)Bu(S)ds \right\|_{\mathcal{W}} \leq \beta \|u(\cdot)\|_{L_2(0,t_1;U)} \qquad \text{(A.40)}$$

for all $u(\cdot) \in L^2(0, t_1; U)$.

(ii) *An operator $C \in \mathcal{L}(\mathcal{W}, Y)$ is called an* admissible output operator for $S(\cdot)$ *if there exist $t_2 > 0$ and $\gamma > 0$ such that*

$$\|CS(\cdot)x\|_{L^2(0,t_2;Y)} \leq \gamma \|x\|_{\mathcal{V}} \text{ for all } x \in \mathcal{W}. \qquad \text{(A.41)}$$

(iii) *Let $B \in \mathcal{L}(U, \mathcal{V})$ and $C \in \mathcal{L}(\mathcal{W}, Y)$ be admissible input and output operators respectively, and $D \in \mathcal{L}$. The system $\Sigma_G = \Sigma(S(\cdot), B, C, D)$ given by*

$$\Sigma_G : \begin{cases} x(t) = S(t)x_0 + \int_0^t S(t-s)Bu(s)ds \\ y(t) = Cx(t) + Du(t), \end{cases} \tag{A.42}$$

where $x_0 \in \mathcal{V}$, $t \geq 0$ *and* $u(\cdot) \in L_2^{loc}(0,\infty)$ *is called a* Pritchard-Salamon system. *If, in addition, we have*

$$D(A^{\mathcal{V}}) \hookrightarrow \mathcal{W}, \tag{A.43}$$

we call Σ_G *a* smooth *Pritchard-Salamon system.*

Remark 24 Let $\Sigma_G = \Sigma(S(\cdot), B, C, D)$ be a smooth Pritchard-Salamon system. In [16] it is shown that if $F \in \mathcal{L}(\mathcal{W}, U)$ is an admissible output operator for $S(\cdot)$, then $A^{\mathcal{V}} + BF$ (with $D(A^{\mathcal{V}} + BF) = D(A^{\mathcal{V}})$) generates a strongly continuous semigroup on $\mathcal{V}$ which restricts to a strongly continuous semigroup on $\mathcal{W}$, and $\Sigma(S_{BF}(\cdot), B, C, D)$ is again a smooth Pritchard-Salamon system (this means that the Pritchard-Salamon class is invariant under output-feedback).

A.6 Weighting Systems Used in the Synthesis

In the controller synthesis algorithm we used a number of weighting systems, as shown in figure 2.4. The weighting systems W_1, W_2, W_3, W_4, W_5 are frequency dependent, while $\overline{W_1}$, W_r, W_p are merely matrices. The details are as follows.

$$W_1(s) = \frac{\sigma_1}{s + \sigma_1} \tag{A.44}$$

where $\sigma_1 = 3 \cdot 10^{-4}$.

$$W_2(s) = \begin{bmatrix} \kappa_2 - \delta_2 & (\gamma_2 - \kappa_2)\sigma_2^\ell \end{bmatrix} \left(sI_{10} - \begin{bmatrix} -\sigma_2^h & 0_{5\times 5} \\ \sigma_2^\ell & -\sigma_2^\ell \end{bmatrix} \right)^{-1} \begin{bmatrix} \sigma_2^h \\ I_5 - \sigma_2^\ell \end{bmatrix} + \delta_2 \tag{A.45}$$

where $\sigma_2^\ell = 0.01 \cdot I_5$, $\sigma_2^h = 5 \cdot I_5$, γ_2, κ_2, δ_2 are diagonal matrices of dimension 5×5 with $\gamma_2^i = 0.015 \cdot k/a_1^i$, $\kappa_2^i = 0.35 \cdot k/a_1^i$, $\delta_2^i = 0.2 \cdot k/a_1^i$ and I_5 is the 5×5 identity matrix.

$$W_3(s) = (\gamma_3 - \kappa_3)(sI_8 + \sigma_3)^{-1}\sigma_3 + \delta_3 \tag{A.46}$$

where γ_3, δ_3 are diagonal matrices of dimension 8×8 with $\gamma_3^i = 0.001$, $\delta_3^i = 0.14$.

$$W_4(s) = \begin{bmatrix} \kappa_4 - \delta_4 & (\gamma_4 - \kappa_4)\sigma_4^\ell \end{bmatrix} \left(sI_{16} - \begin{bmatrix} -\sigma_4^h & 0_{8\times 8} \\ \sigma_4^\ell & -\sigma_4^\ell \end{bmatrix} \right)^{-1} \begin{bmatrix} \sigma_4^h \\ I_8 - \sigma_4^\ell \end{bmatrix} + \delta_4 \tag{A.47}$$

where $\sigma_4^\ell = 0.005 \cdot I_8$, $\sigma_4^h = 0.1 \cdot I_8$,

$$\gamma_4 = 0.011 \begin{bmatrix} -1 & & & & & & & \\ 0.4 & -1 & & & & & & \\ 0.2 & 0.4 & -1 & & & & & \\ 0.1 & 0.22 & 0.4 & -1 & & & & \\ & 0.1 & 0.22 & 0.4 & -1 & & & \\ & & 0.1 & 0.22 & 0.4 & -1 & & \\ & & & 0.1 & 0.22 & 0.4 & -1 & \\ & & & & 0.1 & 0.22 & 0.4 & -1 \end{bmatrix},$$

$\kappa_4 = \gamma_4$, $\delta_4 = \frac{7}{11}\gamma_4$.

$$W_5(s) = \begin{bmatrix} \kappa_5 - \delta_5 & (\gamma_5 - \kappa_5)\sigma_5^\ell \end{bmatrix} \left(sI_{16} - \begin{bmatrix} -\sigma_5^h & 0_{8\times 8} \\ \sigma_5^\ell & -\sigma_5^\ell \end{bmatrix} \right)^{-1} \begin{bmatrix} \sigma_5^h \\ I_8 - \sigma_5^\ell \end{bmatrix} + \delta_5 \tag{A.48}$$

where $\sigma_5^\ell = 0.005 \cdot I_8$, $\sigma_5^h = 0.1 \cdot I_8$,

$$\gamma_5 = 0.0048 \cdot \begin{bmatrix} 1 & 1 & 0 & 0 & 0 & 0 & 0 & 0 \\ 0.25 & 0.5 & 1 & 1 & 0 & 0 & 0 & 0 \\ 0.25 & 0.5 & 1 & 1 & 0 & 0 & 0 & 0 \\ 0.125 & 0.25 & 0.5 & 1 & 1 & 0 & 0 & 0 \\ 0.125 & 0.25 & 0.5 & 1 & 1 & 0 & 0 & 0 \\ 0.125 & 0.25 & 0.5 & 1 & 1 & 0 & 0 & 0 \\ 0 & 0.125 & 0.25 & 0.5 & 1 & 1 & 0 & 0 \\ 0 & 0.125 & 0.25 & 0.5 & 1 & 1 & 0 & 0 \\ 0 & 0 & 0 & 0.125 & 0.25 & 0.5 & 1 & 1 \end{bmatrix},$$

$\kappa_5 = \frac{50}{48} \cdot \gamma_5$,

$$\delta_5 = 0.004 \cdot \begin{bmatrix} 1 & 1 & 0 & 0 & 0 & 0 & 0 & 0 \\ 0 & 0 & 1 & 1 & 0 & 0 & 0 & 0 \\ 0 & 0 & 1 & 1 & 0 & 0 & 0 & 0 \\ 0 & 0 & 0 & 0 & 1 & 0 & 0 & 0 \\ 0 & 0 & 0 & 0 & 1 & 0 & 0 & 0 \\ 0 & 0 & 0 & 0 & 1 & 0 & 0 & 0 \\ 0 & 0 & 0 & 0 & 0 & 1 & 0 & 0 \\ 0 & 0 & 0 & 0 & 0 & 1 & 0 & 0 \\ 0 & 0 & 0 & 0 & 0 & 0 & 1 & 1 \end{bmatrix}.$$

$$\overline{W_1} = \begin{bmatrix} 0.95 & 0.05 \end{bmatrix} \tag{A.49}$$

$$W_r = \begin{bmatrix} 32.04 & 51.77 & 58.14 & 60.24 & 62.63 & 63.18 & 61.27 & 54.85 & 27.17 \end{bmatrix}' \tag{A.50}$$

Notice that W_r was calculated as the steady state response in open loop, with some suitable vector of control signals applied.

$$W_p = \begin{bmatrix} 0.05 & & & & & & & & & \\ & 0.07 & & & & & & & & \\ & & 0.07 & & & & & & & \\ & & & 0.07 & & & & & & \\ & & & & 0.41 & & & & & \\ & & & & & 0.41 & & & & \\ & & & & & & 0.07 & & & \\ & & & & & & & 0.07 & & \\ & & & & & & & & 0.05 & \end{bmatrix}. \qquad \text{(A.51)}$$

A.7 Model Parameters of the Pasteurization Plant

parameter	value	comment
$l = x_i - x_{i-1}$	1.3	length of each zone (m)
v	0.005	velocity of conveyor belt (m/s)
$c1$	0.0539	heat transfer coefficient water/glass (sec^{-1})
$c2$	0.0391	heat transfer coefficient beer/glass (sec^{-1})
$c3$	0.0093	heat transfer coefficient glass/beer (sec^{-1})
η	123	steam temperature(°C)
β	103	parameter related to heat exchangers (sec °C)
a_1^1	0.989	*nominal* cut-off frequency for 1st heat exchanger(rad/sec)
a_1^2	0.853	*nominal* cut-off frequency for 2nd heat exch.(rad/sec)
a_1^3	0.717	*nominal* cut-off frequency for 3rd heat exch.(rad/sec)
a_1^4	0.620	*nominal* cut-off frequency for 4th heat exch.(rad/sec)
a_1^5	0.562	*nominal* cut-off frequency for 5th heat exch.(rad/sec)
a_2^i	0.196	cut-off frequency: upper tanks (rad/sec)
a_3^i	0.028	cut-off frequency: lower tanks (rad/sec)
a_4^i	0.558	coefficient related to heat flow in tunnel (m^{-1})
a_5^i	0.212	coefficient related to heat flow in tunnel (m^{-1})
k	$6.1342 \cdot 10^{-6}$	stationary gain of heat exchangers (sec °C/J)
T_D^i	3.2	delay related to water supply (sec)
T_E^i	2	delay related to water collection (sec)

Appendix B

B.1 Notation

$\hat{i}$	the imaginary unit
τ^i	the ith component of the vector τ
a^i	the ith diagonal entry of the diagonal matrix a
$\overline{\mathbb{C}^+}$	$\{s \in \mathbb{C}$ such that $\mathrm{Re}\{s\} \geq 0\}$
$r_\sigma(\cdot)$	the spectral radius
$\bar{\sigma}(\cdot)$	the largest singular value
I	the identity
Δ_i	the ith diagonal matrix of scalar perturbation systems
W_i	the ith weighting matrix or weighting system
$\|x\|_2$	L^2 norm of x
$\|x\|$	norm of the scalar x
$\|A\|$	induced L^2 norm of the bounded linear operator A
$\|\cdot\|_\infty$	the norm on the Hardy space H_∞
$L^2(0,\infty;H)$	the L^2 space of functions defined on $(0,\infty)$ with values in H
$\mathcal{L}(U,H)$	bounded linear operators from U to H
$D(A)$	domain of the linear operator A
A^*	adjoint of the linear operator A
B'	transpose of B
$\mathcal{F}(G,K)$	linear fractional transformation, defined in (2.42)
$TP(H)$	trigonometric polynomials with values in H
$AP(H)$	almost periodic functions with values in H
$AP_2(H)$	Besicovitch-almost periodic functions based on $AP(H)$
$\|\cdot\|_{ap}$	norm on the Hilbert space of Besicovitch-almost periodic functions

Bibliography

[1] B.D.O. Anderson and Y. Liu. Controller reduction: Concepts and approaches. *IEEE Transactions on Automatic Control*, 34(8):802–812, 1989.

[2] B.D.O. Anderson and J.B. Moore. *Linear Optimal Control.* Prentice-Hall, 1971.

[3] J.P. Aubin. *Applied Functional Analysis.* Wiley, 1979.

[4] H.T. Banks and J.A. Burns. Hereditary control problems: Numerical methods based on averaging approximations. *SIAM Journal of Control and Optimization*, 16(2):169–208, 1978.

[5] H.T. Banks, M.A. Demetriou, and R.C. Smith. An H_∞/minmax periodic control in a two-dimensional structural acoustic model with piezoceramic actuators. *IEEE Transactions on Automatic Control*, 41(7):943–959, 1996.

[6] H.T. Banks, S.L. Keeling, R.J. Silcox, and C. Wang. Linear quadratic tracking problems in Hilbert space: Application to optimal active noise suppression. In *Control of Distributed Parameter Systems*, pages 5–10, Perpignan, France, 1989. IFAC.

[7] A.S. Besicovitch. *Almost Periodic Functions.* Cambridge University Press, 1932.

[8] H. Bohr. *Almost Periodic Functions.* Chelsea Publishing Company, 1947.

[9] H. Bohr and E. Følner. On some types of functional spaces. *Acta Mathematica*, 76:31–155, 1944.

[10] J. Bontsema and R.F. Curtain. A note on spillover and robustness for flexible systems. *IEEE Transactions on Automatic Control*, 33(6):567–569, 1988.

[11] S. Boyd, L. El Ghaoui, E. Feron, and V. Balakrishnan. *Linear Matrix Inequalities in System and Control Theory.* SIAM, 1994.

[12] C. Corduneanu. *Almost Periodic Functions.* Wiley/Interscience, 1968.

[13] R.F. Curtain. Robust stabilizability of normalized coprime factors: the infinite-dimensional case. *International Journal of Control*, 51(6):1173–1190, 1990.

[14] R.F. Curtain. A comparison of finite-dimensional controller designs for distributed parameter systems. *Control-Theory and Advanced Technology*, 9(3):609–628, 1993.

[15] R.F. Curtain and K. Glover. Robust stabilization of infinite dimensional systems by finite dimensional controllers. *Systems & Control Letters*, 7:41–47, 1986.

[16] R.F. Curtain, H. Logemann, St. Townley, and H. Zwart. Well-posedness, stabilizability and admissibility for Pritchard Salamon systems. Technical report, Institut für Dynamische Systeme, Universität Bremen, 1992.

[17] R.F. Curtain, M. Weiss, and Y. Zhou. Closed formulae for a parametric-mixed-sensitivity problem for Pritchard-Salamon systems. *System and Control Letters*, 27:157–167, 1996.

[18] R.F. Curtain and H.J. Zwart. *An Introduction to Infinite Dimensional Systems Theory.* Springer-Verlag New York, 1995.

[19] R. Dautray and J.-L. Lions. *Mathematical Analysis and Numerical Methods for Science and Technology, vol 6, Evolution Problems II.* Springer-Verlag, 1993.

[20] J.C. Doyle, B.A. Francis, and A.R. Tannenbaum. *Feedback Control Theory.* Macmillan Publishing Company, 1992.

[21] J.C. Doyle, K. Glover, P.P. Khargonekar, and B.A. Francis. State-space solutions to standard H_2 and H_∞ control problems. *IEEE Transactions on Automatic Control*, 34(8):831–847, 1989.

[22] B.A. Francis. A course in H_∞ control theory. In *Lecture Notes in Control and Information Sciences*, volume 88. Springer-Verlag, 1987.

[23] B. Friedland. *Advanced Control System Design.* Prentice-Hall, 1996.

[24] L. El Ghaoui, F. Delebecque, and R. Nikoukhah. *Lmitool.*

[25] K. Glover. All optimal Hankel-norm approximations of linear multivariable systems and their L^∞-error bounds. *International Journal of Control*, 39:1115–1193, 1984.

[26] K. Glover. Robust stabilization of linear multivariable systems: relations to approximation. *International Journal of Control*, 43:741–766, 1986.

[27] K. Glover, R.F. Curtain, and J.R. Partington. Realisation and approximation of linear infinite-dimensional systems with error bounds. *SIAM Journal of Control and Optimization*, 26(4):863–898, 1988.

[28] K. Glover and J.C. Doyle. State-space formulae for all stabilizing controllers that satisfy an H_∞-norm bound and relations to risk sensitivity. *System & Control Letters*, 11:167–172, 1988.

[29] K. Glover, J. Lam, and J.R. Partington. Balanced realisation and hankel-norm approximation of systems involving delays. In *25th Conference on Decision and Control*, pages 1810–1815. IEEE, 1986.

[30] M. Green and D.J.N. Limebeer. *Linear Robust Control*. Prentice-Hall, New Jersey, 1995.

[31] G. Guardabassi, A. Locatelli, and S. Rinaldi. What is periodic optimization? In A. Marzollo, editor, *Periodic Optimization*. Springer-Verlag, 1972.

[32] M. Heilbuth and J. Mortensen. Modelling of pasteurizing plant. Master's thesis, Control Engineering Institute, Technical University of Denmark, 1991. (in Danish).

[33] Musyn Inc. and The MathWorks Inc. μ-analysis and synthesis toolbox.

[34] The MathWorks Inc. Matlab.

[35] K. Ito and K.A. Morris. An approximation theory of solutions to operator riccati equations for H_∞ control. In *Proceedings of the 33rd Conference on Decision and Control*, pages 3961–3966. IEEE, 1994.

[36] B. Jacob, M. Larsen, and H. Zwart. Corrections and extensions of "optimal control of linear systems with almost periodic inputs" by G. Da Prato and A. Ichikawa. Technical report, Department of Mathematics, Technical University of Denmark, 1996. Submitted for publication.

[37] O. Jannerup. Modelling of pasteurizer zone. Technical report, Institute of Automatic Control Systems, Technical University of Denmark, 1993.

[38] F. Kappel and D. Salamon. An approximation theorem for the algebraic Riccati equation. *SIAM Journal of Control and Optimization*, 28(5):1136–1147, 1990.

[39] E. Kreyszig. *Introductory Functional Analysis with Applications*. Wiley, 1978.

[40] H. Kwakernaak. Robust control and H_∞-optimization - tutorial paper. *Automatica*, 29(2):255–273, 1993.

[41] J.D. Lambert. *Numerical Methods for Ordinary Differential Systems.* Wiley, 1991.

[42] P. Lancaster and M. Tismenetsky. *The Theory of Matrices.* Academic Press, 1985.

[43] M. Larsen. H_∞ control of linear systems with almost periodic inputs. Technical report, Department of Mathematics, Technical University of Denmark, 1996. Submitted for publication.

[44] M. Larsen and R.F. Curtain. H_∞ tracking problems with almost periodic inputs. In *Proceedings of the 4th IEEE Mediterranean Symposium*, pages 612–616, 1996.

[45] B.M. Levitan and V.V. Zhikov. *Almost periodic functions and differential equations.* Cambridge University Press, 1982.

[46] D.J.N. Limebeer, B.D.O. Anderson, P.P. Khargonekar, and M. Green. A game theoretic approach to H_∞ control for time-varying systems. *SIAM Journal of Control and Optimization*, 30(2):262–283, 1992.

[47] D.J.N. Limebeer, E.M. Kasenally, and J.D. Perkins. On the design of robust two degree of freedom controllers. *Automatica*, 29(1):157–168, 1992.

[48] A. Packard and J. Doyle. The complex structured singular value. *Automatica*, 29(1):71–109, 1993.

[49] A. Pazy. *Semigroups of Linear Operators and Applications to Partial Differential Equations.* Springer-Verlag, 1983.

[50] K. Poolla and A. Tikku. Robust performance against time-varying structured perturbations. *IEEE Transactions on Automatic Control*, 40(9):1589–1602, 1995.

[51] G. Da Prato and A. Ichikawa. Optimal control of linear systems with almost periodic inputs. *SIAM Journal of Control and Optimization*, 25(4):1007–1019, 1987.

[52] A.J. Pritchard and D. Salamon. The linear quadratic control problem for infinite dimensional systems with unbounded input and output operators. *SIAM Journal of Control and Optimization*, 25(1):121–144, 1987.

[53] F. Riesz and B. Sz-Nagy. *Leçons d'analyse fonctionnelle.* Academie des sciences de Hongrie, 1952.

[54] C. Rudolph and S. Weiss. Control of a pasteurization plant. Master's thesis, Control Engineering Institute, Technical University of Denmark, 1990. (In Danish).

[55] M.G. Safonov, D.J.N. Limebeer, and R.Y. Chiang. Simplifying the H_∞ theory via loop shifting, matrix pencil and descriptor concepts. *International Journal of Control*, 50(6):2467–2488, 1990.

[56] Y. Sakawa, F. Matsuno, and S. Fukushima. Modeling and feedback control of a flexible arm. *Journal of Robotic Systems*, 2(4):453–472, 1985.

[57] U. Shaked and C.E. de Souza. Continuous-time tracking problems in an H_∞ setting: A game theory approach. *IEEE Transactions on Automatic Control*, 40(5):841–852, 1995.

[58] M.A. Shubin. Almost periodic functions and partial differential operators. *Russian Mathematical Surveys*, 33(2):1–52, 1978.

[59] B. van Keulen. *H_∞-control for infinite-dimensional systems: a state-space approach.* PhD thesis, University of Groningen, 1993.

[60] B. van Keulen, M. Peters, and R. Curtain. H_∞-control with state-feedback: The infinite dimensional case. *Journal of Mathematical Systems, Estimation, and Control*, 3(1):1–39, 1993.

[61] I. Yaesh and U. Shaked. Two-degree-of-freedom H_∞-optimization of multivariable feedback systems. *IEEE Transactions on Automatic Control*, 36:1272–1276, 1991.

[62] K. Zhou. Frequency-weighted L_∞ norm and optimal Hankel norm model reduction. *IEEE Transactions on Automatic Control*, 40:1687–1699, 1995.

[63] K. Zhou, J. Doyle, and K. Glover. *Robust and Optimal Control.* Prentice-Hall, 1996.